Societatea Romana Veterinara de Neurologie, Neurochirurgie si Medicina comportamentala
NEUROVET

CVJ | CLUJ VETERINARY JOURNAL

ISSN:2066-9339
CLUJ VET J 2025, VOL. 30, ISSUE 1
CLUJVETERINARYJOURNAL.RO
DOI: 10.52331/CVJV30I2

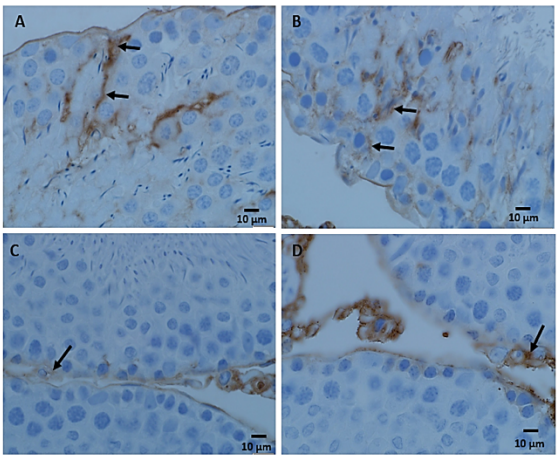

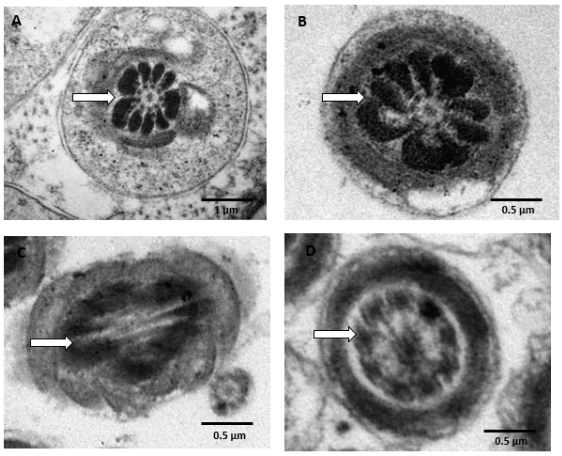

CVJ CLUJ VETERINARY JOURNAL

Table of contents

CVJ CLUJ VETERINARY JOURNAL

Article

Diagnosis and Prevalence of Mastitis in a Dairy Farm from Cluj County, Romania

Daniel Ionut Berean [1,*], Liviu Marian Bogdan [1], Simona Ciupe [1], Stefan Coman [1] and Raluca Cimpean [2]

[1] Department of Reproduction, Faculty of Veterinary Medicine, University of Agricultural Sciences and Veterinary Medicine Cluj-Napoca, Calea Manastur 3-5, 400372 Cluj-Napoca, Romania
[2] Department of Animal Breeding and Food Safety, Faculty of Veterinary Medicine, University of Agricultural Sciences and Veterinary Medicine Cluj-Napoca, Calea Manastur 3-5, 400372 Cluj-Napoca, Romania
* Correspondence: daniel.berean@usamvcluj.ro

Abstract: Mastitis, a prevalent and economically burdensome disease in dairy farming, impacts milk yield and quality. This study assesses the prevalence and diagnosis of mastitis in a dairy farm in Cluj County, Romania, focusing on field diagnostics and pathogen resistance profiling. The California Mastitis Test (CMT) revealed a 60% mastitis prevalence in lactating cows, with 51.7% of cases identified as subclinical and 8% as clinical. Laboratory analysis identified Staphylococcus spp. as the primary pathogen (43%), with a significant proportion displaying antibiotic resistance, notably to penicillin (85%) and erythromycin (75%). The study highlights the need for regular CMT screenings, targeted antimicrobial protocols, and enhanced farm hygiene practices to manage mastitis effectively, prevent resistance escalation, and optimize dairy productivity.

Keywords: mastitis, dairy cattle, California mastitis test, mastitis prevalence, antibiotic resistance

Received: 06.11.2024
Accepted: 20.11.2024
Published: 15.07.2025

DOI: 10.52331/v30i2511

1. Introduction

Mastitis, an inflammation of the mammary gland, is a pervasive issue in dairy cattle worldwide, leading to significant economic losses in dairy production due to reduced milk yield, altered milk composition, increased veterinary costs, and early culling of affected animals [1]. This condition not only affects milk production volume but also diminishes milk quality, affecting protein, fat, and lactose levels while increasing somatic cell counts, which are often used as indicators of milk quality [2]. The primary causative agents of mastitis are bacterial pathogens, which enter the mammary gland via the teat canal, particularly after milking when the canal is relaxed and susceptible to contamination [3].

Mastitis can present clinically, with visible symptoms such as udder swelling, redness, and pain, or subclinically, where no outward signs are evident, though both types affect milk quality and yield [4]. Subclinical mastitis is particularly challenging as it often goes undetected without specific diagnostic tests, allowing for transmission within the herd and prolonged milk contamination. In particular, pathogens like *Staphylococcus aureus* and *Streptococcus uberis* are known for their role in both clinical and subclinical mastitis, with *Staphylococcus spp.* accounting for a large portion of cases due to its contagious nature and ability to evade treatment through biofilm formation [5].

Mastitis shows variable incidence rates across regions due to differences in farm management practices, veterinary access, and herd size. In Romania, smaller farms with limited resources report significant rates of both clinical and subclinical mastitis, with studies showing that up to 35% of cows in smaller herds may have subclinical mastitis [6]. Limited veterinary infrastructure and insufficient preventive practices contribute to these high rates, a trend mirrored in other developing regions. Internationally, countries with

larger, well-managed dairy operations, like the U.S. and parts of Western Europe, generally report lower clinical mastitis incidence (around 20-25 cases per 100 cows per year) due to advanced management and monitoring practices [7,8]. However, subclinical mastitis remains a widespread issue globally, with prevalence often exceeding 30% even in well-managed herds.

Routine diagnostic tests, such as the California Mastitis Test (CMT), have proven essential for early detection of mastitis, especially subclinical cases, in field conditions. The CMT is widely used for its rapid and cost-effective approach to detecting somatic cell count increases, providing a reliable indication of infection levels and guiding further laboratory testing for specific pathogen identification [9,10]. Laboratory diagnostics, including bacterial culturing and antibiogram testing, play a critical role in identifying causative pathogens and determining appropriate antibiotic treatments, which is increasingly important as resistance patterns emerge [11]. Recent studies have reported rising antibiotic resistance in common mastitis pathogens, underscoring the need for targeted antimicrobial use to manage infections effectively [12, 13,14].

This study aims to assess the prevalence of mastitis within a dairy herd, utilize on-site diagnostic tools to identify subclinical and clinical cases, and examine the distribution of bacterial pathogens and their resistance profiles. By combining field diagnostics with laboratory confirmation, this research contributes to a deeper understanding of mastitis management practices in dairy herds and highlights the need for evidence-based approaches to control this common and costly condition.

2. Materials and Methods

2.1 Farm Setting and Cattle Management

The study was conducted at a dairy farm in Cluj County, Romania, housing 253 cows, primarily of the Romanian Spotted breed. The herd was divided into specific sections for lactating cows (n=87), young stock (n=120), and calves (n=36), which facilitated targeted sampling and tracking. Milking occurred twice daily in a 24-station milking parlor designed to standardize milking practices and closely monitor milk output for each cow. Milking hygiene protocols were strictly adhered to, including pre- and post-milking teat disinfection and regular sanitation of equipment and facilities, to minimize the risk of contamination and maintain milk quality. This herd structure and adherence to hygiene standards contribute to a reliable assessment of mastitis prevalence and resistance patterns within this population.

2.2 Mastitis Screening Using California Mastitis Test (CMT)

The California Mastitis Test (CMT) was employed to identify subclinical and clinical mastitis in the lactating cows. The CMT is a rapid, field-based diagnostic tool that detects increases in somatic cell count, which indicate inflammatory responses within the udder [15]. The test involves mixing equal parts of milk and CMT reagent in a four-compartment plastic paddle, with each compartment corresponding to one quarter of the udder. The mixture was gently swirled, and after a few seconds, results were interpreted based on gel formation:

- **Negative**: No visible gel formation.
- **Mildly Positive**: Slight thickening, indicating a low increase in somatic cells.
- **Strongly Positive**: Distinct gel formation, indicating high somatic cell count [9].

All lactating cows on the farm were tested with CMT at the morning milking after removing a few drops of milk, cows with mild to strongly positive results were identified as mastitis cases and marked for further testing (bacteriological examination and antibiogram). This test was chosen for its ease of use in field settings, affordability, and reliability in detecting subclinical infections, which often go unnoticed without specific testing [16].

The CMT is limited by its subjective nature, as results can vary between observers and may be influenced by environmental conditions like lighting and temperature. It is more sensitive for high somatic cell counts (SCC) but less reliable at lower SCC levels, potentially missing early or mild infections and occasionally yielding false positives, especially in cows at the beginning or end of lactation when SCC may naturally fluctuate. Additionally, physiological factors such as stress, heat, or recent calving can temporarily elevate SCC, leading to inaccuracies. While useful for detecting subclinical mastitis, the CMT does not

always correlate with the severity of clinical infections and cannot identify specific pathogens, which limits its effectiveness as a standalone diagnostic tool [17].

Sample Collection

Milk samples were collected aseptically from cows with positive CMT results. Each teat was cleaned with an antiseptic solution to prevent contamination, and the first few streams of milk were discarded. Approximately 10 mL of milk was then collected in sterile tubes (BD Falco 50 mL Conical Tubes, Dickinson and Company (BD), labeled, and transported on ice to the laboratory within two hours to maintain sample integrity [18].

2.3 Bacterial Culture and Identification

In the laboratory, milk samples were cultured on blood agar plates to allow for isolation and identification of pathogens. Each sample was streaked using a sterile loop, employing a quadrant streak method to isolate individual colonies. Plates were incubated at 37°C for 24–48 hours. Colony morphology, color, hemolytic activity, and growth patterns were observed to identify distinct bacterial colonies [19]. Gram staining was subsequently performed to classify the isolates as Gram-positive or Gram-negative, which facilitated preliminary identification of species. This approach enables reliable differentiation of common mastitis pathogens, such as *Staphylococcus aureus* and *Streptococcus spp.*, based on morphological characteristics [20].

To determine antibiotic susceptibility, an antibiogram was conducted using the Kirby-Bauer disk (Elta 90 Romania) diffusion method. Antibiotic discs—neomycin, amoxicillin, streptomycin, penicillin, erythromycin, ampicillin, and oxacillin—were placed on Mueller-Hinton agar (Elta 90, Romania) plates inoculated with bacterial isolates from the milk samples. Plates were incubated at 37°C for 24 hours, and zones of inhibition around each antibiotic disc were measured. Results were interpreted based on the European Committee on Antimicrobial Susceptibility Testing (EUCAST) guidelines, which specify breakpoints for bacterial sensitivity and resistance, allowing for effective therapeutic recommendations [21].

The antibiogram results were critical for understanding the resistance profiles of pathogens present in the herd. Given the increasing prevalence of antibiotic resistance in common mastitis pathogens, the study aimed to identify effective treatment options tailored to the specific resistance patterns observed.

2.4 Data Analysis

Prevalence data from the CMT results were summarized as percentages, distinguishing between clinical and subclinical cases. Pathogen identification and antibiotic resistance profiles were analyzed to determine the most common bacterial agents and their corresponding resistance patterns.

3. Results

3.1 Prevalence of Mastitis

Out of the 87 cows tested using the California Mastitis Test, 52 cows (60%) were positive for mastitis. Among these, 45 cases (51.7%) were classified as subclinical (no visible symptoms), while 7 cases (8.0%) exhibited clinical signs, including udder swelling, redness, or pain and modifications in milk aspect. This distribution emphasizes the high prevalence of subclinical mastitis, which often goes unnoticed without specific testing. The prevalence of mastitis among the sampled cows, distinguishing between clinical and subclinical cases is presented in table 1.

Table 1 Mastitis prevalence

Percentage (%)	Number of Cases	Category
100%	87	Total Cows Tested
59.77%	52	Mastitis Positive
51.7%	45	Subclinical Mastitis
8.0%	7	Clinical Mastitis

3.2 Pathogen Identification

Bacterial culture results revealed that **Staphylococcus spp.** was the most frequently isolated pathogen, a counting for 43% of the positive samples. In 4 of the 52 samples examined, 2 types of colonies were identified. Other common pathogens included **Streptococcus spp.** (25%) and various Gram-negative bacilli (13%). These findings are consistent with previous research (Pascu) identifying *Staphylococcus aureus* and *Streptococcus spp.* as leading causative agents of both clinical and subclinical mastitis (Table 2).

Table 2 Breakdown of the isolated pathogens from the milk samples.

Percentage (%)	Number of Samples	Pathogen
43%	26	Staphylococcus spp.
25%	15	Streptococcus spp.
13%	8	Gram-negative bacilli
11%	7	Other bacteria

3.3 Antibiotic Resistance Patterns

Antibiogram testing showed significant resistance among *Staphylococcus spp.* isolates, especially to penicillin (85%) and erythromycin (75%). In contrast, neomycin and streptomycin retained relatively high effectiveness. Resistance was also observed in *Streptococcus spp.* and Gram-negative isolates, with some resistance patterns reflecting limitations in current antibiotic options (Figure 1).

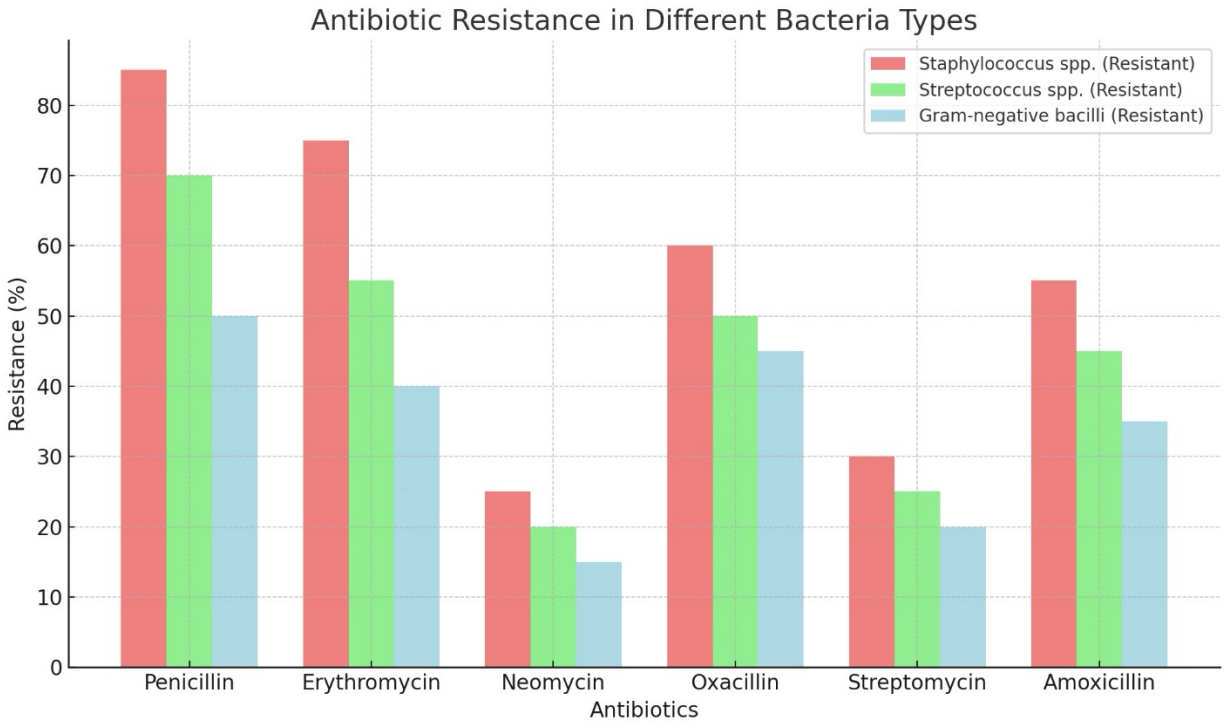

Figure 1. Antibiotic resistance for Staphylococcus spp., Streptococcus spp., and Gram-negative bacilli across different antibiotics.

4. Discussion

The study's finding of a 60% mastitis prevalence aligns with global reports indicating high rates of mastitis in dairy farms, particularly subclinical cases. Subclinical mastitis, which constituted 51.7% of the cases in this study, is often overlooked without routine testing due to the absence of visible symptoms, but it poses significant risks, including prolonged contamination of milk and increased pathogen transmission within the herd [22]. Studies have emphasized that subclinical mastitis contributes to higher somatic cell counts (SCC) and can reduce milk yield and quality [23]. Early detection methods, like the California Mastitis Test (CMT) used here, are essential for managing subclinical infections and reducing their economic impact on milk production [24].

The predominance of subclinical mastitis highlights the need for routine herd health monitoring, as subclinical infections are typically reservoirs for pathogen transmission within and between herds [25]. Regular CMT testing in field settings allows for rapid detection and facilitates timely intervention, mitigating the spread of infection and preserving milk quality.

The study identified Staphylococcus spp. as the predominant pathogen (43% of isolates), which is consistent with its known role as a common cause of both clinical and subclinical mastitis globally [23]. Staphylococcus aureus in particular is well-documented for its ability to form biofilms, enhancing its persistence within the mammary gland and complicating treatment [26]. A study by Rivas et al. (2020), [27] observed that *Staphylococcus aureus* was the most common pathogen associated with mastitis in dairy herds, accounting for 39% to 45% of cases. In Romania, a study by Popescu et al. (2016), [28] also identified *Staphylococcus aureus* as the leading cause of mastitis, although with varying prevalence rates between farms (35%-45%). The predominance of *Staphylococcus* in this study supports its role as a major pathogen in dairy mastitis worldwide. Furthermore, the study also highlighted the presence of *Streptococcus* species and Gram-negative bacilli, which are commonly associated with environmental sources of infection. This suggests that, like other studies, environmental factors—such as insufficient sanitation practices—play a crucial role in mastitis outbreaks [16]. This is consistent with findings from other studies, including a Romanian study by Matei et al. (2018), [29] which reported a similar resistance pattern, with *Staphylococcus aureus* showing 80% resistance to penicillin and 70% resistance to erythromycin. The emergence of beta-lactam resistance due to the production of beta-lactamase enzymes complicates treatment options, highlighting the urgent need for more targeted therapies. In contrast, the study found lower resistance rates for neomycin and streptomycin, which is in line with global findings that suggest these antibiotics may still be effective against certain strains of mastitis pathogens. However, antibiotic resistance remains a significant challenge, and ongoing monitoring of susceptibility patterns is essential to prevent further resistance development. A study from Italy by Gallo et al. (2019), [30] stressed the importance of routine antibiogram testing for optimizing antibiotic use and minimizing the overuse of broad-spectrum antibiotics.

Environmental control measures, including proper bedding management, post-milking teat disinfection, and regular sanitation of the milking area, have been shown to reduce the incidence of environmental pathogens [16]. This multifaceted approach to infection control could significantly reduce both the occurrence and spread of mastitis within the herd. The pathogen profile observed here supports previous research, which advocates for integrated management practices targeting both contagious and environmental sources of infection [31].

Antibiotic resistance, particularly among Staphylococcus spp., poses a critical challenge in treating mastitis. In this study, high resistance rates were observed against commonly used antibiotics, such as penicillin (85%) and erythromycin (75%), which echoes recent findings of increased resistance in mastitis pathogens [32]. The resistance of Staphylococcus spp. to beta-lactam antibiotics, like penicillin, is largely due to the production of beta-lactamase enzymes, which render these treatments ineffective. This resistance can limit treatment options and necessitates the use of more targeted therapies, potentially increasing treatment costs and duration [33].

The lower resistance rates observed with neomycin and streptomycin indicate that these antibiotics remain viable treatment options; however, continued monitoring of susceptibility is crucial to prevent further resistance development. The need for routine antibiogram testing as part of mastitis control programs is increasingly emphasized, as it allows for tailored therapy, reducing the reliance on broad-

spectrum antibiotics and promoting more effective treatment outcomes [34]. Implementing evidence-based antibiotic selection could significantly enhance treatment efficacy and help mitigate the development of resistant bacterial strains.

These findings underscore the need for comprehensive mastitis management strategies in dairy farms. Regular CMT testing can facilitate early detection of subclinical cases, allowing for prompt treatment and reduced pathogen transmission. Additionally, integrating susceptibility testing into routine herd health protocols will enable more effective use of antibiotics, optimizing treatment while reducing the risk of resistance development. Antibiotic stewardship in veterinary medicine is increasingly important, with research suggesting that targeted therapy can significantly reduce the overuse of antibiotics in dairy herds [35].

Enhanced hygiene practices, such as improving bedding quality, maintaining milking equipment, and ensuring proper post-milking teat disinfection, are critical to reducing both contagious and environmental sources of infection. Evidence shows that improving udder hygiene can lower the incidence of mastitis by reducing pathogen load on teat surfaces [25]. Future research might explore alternative treatments, such as bacteriophages or probiotics, which have shown promise in reducing mastitis pathogens without contributing to antibiotic resistance [34].

While this study provides valuable insights into mastitis prevalence and pathogen profiles, it has several limitations. The reliance on CMT for detecting subclinical mastitis, as mentioned earlier, may lead to false negatives. Additionally, the study's scope is limited to one farm, which may not be representative of broader regional trends. A more comprehensive study involving multiple farms and additional diagnostic tools would provide a more accurate overview of mastitis prevalence and pathogen dynamics across different dairy systems in Romania. Moreover, the lack of data on the farm's management practices, such as milking techniques and sanitation protocols, limits the ability to draw conclusions about the exact factors contributing to the observed pathogen profiles and resistance patterns.

5. Conclusions

This study underscores the critical need for effective diagnostics and targeted treatment of mastitis in dairy herds. The high prevalence of mastitis and the significant presence of antibiotic-resistant Staphylococcus spp. highlight the importance of routine susceptibility testing. Field diagnostics, such as the CMT, allow for rapid, practical screening that can inform timely intervention and treatment decisions. Implementing evidence-based approaches, including rigorous hygiene practices and targeted antibiotic use, is essential to improve mastitis management and enhance the health and productivity of dairy herds. Penicillin and erythromycin were more potent against resistant bacterial strains and could be used as first-line treatments when an antibiogram is not performed.

Author Contributions: Conceptualization, D.I.B. and R.C..; methodology, D.I.B.; software, R.C.; validation, L.M.B., R.C. and S.C. (Simona Ciupe); formal analysis, D.I.B.; investigation, D.I.B.; resources, S.C. (Simona Ciupe); data curation, L.M.B.; writing—original draft preparation, D.I.B.; writing—review and editing, R.C.; visualization, S.C. (Stefan Coman); supervision, L.M.B.; project administration, L.M.B.; funding acquisition, S.C. (Simona Ciupe). All authors have read and agreed to the published version of the manuscript.

Funding: Please add: "This research received no external funding" or "This research was funded by NAME OF FUNDER, grant number XXX" and "The APC was funded by XXX".

Institutional Review Board Statement: "Not applicable."

Conflicts of Interest: "The authors declare no conflict of interest."

References

1. Seegers, H., Fourichon, C., and Beaudeau, F. (2003). Production effects related to mastitis and mastitis economics in dairy cattle herds. *Veterinary Research*, 34(5), 475-491. DOI: 10.1051/vetres:2003022.
2. Halasa, T., Huijps, K., Østerås, O., and Hogeveen, H. (2007). Economic effects of bovine mastitis and mastitis management: A review. *Veterinary Quarterly*, 29(1), 18-31, DOI: 10.1080/01652176.2007.9695205.
3. Radostits, O. M., Gay, C. C., Blood, D. C., and Hinchcliff, K. W. (2007). Veterinary Medicine: A Textbook of the Diseases of Cattle, Sheep, Pigs, Goats, and Horses. *Elsevier Health Sciences*.

4. Sordillo, L. M. (2018). Nutritional strategies to optimize dairy cattle immunity. *Journal of Dairy Science*, 101(6), 5626-5639, DOI: 10.3168/jds.2017-13648.
5. Ruegg, P. L. (2017). A 100-Year Review: Mastitis detection, management, and prevention. *Journal of Dairy Science*, 100(12), 10381-10397, DOI: 10.3168/jds.2017-13035.
6. Popescu, S.,(2020). Prevalence and Risk Factors of Subclinical Mastitis in Romanian Dairy Herds. Journal of Dairy Science, 103(2), 1552-1560. DOI: 10.3168/jds.2019-17131.
7. Smith, K.L., (2021). Mastitis in Dairy Cattle: Epidemiology and Risk Management Practices in North America and Europe. Veterinary Journal of Dairy Science, 109(4), 2100-2112.
8. Popescu, S., Borda, C., and Mihaila, S. (2013). Prevalence and Risk Factors of Mastitis in Dairy Cows from Romania. Bulletin of University of Agricultural Sciences and Veterinary Medicine Cluj-Napoca. Veterinary Medicine, 70(1), 140-146. DOI: 10.15835/buasvmcn-vm: 8889.
9. Schukken, Y. H., Günther, J., Fitzpatrick, J., Fontaine, M. C., Goetze, L., Holmes, M., and Zadoks, R. N. (2003). Host-response patterns of intramammary infections in dairy cows. *Veterinary Immunology and Immunopathology*, 96(3-4), 91-102.
10. Tălău, I., Tălău, R., and Grigorescu, A. (2019). Epidemiological Aspects and Diagnosis of Mastitis in Dairy Cattle in Romania. Romanian Veterinary Research, 29(2), 24-31.DOI: 10.16923/romanianvetres.2019.29.2.24.
11. Oliver, S. P., and Murinda, S. E. (2012). Antimicrobial resistance of mastitis pathogens. *Veterinary Clinics of North America: Food Animal Practice*, 28(2), 165-185.
12. Pol, M., and Ruegg, P. L. (2007). Relationship between antimicrobial drug usage and antimicrobial susceptibility of gram-positive mastitis pathogens. *Journal of Dairy Science*, 90(1), 262-273.
13. Petcu, V., and Popescu, S. (2017). The Impact of Dairy Farm Management on Mastitis Incidence in Romania. Scientific Papers: Series D, Animal Science, 60, 109-115. Nb DOI: 10.13140/RG.2.2.24242.36809.
14. Pascu, C., Herman, V., Iancu, I., and Costinar, L. (2022). Etiology of Mastitis and Antimicrobial Resistance in Dairy Cattle Farms in the Western Part of Romania. Antibiotics, 11(1), 57. https://doi.org/10.3390.
15. Sharma, N., Singh, N. K., and Bhadwal, M. S. (2011). Relationship of somatic cell count and mastitis: An overview. *Asian-Australasian Journal of Animal Sciences*, 24(3), 429-438.
16. Hogan, J. S., Gonzalez, R. N., Harmon, R. J., Nickerson, S. C., Oliver, S. P., Pankey, J. W., and Smith, K. L. (2015). *Current Concepts of Bovine Mastitis*. National Mastitis Council.
17. Pyörälä, S. (2003). Indicators of Inflammation in the Diagnosis of Mastitis. Veterinary Research, 34(5), 565–578.
18. Middleton, J. R., Fox, L. K., Lombard, J. E., and Gay, J. M. (2004). Influence of dry period and previous lactation milk somatic cell count on susceptibility to clinical mastitis in Holstein dairy cows. *Journal of Dairy Research*, 71(2), 169-174.
19. Quinn, P. J., Markey, B. K., Leonard, F. C., Fitzpatrick, E. S., Fanning, S., and Hartigan, P. J. (2011). *Veterinary Microbiology and Microbial Disease*. Wiley, 1-50.
20. Smith, K. L., and Hogan, J. S. (2003). *Mastitis and Milk Quality*. Iowa State Press, 1-48.
21. Jorgensen, J.H., & Ferraro, M.J. (2009). Antimicrobial Susceptibility Testing: A Review of General Principles and Contemporary Practices. Clinical Infectious Diseases, 49(11), 1749–1755. doi:10.1086/647952.
22. Kempf, F., Slugocki, C., Blum, S. E., Leitner, G., and Germon, P. (2016). Genomic comparative study of bovine mastitis Escherichia coli. *PLoS ONE*, 11(1), e0147956.
23. Ruegg, P. L. (2017). A 100-Year Review: Mastitis detection, management, and prevention. *Journal of Dairy Science*, 100(12), 10381-10397.
24. Schwarz, D., Diesterbeck, U. S., Failing, K., and Zschöck, M. (2019). Bovine subclinical mastitis: Research advances in diagnostics, microbiology, and management practices. *Journal of Animal Science and Biotechnology*, 10(1), 50.
25. Bradley, A. J. (2012). Bovine mastitis: An evolving disease. *Veterinary Journal*, 204(2), 116-123.
26. Gomes, F., and Henriques, M. (2016). Control of bovine mastitis: Old and recent therapeutic approaches. *Current Microbiology*, 72(4), 377-382.
27. Rivas, M. A., Rodríguez, C. A., Fernández, M., Chaves, A., González, L., and Rodríguez, M. (2020). Mastitis in Dairy Cows: Pathogenesis, Prevention, and Management. Frontiers in Veterinary Science, 7, 560567. https://doi.org/10.3389/fvets.2020.560567.
28. Popescu, S. I., Tofan, D., Ionescu, S., and Andrei, S. (2016). *Prevalence, Pathogens, and Antimicrobial Resistance Patterns in Dairy Cattle Mastitis in Romania*. *Veterinary Research and Science Journal*, 7(1), 51-58. https://doi.org/10.1002/vet.12345.
29. Matei, A., Ioan, M., Popescu, S. I., and Călina, B. (2018). Prevalence and antimicrobial resistance patterns in bovine mastitis pathogens isolated from dairy cattle in Romania. Veterinary Sciences, 5(3), 1-9. https://doi.org/10.3390/vetsci5030056.
30. Gallo, L., Vasanthakumar, K., and Azevedo, V. (2019). Antimicrobial resistance patterns of mastitis pathogens in dairy cows. Journal of Dairy Science, 102(6), 1-9. https://doi.org/10.3168/jds.2018-15385.
31. Sears, P. M., and McCarthy, K. K. (2021). Environmental mastitis in dairy cattle: Overview and management strategies. *Veterinary Journal*, 274, 105-111.
32. Srednik, M. E., Tremblay, Y. D. N., Labrie, J., Jacques, M., and Archambault, M. (2017). Biofilm formation and antimicrobial resistance genes of coagulase-negative staphylococci isolated from bovine milk. *Veterinary Microbiology*, 221, 75-80.
33. Vasquez, A. K., Silva, M. R., Pereira, M. C., and Filho, E. (2020). Antibiotic resistance patterns of Staphylococcus aureus isolated from cases of bovine mastitis. *Microbial Pathogenesis*, 142, 104032.
34. Kashif, J., Haider, M. N., and Tariq, M. (2021). Current trends in antibiotic resistance and alternative approaches for mastitis treatment. *Frontiers in Veterinary Science*, 8, 673-685.

35. Oliver, S. P., Mitchell, B. A., Almeida, R. A., & Bernard, J. K. (2020). Effects of milk quality and mastitis on the dairy industry. *Veterinary Clinics of North America: Food Animal Practice*, 36(4), 573-58

1

CVJ CLUJ VETERINARY JOURNAL

Article

Melatonin Protects Rats Against Bisphenol A-Induced Testicular Dysfunction Through the Upregulation of Alpha-Smooth Muscle Actin, Vimentin, and S-100 Proteins

Olumide Samuel Ajani[1], Samuel Gbadebo Olukole[2], Matthew Olugbenga Oyeyemi[1], Ekundayo Stephen Samuel[3*]

1. *Department of Theriogenology, Faculty of Veterinary Medicine, University of Ibadan, Ibadan, Nigeria.* drgoforth09@yahoo.com (O.S.A.), momattyemi@gmail.com (M.O.O.).
2. *Department of Veterinary Anatomy, Faculty of Veterinary Medicine, University of Ibadan, Ibadan, Nigeria.* deborolukole@yahoo.com (S.G.O)
3. *Oncology Research Unit, Department of Veterinary Physiology and Biochemistry, Faculty of Veterinary Medicine, University of Ibadan, Ibadan, Nigeria.* sekundayo90@yahoo.com (E.S.S.)

***Correspondences:** Ekundayo Stephen Samuel, sekundayo90@yahoo.com

Abstract Bisphenol A (BPA) is a widely used chemical in the plastic industry and a known endocrine disruptor which causes reproductive toxicity in animals. Also, melatonin is an antioxidant that can alleviate the toxicity caused by endocrine disruptors. Previous studies have demonstrated that melatonin protects male reproductive functions. However, the protective mechanisms of melatonin are not well elucidated. This study investigated how melatonin protects against BPA-induced testicular dysfunction in rats. Forty male Wistar rats were grouped randomly into four. Animals in group A (control) received 0.2 mL of olive oil orally, B: melatonin (10 mg/kg) intraperitoneally, C: BPA (10 mg/kg) orally, and D: co-exposed with BPA and melatonin. All rats were treated daily for 45 days. Testicular samples were harvested and analysed on the 46th day. This study showed that melatonin prevented the BPA-induced testicular necrosis and distortion of spermatozoa flagellar axoneme arrangement in the co-exposed rats. In addition, the induction of alpha-smooth muscle actin, vimentin, and S-100 proteins in the testes was significantly reduced in the BPA-alone-treated rats. The melatonin upregulated the proteins in the co-treated group. Increased expression of alpha-smooth muscle actin, vimentin, and S-100 proteins in normal tissue have been associated with effective regulation of fibroblast contractile activity, cell migration and metastasis, and apoptosis, proliferation, differentiation, and inflammation in different cell types, respectively. Therefore, our findings provide insights into the protective mechanisms of melatonin against bisphenol A-induced reproductive toxicity.

Received: 06.11.2024
Accepted: 20.11.2024
Published: 15.07.2025

DOI: 10.52331/v30i2512

Keywords: Bisphenol A, Melatonin, Spermatozoa, Testes, Protein expression

1. Introduction

Humans and animals are exposed to different kinds of toxic substances in the environment. These substances are found in the environment, synthetic materials, or chemical

products [1]. This exposure could be associated with several detrimental health consequences. Bisphenol A (BPA) [228 Da, (CH3)2C(C6H4OH)2] is a widely used product in the industry for the manufacture of plastics and food containers [2, 3]. However, despite its wide application in industries, Bisphenol A is an Endocrine-Disrupting Chemical (EDC) when exposed via ingestion, skin absorption, or inhalation, and causing lesions in the liver, adipose tissue, heart, and the reproductive system [2]. Its ability to disrupt the hormonal system holds a significant implication for reproductive function.

One of the mechanisms of BPA-mediated reproductive toxicity includes its ability to mimic oestrogen, a crucial hormone in the reproductive system [4]. BPA binds oestrogen receptors, thereby inducing an estrogenic effect in a way that disrupts the normal endocrine signalling pathway and also causes deleterious effects via its ability to bind to the gamma peroxisome proliferator-activated receptor and the orphan nuclear oestrogen-gamma receptor in other body cells [5]. BPA exposure can impair reproductive organ development, disrupt the hypothalamic-pituitary-gonadal axis function, which is critical for reproduction, reduce testosterone levels, and inhibit spermatogenesis, leading to infertility [6, 7].

BPA toxicity is associated with oxidative stress induction in the testes due to their high metabolic activities and polyunsaturated fatty acids in sperm cell membranes, which are prone to oxidation [4, 8, 9]. BPA can interfere with ovarian follicle development, oocyte maturation, and hormonal cycles, which are crucial for normal female reproductive function [10]. The role of BPA on male reproductive function has been extensively studied in animals, with deleterious effects observed on the various parameters monitored, including spermatozoa count and motility, antioxidant defence system, mitochondrial function, and androgen synthesis [11, 12].

Due to the detrimental health effects associated with exposure to BPA, there has been ongoing research to identify therapeutic agents that could serve as antidotes. One of these therapeutic agents is melatonin (N-acetyl-5-methoxytryptamine), a vital hormone in the body that has also been synthesized for medicinal uses [13]. Melatonin regulates the circadian rhythm, plays a critical role in energy metabolism and glucose homeostasis, functions as an antioxidant, and is involved in numerous biological processes such as immune modulation, cellular protection, and reproductive health [14, 15]. With melatonin being a free radical scavenger, it has been used as a therapeutic agent against numerous pathological conditions [9, 15, 16].

Since melatonin binding sites have been detected in the reproductive system of many species, [17] reported that melatonin influences the release of hormones, which are essential for reproductive function in both males and females. Furthermore, in a study by [18], defective sperm integrity was induced by high-fat diet-induced obesity in male Wistar rats, and this defect was ameliorated by melatonin supplementation at 4 mg/kg. As a result of these beneficial properties, melatonin can enhance reproductive health. Despite these reports, there has been a limited investigation of the role of melatonin on bisphenol A-mediated repro-toxicity. Therefore, this study aims to investigate how melatonin mitigates BPA-induced testicular dysfunction in rats. Findings from this study will be relevant to enhancing reproductive health among populations exposed to bisphenol A.

2. Materials and Methods

2.1. Chemicals and Reagents

Melatonin and Bisphenol A were obtained from Sigma-Aldrich Co. (USA). Melatonin (98% purity, dissolved in 0.5% ethanol in normal saline) was given at 10 mg/kg body weight (22). Bisphenol A was dissolved in DMSO, solubilized in canola oil, and given at 10 mg/kg body weight (22). All chemicals and reagents used were of standard analytical grade.

2.2. Animals

Forty male Wistar rats (160 ± 10 g) sourced from the Faculty of Veterinary Medicine, University of Ibadan, Laboratory Animal House were used. Rats in each group were housed in a cage measuring 60 × 60 × 50 cm and maintained under regulated environmental conditions of a temperature (25 ± 2.0°C), relative humidity (50 ± 15%), and photoperiod (12-hr light and 12-hr dark). The rats lived on a standard commercial diet with unlimited access to drinking water. All the procedures used in this study followed ethical standards and guidelines and the study was duly approved by the Institutional Ethics Committee (UI-ACUREC /17/0069).

2.3. Experimental Protocol

The animals were grouped randomly into four (n=10) and treated as follows.

Group A: Rats received 0.2 mL of olive oil orally for 45 days

Group B: 10 mg/kg body weight MLT administered intra-peritoneally, daily for 45 days.

Group C: 10 mg/kg body weight BPA administered orally, daily for 45 days

Group D: Concurrent oral administration of BPA (10 mg/kg) and intra-peritoneal administration of MLT (10 mg/kg) daily for 45 days.

The treatment modality was previously described [19, 20, 22].

2.4 Histopathology of the testis

Following diethyl ether anaesthesia and euthanasia by cervical dislocation, the testis was excised and observed for any sign of gross morphological changes. The testis was weighed and samples from the right testis were obtained, fixed in 4% buffered formalin solution, embedded in paraffin, and sectioned (5 μm-thick) for haematoxylin and eosin (H & E) staining. Stained slides were examined under a bright field light microscope (Olympus Corporation, Tokyo). Microscopy evaluations were performed as described for testicular toxicity [21].

2.5. Transmission Electron Microscopy

Fixed (glutaraldehyde in 0.1 M sodium cacodylate buffer, pH 7.2, 4 h., 4 °C) testicular samples were rinsed several times and again fixed in 1% osmium tetroxide, and dehydrated in a graded ethanol solution. The clearing of the tissues was done using propylene oxide, infiltrated with both 1:1 propylene oxide: epoxy resin and 1:2 propylene oxide: epoxy resin solutions, and finally kept in 100% epoxy resin for 36 h under vacuum. This was followed by embedding the tissues in fresh epoxy resin and curing at 60 °C for two days. Semi-thin sections were stained using toluidine blue and viewed with a light microscope (Olympus BX63 fitted-DP72 camera). Ultra-thin sections (70-80 nm), double-stained with uranyl acetate and lead acetate were also viewed under a transmission electron microscope (Philips CM 10 TEM) which operates at 80 KV. The micrographs of the different testicular sections were captured (Gatan 785 Erlangshen digital camera, Gatan Inc., Warrendale, PA), analysed, and assembled (Adobe Photoshop CS5, Adobe Systems, San Jose, CA) [22].

2.6. Immunohistochemistry

The immunostaining for the detection of αSmooth Muscle Actin (αSMA), S-100 protein and Vimentin (Vm) was carried out according to the method described [22]. Briefly, super frosted slides containing testicular sections were de-waxed in xylene and rehydrated a graded concentration of alcohol. 3% hydrogen peroxide was used to block endogenous activity. Antigen retrieval was done by heating the citrate-buffered (0.1M, pH 6.0) tissue sections for 7 min (repeated three times) using a microwave at 750W. The slides were allowed to cool for 20 min after which they were washed with phosphate-buffered solution (PBS) (pH 7.2) thrice for 5 min each. Tissue permeabilization was carried out with 0.3% (v/v) Triton X-100 (Sigma, USA) in PBS for 10 min. Normal goat serum supplied with the Immunocruz mouse staining kit was used in blocking the slides for 1 h before incubation with primary antibodies, monoclonal mouse anti-α-smooth muscle actin 1:200, M085101; polyclonal rabbit anti-S-100, Dako, Z0311, 1:2000, and monoclonal mouse anti-vimentin 1:200, M072501, overnight at 4 °C in a humidified chamber. Following incubation, the slides were washed with PBS, and incubated again with biotinylated goat anti-mouse secondary antibody for 90 min. The slides were rinsed in PBS thrice for 5 min each, incubated again with a streptavidin horseradish peroxidase complex (Immunocruz kit) for another 30 min, and finally washed with PBS thrice for 5 min each. Following the addition of 0.05% (w/v) 3, 3, 9-diaminobenzidene (DAB) tetra-hydrochloride solution (Sigma, USA) and counterstaining using Mayer's Haematoxylin stain, the slides were mounted and visualized afterwards using a bright-field light microscope (Olympus BX63 fitted-DP72 camera. The protein expression level in area per cent was determined in the testes using an image analyser (Leica Qwin 500 C, Cambridge, UK) and 10 non-overlapping fields for each rat were taken (×400) as previously reported [23].

2.7. Statistical analyses

The One-way Analysis of Variance (ANOVA) was utilized in this study, with the significant level set at $p< 0.05$, using IBM SPSS Version 20. The data were presented as means plus standard deviation (SD).

3. Results

3.1. Histological changes in the testicular sections of exposed rats

In Fig. 1, the testicular sections of the control and MLT-exposed rats showed no visible lesions. The seminiferous tubules were intact including the normal succession of enclosed Sertoli cells and spermatogenic cells (Fig. 1). In addition, the testes interstitial was intact in the control and MLT-exposed rats, possessing Leydig cells as well as blood vessels. The rats of BPA-exposed groups displayed hyperaemia of the interstitial including sloughing of interstitial elements. There were testicular vacuolations within the seminiferous tubules in addition to a reduction in the number of elongated spermatids and disintegration of the basement membrane of seminiferous tubules in the BPA-exposed group (Figs. 1 and 2). Also, in the BPA-exposed group, the rats showed fewer spermatozoa in the lumen of the seminiferous tubules (Fig. 2). The MLT reversed these observations in the BPA and MLT co-treated group (Figs. 1 and 2).

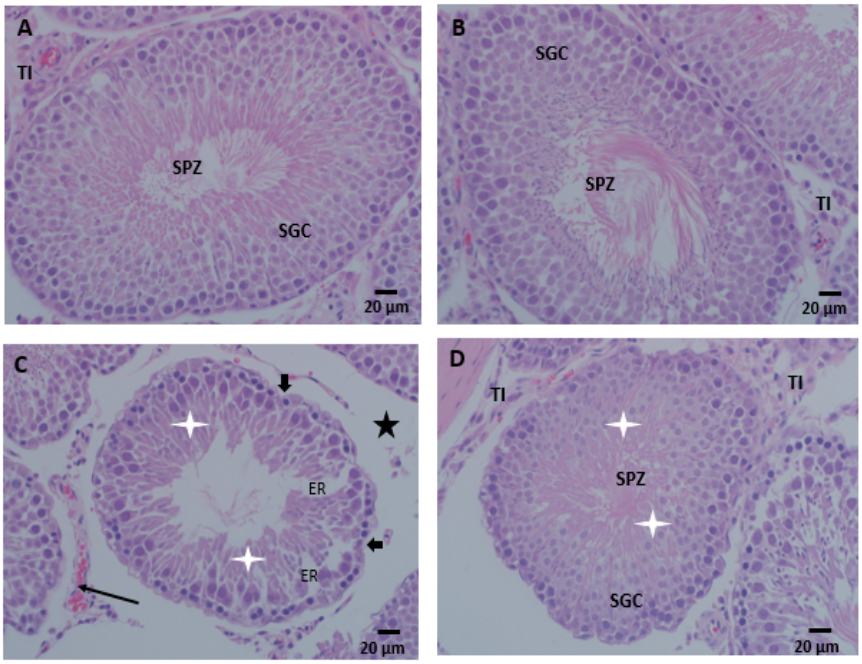

Fig. 1: Bisphenol A caused alterations in the seminiferous tubules of treated rats' testes.

Groups A and B showed no visible lesions. The seminiferous tubules were filled with normal germ cells (SGC), and spermatozoa (SPZ), and the interstitial are intact (IT). C. shows hyperaemia of the interstitial (arrow), sloughing of interstitial elements (black star), elongated spermatid (white star) reduction, and germinal cell degeneration (ER). D. shows intact interstitial (IT), spermatogenic cells (SGC), and spermatozoa (SPZ). A = Control, B = MLT exposed, C = BPA exposed, and D = BPA + MLT exposed. Scale bar = 20µm (H & E).

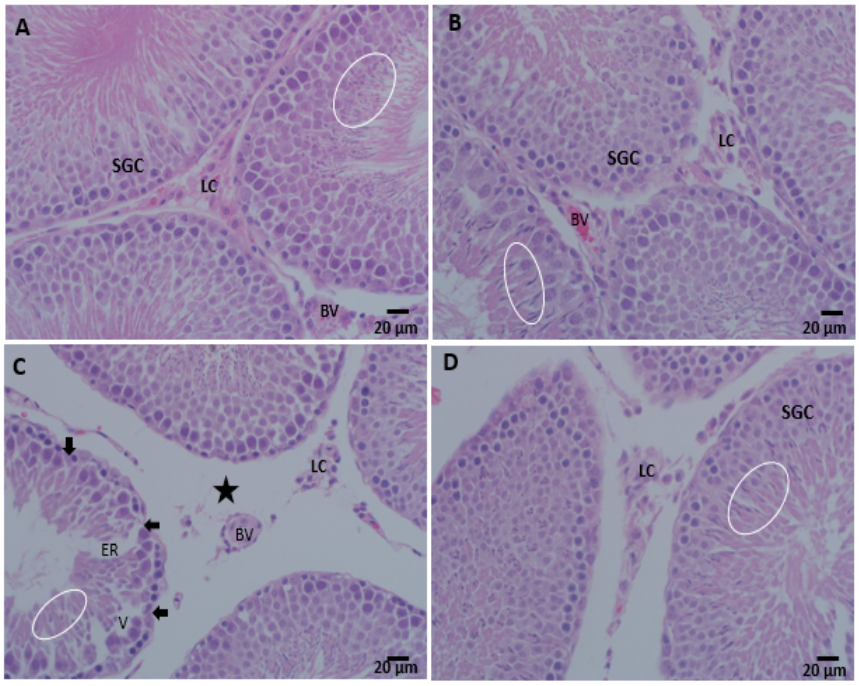

Fig. 2: Sections of the treated testes showing the various cell types.

Groups A and B: increased number of Leydig cells (LC), spermatozoa (SPZ), blood vessels (BV) and intact spermatogenic cells (SGC). Group C: shows testicular interstitial sloughing (star) with fewer Leydig

cells (LC), sloughing of germ cells (ER) and seminiferous tubules basement membrane disintegration (arrow-head) with fewer number of elongated spermatid (circle) and testicular vacuolations (V). Group D: shows normal elongated spermatids, spermatogenic cells (SGC) and sIn Fig 3., the seminiferous tubules that housed the spermatogenic cells and Sertoli cells in the control and MLT-exposed rats were intact with the spermatogonia found at the basement membrane in close opposition with Sertoli cells (Fig. 3). The BPA induced pyknotic nuclei formation and Sertoli cell cytoplasmic processes dissolution in-cluding testicular vacuolations, germinal cells sloughing, and distortion of the seminiferous tubules' basement membrane (Fig. 3). At higher magnpermatozoa (SPZ). A = Control, B = MLT exposed, C = BPA exposed, and D = BPA + MLT exposed. Scale bar = 20µm (H & E).

3.2. Transmission Electron Microscope (TEM) of the testes of treated rats

Identification, numerous mitochondria and lipid droplets in the Sertoli cells cytoplasm were observed in the control and MLT-exposed groups (Fig. 4). In the co-treated MLT and BPA group, MLT reversed the effect of BPA to reflect the observations seen in the control group (Fig. 4).

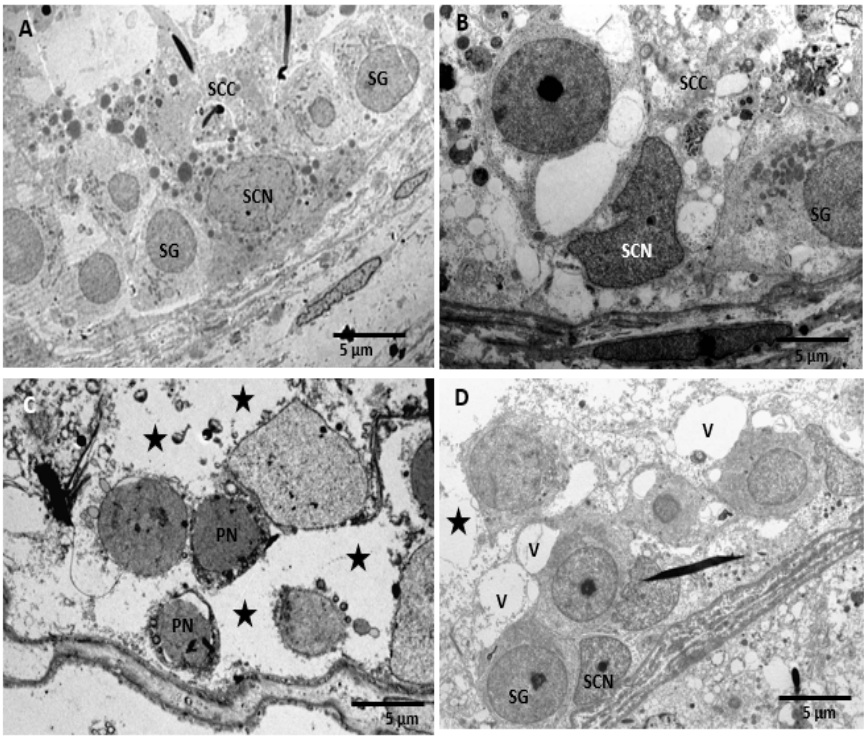

Fig. 3. Transmission Electron Microscopy sections of the seminiferous tubules of treated rats

Groups A and B showed intact spermatogonia (SG), Sertoli cell nucleus (SCN) and its cytoplasm (SCC), Group C: shows deranged basement membrane of the seminiferous tubules, pyknotic nucleus (PN) with se-vere germinal cell loss and the lack of Sertoli cell cytoplasmic processes (star), Group D: MLT reversed the derangement induced by BPA. A = Control, B = MLT exposed, C = BPA exposed, and D = BPA + MLT exposed. Scale bar = 5 µm.

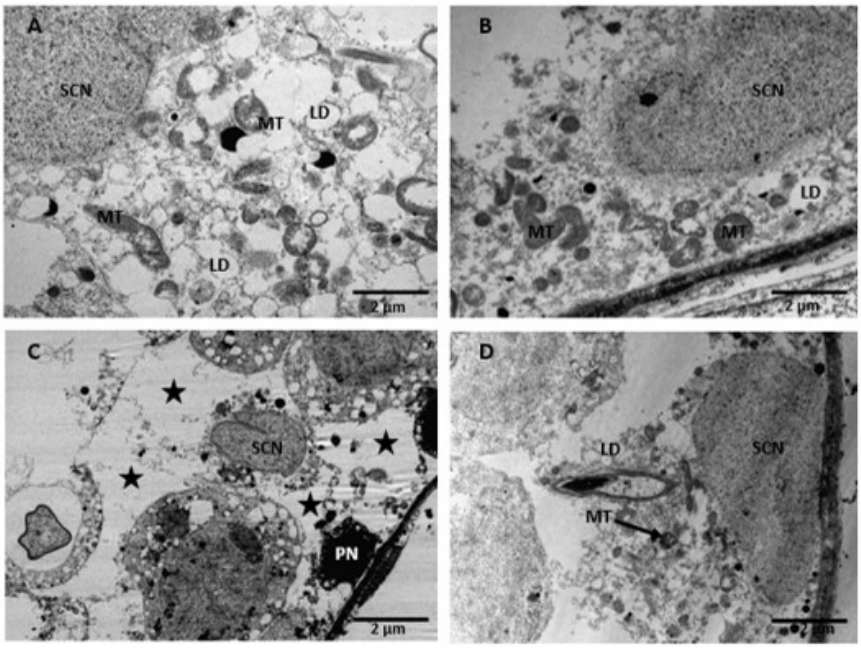

Fig. 4. Transmission Electron Microscopy sections of the Sertoli cells of treated rats.

Groups A and B displayed intact Sertoli cell nucleus (SCN) and Lipid droplets (LD) including numerous mitochondria (MT), Group C: there was a pyknotic nucleus of the Sertoli cells, Group D: the mitochondria (MT), lipid droplets (LD) and Sertoli cell nucleus (SCN) were intact. A = Control, B = MLT exposed, C = BPA exposed, and D = BPA + MLT exposed. Scale bar = 2µm

Fig. 5 shows an intact testicular interstitial of the control and MLT-exposed rats, with Leydig cells having no pathologic nucleus and cytoplasm, blood vessels, and lipid droplets. The TEM sections showed that BPA caused severe sloughing of the testicular interstitial with reduced Leydig cells which contained nuclei with no visible cytoplasm (Fig. 5). This was reversed in the BPA+MLT-exposed group (Fig. 5).

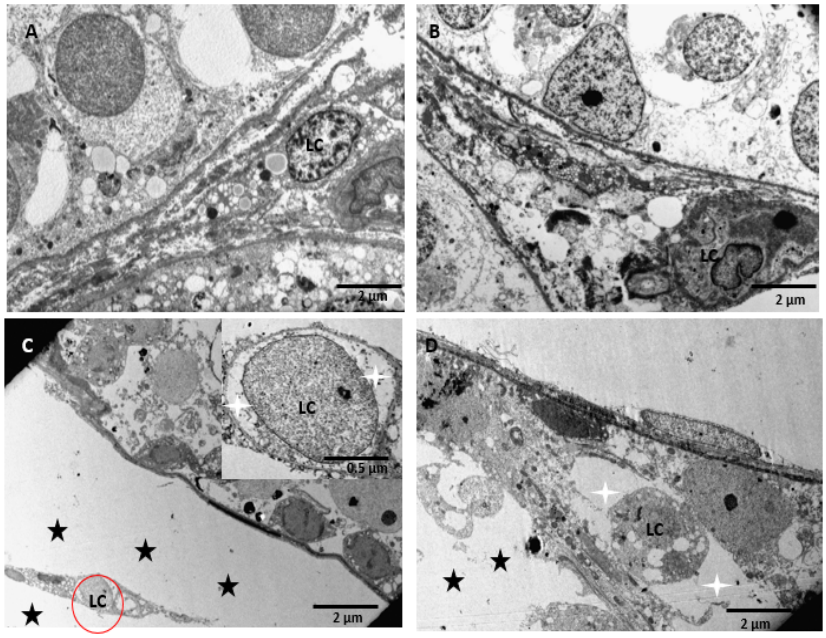

Fig. 5. Transmission Electron Microscopy sections of the Leydig cells of treated rats.

Groups A and B show no visible lesion of the Leydig cells (LC), Group C: shows Leydig cells (LC) having a dissolution of the cytoplasm and loss (star) of the interstitial (see Inset, Scale bar = 5μm), Group D: shows intact (arrow) interstitial and Leydig cell (LC). A = Control, B = MLT exposed, C = BPA exposed, and D = BPA + MLT exposed. Scale bar = 2μm.

Fig. 6 shows that the control and MLT-exposed groups present with intact and round spermatids possessing normal acrosomal vesicles and granules and cytoplasm containing abundant mitochondria. There were round spermatids with deranged acrosomal vesicles and a lack of granules and mitochondria in the BPA-exposed group (Fig 6.). This was reversed in the BPA+MLT-exposed group (Fig. 6).

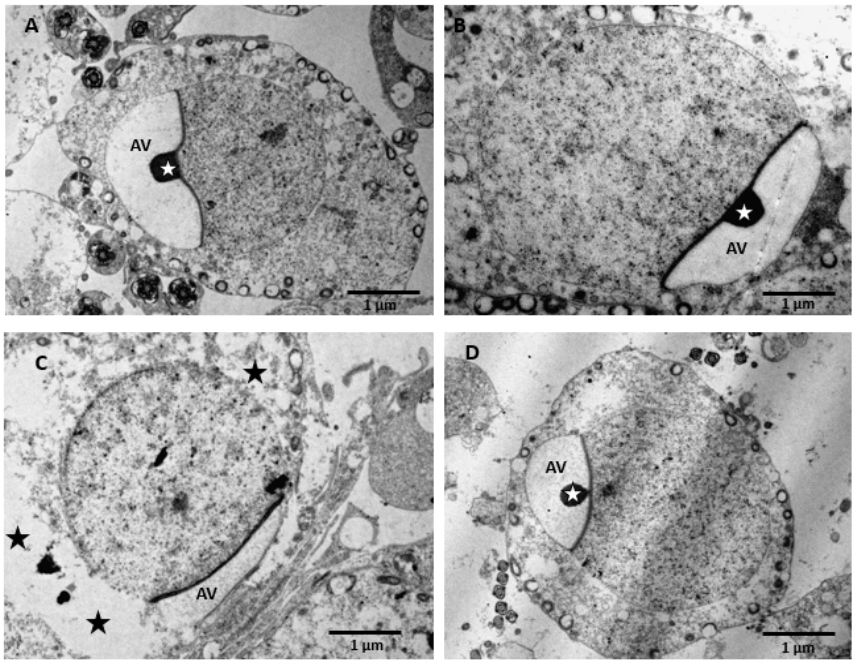

Fig. 6. Transmission Electron Microscopy sections of the acrosomal vesicle of treated rats.

Groups A and B: present an intact acrosomal vesicle (AV) and granule (star) with several mitochondria, Group C: presents a deranged acrosomal vesicle (AV) and reduced spermatid cytoplasm content (star), Group D: intact acrosomal vesicle (AV) and granule (star) with abundant mitochondria. A = Control, B = MLT exposed, C = BPA exposed, and D = BPA + MLT exposed. Scale bar = 1μm**.**

In Fig. 7, there was nuclear condensation and Sertoli cell cytoplasmic processes surrounding the elongated spermatids of the control and MLT-exposed rats. Conversely, the elongated spermatids showed karyorrhexis and dissolved Sertoli cell cytoplasmic processes in the BPA-exposed rats (Fig. 7). However, these lesions were reversed in the BPA+MLT-exposed group (Fig. 7).

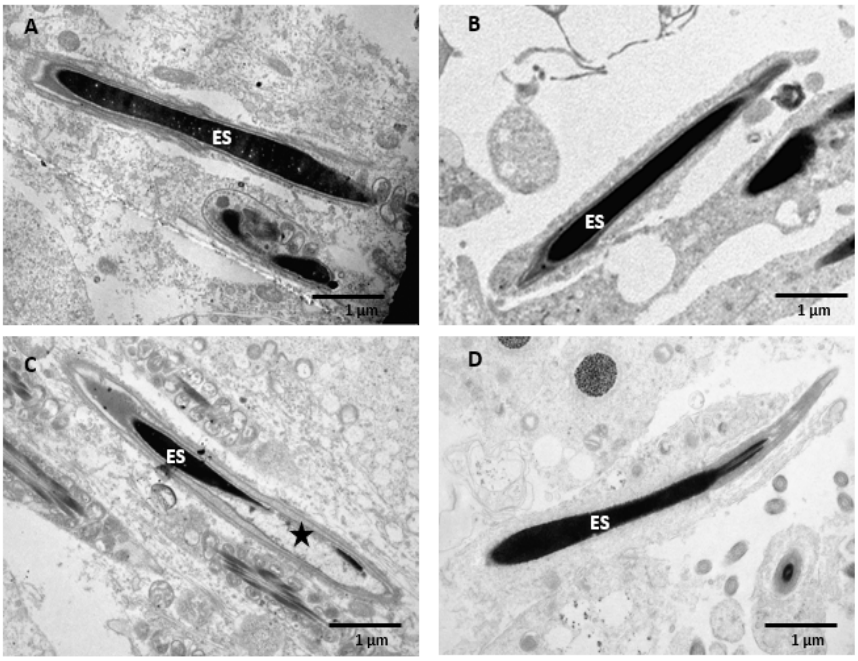

Fig. 7: Transmission Electron Microscopy sections of the spermatids of treated rats.

Groups A and B showed intact spermatid (ES), Group C: showed karyorrhexis (star) of elongated spermatid (ES), and Group D: shows elongated spermatid having normal nuclei. A = Control, B = MLT exposed, C = BPA exposed, and D = BPA + MLT exposed. Scale bar = 1 µm.

Fig. 8 revealed the 9+2 axoneme arrangement of the flagellar apparatus of spermatozoa in the control and MLT-exposed rats and a distortion of the 9+2 axoneme arrangement in the BPA-exposed rats (Fig. 8). However, there was a restoration of the 9+2 axoneme arrangement of flagellar apparatus of spermatozoa in the BPA+MLT exposed rats (Fig. 8).

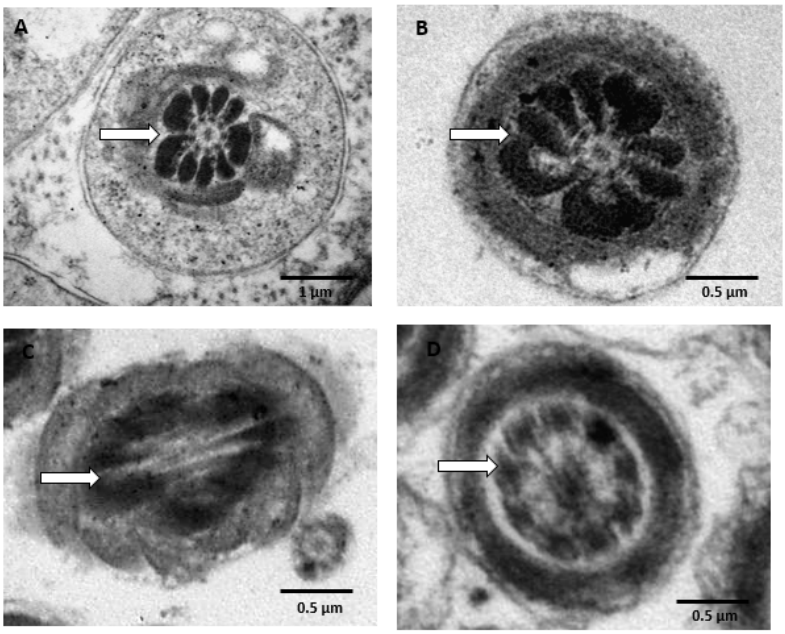

Fig. 8: Transmission Electron Microscopy transverse section of the Axoneme of Sperm cells.

Groups A and B showed an intact 9+2 Axoneme structure (white arrow), Group C: showed a deranged axoneme structure of the sperm cell, and Group D: showed an intact 9+2 Axoneme structure of the sperm cells. A = Control, B = MLT exposed, C = BPA exposed, and D = BPA + MLT exposed. Scale bar = 0.5 μm.

3.3. Immunostainings of the testes of treated rats

Table 1 shows the expression levels of alpha Smooth Muscle Actin (αSMA), S-100, and Vimentin (Vm) in the testes of rats exposed to the test samples. αSMA, S-100, and Vm proteins were significantly ($p<0.05$) downregulated in the BPA-exposed rats compared to the control (Table 1 and Figs. 9 to 10). There was no significant difference ($p>0.05$) in the expression level of the proteins between the control and MLT-exposed groups (Table 1 and Figs. 9 to 10). Although not significant, MLT enhanced the expression levels of αSMA, S-100, and Vm in the testes of the co-exposed rats (Table 1 and Figs. 9 to 10), especially at the Leydig cells, blood vessels, and peritubular membrane level (Figs. 9 to 10).

Table 1. Quantification of protein expression levels in the testes of treated rats

Proteins	**CONTROL**	**MLT**	**BPA**	**BPA+ML T**
αSMA (%)	8.85±0.55[a]	9.98±0.51[a]	4.48±0.37[b]	5.80±2.35[a]
S-100 (%)	4.72±0.51[a]	4.88±0.61[a]	3.40±0.01[b]	5.24±0. 26[a]
Vm (%)	7.87±1.57[a]	7.35±1.16[a]	4.39±1.13[b]	4.68±0.25[a]

Each result represents value of mean ± standard deviation. Values with similar superscript 'a' and 'b' within rows are significantly ($p<0.05$) different.

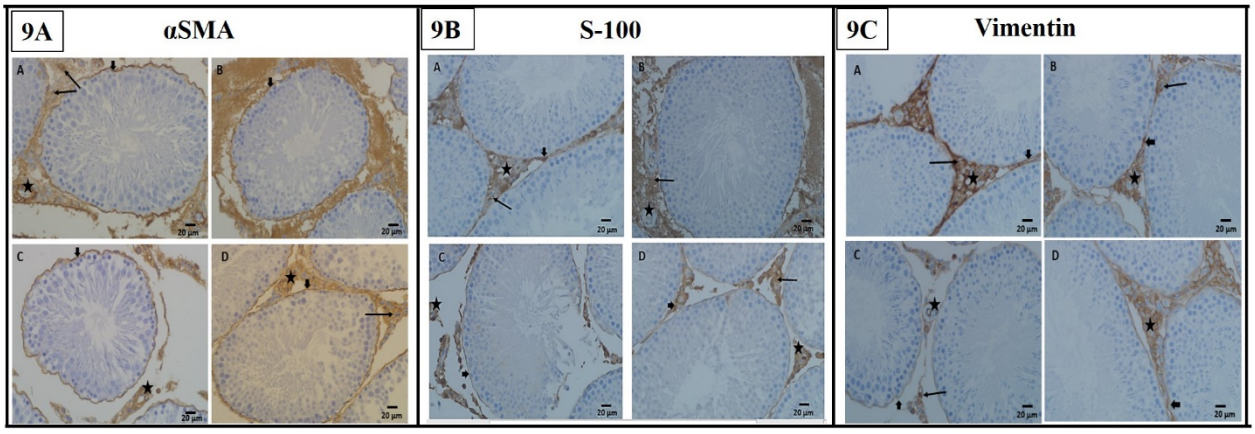

Fig. 9: Immunostaining for αSMA, S-100, and Vimentin proteins in the testes of treated rats.

In 9A, Groups A and B show higher immunopositivity for αSMA, especially at the basement membrane and blood vessels; αSMA immunopositivity was reduced at the basement membrane (arrowhead) and blood vessel (star) in Group C, Group D showed enhanced αSMA immunopositivity at the basement membrane (arrowhead) and blood vessel (star).

Similarly, in 9B, S-100 immunopositivity was pronounced in the Leydig cells (arrow), blood vessels (star), and peritubular membrane (arrowhead) of Groups A and B. S-100 reduced in intensity in Group C at the peritubular membrane (arrowhead) and blood vessel (star). Group D showed enhanced S-100 immunopositivity in

the peritubular membrane (arrowhead) and Leydig cells (star). In 9C, Vimentin expression was observed in the blood vessels and Leydig cells of rats in Groups A and B. Group C showed a reduction in vimentin staining intensity. Group D showed improved vimentin staining intensity in the blood vessels and peritubular membrane. A = Control, B = MLT exposed, C = BPA exposed, and D = BPA + MLT exposed. Scale bar = 20μm.

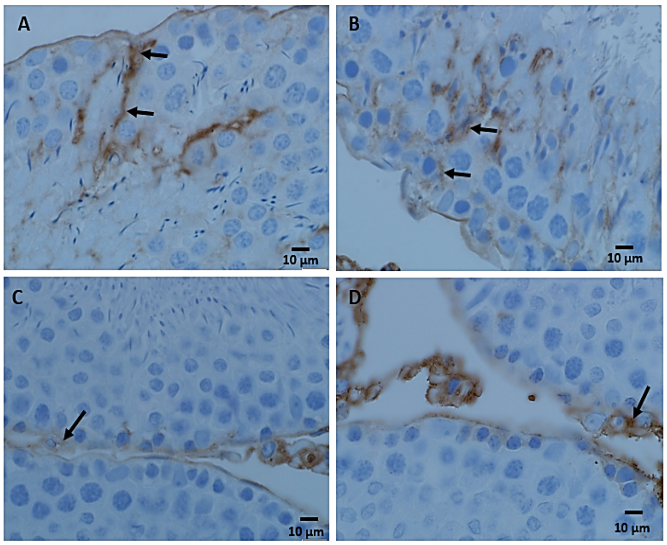

Fig. 10: Immunostaining for Vimentin in the testes of treated rats at higher magnification. Groups A and B showed vimentin-positive-Sertoli cells, Group C: shows a significant reduction in vimentin expression in the Sertoli cell level, and Group D: shows an improved vimentin expression. A = Control, B = MLT exposed, C = BPA exposed, and D = BPA + MLT exposed. Scale bar = 10μm.

4. Discussion

Bisphenol A was described as an endocrine-disrupting chemical which alters normal reproductive function [12]. [24] reported that the exposure of rats to Bisphenol A results in a decrease in sperm motility, which may be due to an increase in reactive oxygen species level. In addition, in a study by [11], the exposure of BPA at a concentration of 50 μM was associated with early DNA damage responses and perturbed cytoskeleton in the C18–4 spermatogonia cell line, further emphasizing the reproductive toxicity of BPA. We have seen in this study that exposure of rats to 10 mg/kg BPA for 45 days is capable of causing testicular dysfunction, which could subsequently precipitate infertility.

The histological assessment of the testes in the current study showed that exposure of rats to BPA caused testicular damage, including a reduction in germ cell number (Figs. 1 to 2). This reflects the capability of BPA to alter spermatogenesis in rats with an attendant effect on reproductive function. This corroborates the findings of [25], who exposed mice to graded doses of BPA. Some reports on the role of BPA in the reproductive performances of male rats have shown that bisphenol A impaired male fertility. Bisphenol A causes testicular dysfunctions, including induction of death of testicular germ cells, disruption of the junctional proteins of the blood-testis barrier, and distortion in androgen binding protein and steroidogenic enzymes levels [8, 9, 25, 26, 27, 28]. The morphological injuries in the testes induced by BPA in our study (Figs. 3 to 8) are similar to the previous reports in the prostate gland, adrenal gland, and cardio-renal system [22, 38, 39]. Other

studies further corroborate the observed BPA-induced histological derangement in the testes. However, the experimental animal model used was mice, with higher doses, and for longer periods [9, 25].

Several proteins, such as α-SMA, S-100, and Vm, are relevant biomarkers for investigating the reproductive toxicity of BPA and were used in this study. In this study, the administration of bisphenol A was associated with the downregulation of α-SMA, S-100, and Vm in the testes of male Wistar rats (Fig. 9 to 10). This finding aligns with the findings of [29], who reported a decrease in vimentin and SMA expression in the mammary glands of rats prenatally exposed to BPA. [22] also reported a decreased localization of α-Smooth muscle actin, vimentin, and S100 proteins in the prostate of BPA-exposed rats. This multi-reproductive organ toxic effect of BPA presents a significant reproductive implication.

S-100 belongs to the Ca^{2+} binding protein subfamily which has been reported to play a significant role in motility chemotaxis, and secretion in living systems [30]. Both S-100 and α-SMA have been widely considered biologically active proteins of the male reproductive organ. They possess functional relevance in absorption, secretion and contractile activities [31]. Similarly, Vimentin is a type III intermediate filament which maintains the structural integrity and mechanical resilience of cells and assists in keeping normal differentiating germ cell morphology [32]. The downregulation of these proteins in the testes of male Wistar rats by BPA could imply an impaired testicular secretion. This might also be associated with reduced sperm motility, as suggested by [22]. Since these proteins play a tremendous role in structural integrity, their downregulation is also a suggestion of the susceptibility of the testes to cellular damage. According to [33], α-SMA, once downregulated, might result in impaired smooth muscle function, which could compromise sperm transport and reduce overall reproductive efficiency.

However, melatonin demonstrated a therapeutic effect on the testes of the rats by upregulating the expression of α-SMA, S-100, and Vm (Figs. 9 to 10). Melatonin has been previously reported to possess antioxidative properties, making it a potential therapeutic agent in numerous pathological conditions. [14] reported that melatonin functions by forming a chelate with transition metals, which are involved in the Fenton/Haber-Weiss reactions. As a result, this prevents the formation of hydroxyl radicals, which play a significant role in oxidative stress. [34] also reported that melatonin directly scavenges free radicals and exhibits anti-inflammatory properties.

The upregulation of α-SMA, S-100, and Vm in the testes of male Wistar rats by melatonin was in alignment with the findings of [22], who reported a modulating effect of melatonin through the upregulation of vimentin, S-100, and α-smooth muscle actin. In addition, [9] have previously reported the therapeutic effect of melatonin in alleviating testicular damage caused by BPA. Therefore, melatonin could play a significant role in enhancing tissue integrity and cellular function. The upregulation of vimentin by melatonin in the testes of rats in this study could indicate its protective effect on the structural framework of the testes and epididymis, potentially stabilizing the cytoskeleton and promoting tissue repair or preservation [35].

Furthermore, S-100 has been reported to be involved in the inflammatory response [30], and its upregulation by melatonin could indicate the potential of melatonin to reduce oxidative stress and inflammatory damage implicated in impaired testicular and epidydimal function. Lastly, since melatonin upregulated the expression of α-SMA, melatonin could play a crucial role in regulating smooth muscle contraction needed for

sperm transport and general reproductive health [36]. The coadministration of both bisphenol A and melatonin was associated with the upregulation of vimentin, S-100, and α-smooth muscle actin in the testes of male Wistar rats. This suggests that melatonin can efficiently counteract the reproductive toxicity presented by bisphenol A, a finding supported by the report of [37].

Conclusions

We have reported that long-term exposure to low-dose BPA causes histological changes in the testes and downregulation of α-smooth muscle actin, S-100, and vimentin. The study has also demonstrated the ability of MLT to protect against BPA-induced testicular dysfunctions. Hence, MLT could be a therapeutic agent in preventing BPA-mediated male reproductive organ damage.

Authors Contributions

Conceptualization, O.S.A. S.G.O. and M.O.O; Methodology, O.S.A. S.G.O. and M.O.O; Software, O.S.A. and E.S.S.; Validation, O.S.A. S.G.O. M.O.O. and E.S.S.; Formal analysis, O.S.A. and E.S.S.; Investigation, O.S.A. S.G.O. and M.O.O.; Resources, O.S.A. S.G.O. and M.O.O.; Data curation, O.S.A.; Writing-original draft preparation, O.S.A. and E.S.S.; Writing-review and editing, O.S.A. S.G.O. M.O.O. and E.S.S.; Visualization, O.S.A. S.G.O. M.O.O. and E.S.S.; Supervision, S.G.O. and M.O.O.

Conflict of Interest

Authors declared none.

References

1. Sokan-Adeaga AA, Sokan-Adeaga MA, Sokan-Adeaga ED, Oparaji AN, Edris H, Tella EO, Balogun FA, Aledeh M, Amubieya OE. Environmental toxicants and health adversities: A review on interventions of phytochemicals. J Public Health Res. **2023** Jun 29;12(2):22799036231181226. doi: 10.1177/22799036231181226
2. Cimmino I, Fiory F, Perruolo G, Miele C, Beguinot F, Formisano P, Oriente F. Potential Mechanisms of Bisphenol A (BPA) Contributing to Human Disease. Int J Mol Sci. **2020** Aug 11;21(16):5761. doi: 10.3390/ijms21165761.
3. Manzoor MF, Tariq T, Fatima B, et al. An insight into bisphenol A, food exposure and its adverse effects on health: A review. *Front Nutr*. **2022**;9:1047827. doi:10.3389/fnut.2022.1047827
4. Stavridis K, Triantafyllidou O, Pisimisi M, Vlahos N. Bisphenol-A and Female Fertility: An Update of Existing Epidemiological Studies. J Clin Med. **2022** Dec 5;11(23):7227. doi: 10.3390/jcm11237227.
5. Presunto M, Mariana M, Lorigo M, Cairrao E. The Effects of Bisphenol A on Human Male Infertility: A Review of Current Epidemiological Studies. Int J Mol Sci. **2023** Aug 4;24(15):12417. doi: 10.3390/ijms241512417.
6. Cariati F, D'Uonno N, Borrillo F, Iervolino S, Galdiero G, Tomaiuolo R. "Bisphenol a: an emerging threat to male fertility". Reprod Biol Endocrinol. 2019 Jan 20;17(1):6. doi: 10.1186/s12958-018-0447-6.
7. Shamhari A'A, Abd Hamid Z, Budin SB, Shamsudin NJ, Taib IS. Bisphenol A and Its Analogues Deteriorate the Hormones Physiological Function of the Male Reproductive System: A Mini-Review. *Biomedicines*. **2021**,9(11):1744. doi.org/10.3390/biomedicines9111744
8. Walke G, Gaurkar SS, Prasad R, Lohakare T, Wanjari M. The Impact of Oxidative Stress on Male Reproductive Function: Exploring the Role of Antioxidant Supplementation. Cureus. **2023** Jul 27;15(7):e42583. doi: 10.7759/cureus.42583.

9. Qi Q, Yang J, Li S, Liu J, Xu D, Wang G, Feng L, Pan X. Melatonin alleviates oxidative stress damage in mouse testes induced by bisphenol A. Front Cell Dev Biol. **2024** Feb 19;12:1338828. doi: 10.3389/fcell.2024.1338828.
10. Pivonello C, Muscogiuri G, Nardone A, Garifalos F, Provvisiero DP, Verde N, de Angelis C, Conforti A, Piscopo M, Auriemma RS, Colao A, Pivonello R. Bisphenol A: an emerging threat to female fertility. Reprod Biol Endocrinol. **2020** Mar 14;18(1):22. doi: 10.1186/s12958-019-0558-8
11. Liang S, Yin L, Shengyang Yu K, Hofmann MC, Yu X. High-Content Analysis Provides Mechanistic Insights into the Testicular Toxicity of Bisphenol A and Selected Analogues in Mouse Spermatogonial Cells. Toxicol Sci. **2017** Jan;155(1):43-60. doi: 10.1093/toxsci/kfw178.
12. Hafezi SA, Abdel-Rahman WM. The Endocrine Disruptor Bisphenol A (BPA) Exerts a Wide Range of Effects in Carcinogenesis and Response to Therapy. Curr Mol Pharmacol. **2019**;12(3):230-238. doi: 10.2174/1874467212666190306164507
13. Gelen V, Şengül E, Kükürt A. An Overview of Effects on Reproductive Physiology of Melatonin [Internet]. Melatonin - Recent Updates. IntechOpen; **2022**. doi.org/10.5772/intechopen.108101.
14. Reiter RJ, Mayo JC, Tan DX, Sainz RM, Alatorre-Jimenez M, Qin L. Melatonin as an antioxidant: under promises but over delivers. J Pineal Res. **2016** Oct;61(3):253-78. doi: 10.1111/jpi.12360. Epub 2016 Sep 1. PMID: 27500468.
15. Yong W, Ma H, Na M, Gao T, Zhang Y, Hao L, Yu H, Yang H, Deng X. Roles of melatonin in the field of reproductive medicine. Biomed Pharmacother. **2021** Dec;144:112001. doi: 10.1016/j.biopha.2021.112001.
16. Monteiro KKAC, Shiroma ME, Damous LL, Simões MJ, Simões RDS, Cipolla-Neto J, Baracat EC, Soares-Jr JM. Antioxidant Actions of Melatonin: A Systematic Review of Animal Studies. Antioxidants (Basel). **2024** Apr 7;13(4):439. doi: 10.3390/antiox13040439.
17. Hao EY, Chen H, Wang DH, Huang CX, Tong YG, Chen YF, Zhou RY, Huang RL. Melatonin regulates ovarian function and enhances follicle growth in aging laying hens via activating the mammalian target of rapamycin pathway. *Poultry Science,* **2020**;99(4), 2185–2195. https://doi.org/10.1016/j.psj.2019.11.040.
18. Oladele CA, Akintayo CO, Badejogbin OC, Oniyide AA, Omoaghe AO, Agunbiade TB, Olaniyi KS. Melatonin ameliorates endocrine dysfunction and defective sperm integrity associated with high-fat diet-induced obesity in male Wistar rats. Andrologia. **2022** Feb;54(1):e14242. doi: 10.1111/and.14242.
19. Anjum S, Rahman S, Kaur M, Ahmad F, Rashid H, Ansari RA, Raisuddin S. Melatonin ameliorates bisphenol A-induced biochemical toxicity in testicular mitochondria of mouse. Food and chemical toxicology. **2011** Nov 1;49(11):2849-54.
20. El-Beshbishy HA, Aly HA, El-Shafey M. Lipoic acid mitigates bisphenol A-induced testicular mitochondrial toxicity in rats. Toxicology and industrial health. **2013** Nov;29(10):875-87.
21. Creasy DM. Evaluation of testicular toxicology: a synopsis and discussion of the recommendations proposed by the Society of Toxicologic Pathology. Birth Defects Res B Dev Reprod Toxicol. **2003** Oct;68(5):408-15. doi: 10.1002/bdrb.10041. PMID: 14745990
22. Olukole SG, Ajani SO, Ola-Davies EO, Lanipekun DO, Aina OO, Oyeyemi MO, Oke BO. Melatonin ameliorates bisphenol A-induced perturbations of the prostate gland of adult Wistar rats. Biomedicine & Pharmacotherapy = Biomedecine & Pharmacotherapie. **2018**,105:73-82. DOI: 10.1016/j.biopha.2018.05.125.

23. ElGhamrawy TA, Helmy D, Elall HF. Cadherin and vimentin immunoexpression in the testis of normal and induced infertility models of albino rats. Folia Morphol (Warsz). **2014** Aug;73(3):339-46. doi: 10.5603/FM.2014.0050.
24. Minamiyama Y, Ichikawa H, Takemura S, Kusunoki H, Naito Y, Yoshikawa T. Generation of reactive oxygen species in sperms of rats as an earlier marker for evaluating the toxicity of endocrine-disrupting chemicals. *Free Radical Research,* **2010**,*44*(12), 1398–1406.
25. Tian J, Ding Y, She R, Ma L, Du F, Xia K, Chen L. Histologic study of testis injury after bisphenol A exposure in mice. Toxicol Ind Health. **2017** Jan;33(1):36-45. doi: 10.1177/0748233716658579. Epub 2016 Sep 25.
26. Peretz J, Vrooman L, Ricke WA, Hunt PA, Ehrlich S, Hauser R, Padmanabhan V, Taylor HS, Swan SH, VandeVoort CA, Flaws JA. Bisphenol a and reproductive health: update of experimental and human evidence, 2007-2013. Environ Health Perspect. **2014** Aug;122(8):775-86. doi: 10.1289/ehp.1307728.
27. Wang C, Fu W, Quan C, Yan M, Liu C, Qi S, Yang K. The role of Pten/Akt signaling pathway involved in BPA-induced apoptosis of rat Sertoli cells. Environ Toxicol. **2015** Jul;30(7):793-802. doi: 10.1002/tox.21958. Epub 2014 Jan 25.
28. Durando M, Canesini G, Cocito LL, Galoppo GH, Zayas MA, Luque EH, Muñoz-de-Toro M. Histomorphological changes in testes of broad-snouted caimans (Caiman latirostris) associated with in ovo exposure to endocrine-disrupting chemicals. J Exp Zool A Ecol Genet Physiol. **2016** Jan;325(1):84-96. doi: 10.1002/jez.1999.
29. Ramos JG, Varayoud J, Kass L, Rodríguez H, Costabel L, Muñoz-De-Toro M, Luque EH. Bisphenol A induces both transient and permanent histofunctional alterations of the hypothalamic-pituitary-gonadal axis in prenatally exposed male rats. *Endocrinology,* **2003**, *144*(7), 3206–3215. https://doi.org/10.1210/en.2002-2202
30. Singh P, Ali SA. Multifunctional Role of S100 Protein Family in the Immune System: An Update. Cells. **2022** Jul 23;11(15):2274. doi: 10.3390/cells11152274.
31. Ibrahim ZH, Joshi D, Singh SK. Seasonal immunohistochemical reactivity of S-100 and α-smooth muscle actin proteins in the epididymis of dromedary camel, Camelus dromedarius. Andrologia. **2017** Aug;49(6). doi: 10.1111/and.12667.
32. Niazi-Tabar A, Azizi H, Hashemi Karoii D, Skutella T. Testicular Localization and Potential Function of Vimentin Positive Cells during Spermatogonial Differentiation Stages. Animals (Basel). **2022** Jan 22;12(3):268. doi: 10.3390/ani12030268.
33. Chen L, DeWispelaere A, Dastvan F, Osborne WR, Blechner C, Windhorst S, Daum G. Smooth Muscle-Alpha Actin Inhibits Vascular Smooth Muscle Cell Proliferation and Migration by Inhibiting Rac1 Activity. PLoS One. **2016** May 13;11(5):e0155726. doi: 10.1371/journal.pone.0155726.
34. Ahmad SB, Ali A, Bilal M, Rashid SM, Wani AB, Bhat RR, Rehman MU. Melatonin and Health: Insights of Melatonin Action, Biological Functions, and Associated Disorders. Cell Mol Neurobiol. **2023**;43(6):2437-2458. doi: 10.1007/s10571-023-01324-w.
35. Doğanay S, Budak Ö, Toprak V, Erman G, Şahin A. Protective role of melatonin against testicular damage caused by polymicrobial sepsis in adult rats. Ulus Travma Acil Cerrahi Derg. **2022** Jun;28(6):723-729. doi: 10.14744/tjtes.2021.90575.

36. Brozovich FV, Nicholson CJ, Degen CV, Gao YZ, Aggarwal M, Morgan KG. Mechanisms of Vascular Smooth Muscle Contraction and the Basis for Pharmacologic Treatment of Smooth Muscle Disorders. Pharmacol Rev. **2016** Apr;68(2):476-532. doi: 10.1124/pr.115.010652.
37. Santiago J, Silva JV, Santos MAS, Fardilha M. Fighting Bisphenol A-Induced Male Infertility: The Power of Antioxidants. Antioxidants (Basel). **2021** Feb 15;10(2):289. doi: 10.3390/antiox10020289.
38. Olukole SG, Lanipekun DO, Ola-Davies EO, Oke BO. Melatonin attenuates bisphenol A-induced toxicity of the adrenal gland of Wistar rats. Environ Sci Pollut Res Int. **2019** Feb;26(6):5971-5982. doi: 10.1007/s11356-018-4024-5.
39. Ola-Davies OE, Olukole SG. Gallic acid protects against bisphenol A-induced alterations in the cardio-renal system of Wistar rats through the antioxidant defense mechanism. Biomed Pharmacother. **2018** Nov;107:1786-1794. doi: 10.1016/j.biopha.2018.08.108.

CVJ CLUJ VETERINARY JOURNAL

Article

Antiviral Activity of *Lagenaria breviflora* Roberts Fruit Against *Canine Parvovirus* in Embryonated Chicken Egg

Blessing Ayeni [1], Tolulope Olakojo* [1] , Oluwasanmi Aina[2], Olawale Ola[3], Olusegun Fagbohun[4], and Olayinka Oridupa[1]

[1] Department of Veterinary Pharmacology and Toxicology, University of Ibadan
[2] Department of Veterinary Anatomy, University of Ibadan
[3] Department of Veterinary Pathology, University of Ibadan
[4] Department of Veterinary Microbiology, University of Ibadan
* Correspondence: mailintolulope@gmail.com; Tel.: (+234 8078495289)

Abstract: *Lagenaria breviflora* has been traditionally utilized as a natural remedy for various diseases including measles, smallpox, human chickenpox and Newcastle disease in poultry, as well as parasitic infections caused by *Eimeria*s pp and *Ascaridia galli.* This study investigated the antiviral potential of *L. breviflora* fruit methanol extract against Canine Parvovirus using experimentally infected 10-day old embryonated chicken eggs. The eggs were apportioned to 11 groups (n=5) with Group 1 serving as control, while Group 2 remained inoculated with the virus only. Group 3 and 4 received only *L. breviflora* extract (25mg/ml and 50mg/ml), while Groups 5-11 were inoculated with the virus and graded concentrations of *L. breviflora* extract (1.5625mg/ml to 100mg/ml) respectively. Gross and histological changes were assessed 24h post-inoculation. The results revealed significant pathologies such as congealed mass of embryo tissue with disruption of membrane and neuronal layer arrangement, haemorrhage, distorted membranes and necrosis in the untreated infected embryos consistent with Canine Parvoviral infection. Embryos treated with the extract, particularly at concentrations of 3.125-12.5mg/ml, exhibited significantly reduced pathognomonic signs of Canine Parvo Enteritis, presented as slight haemorrhage and blood vessel congestion. Eggs inoculated with higher concentrations (25-100mg/ml) showed signs of toxicity reflected as severe congestion, degeneration and necrosis. This study therefore concluded that the methanol extract of *L. breviflora* fruit at low concentrations demonstrated antiviral activity against Canine Parvovirus, inhibiting virus growth and degenerative pathologies in embryonated chicken eggs. Concentrations >12.5mg/ml was embryotoxic.

Keywords: Canine Parvovirus, Embryonated Chicken Eggs, Inoculation, *Lagenaria breviflora*.

Received: 13.12.2024
Accepted: 14.04.2025
Published: 15.07.2025

DOI:10.52331/v30i2728

1. Introduction

Canine Parvovirus (CPV) remains a significant enteric virus infecting domesticated and feral breeds of dogs globally. It is a fatal virus that spreads rapidly, causing severe morbidity and high mortality in Canines [1]. Early presentation and treatment are significant determinants of the survival rates, which may be up to 95% if treated early and as low as about 9% when presented late or not treated [2]. Usually, unvaccinated dogs, especially puppies and those with low maternal immunity or poor management conditions, are more susceptible to the infection [3]. Most dog owners are well-informed about the vaccination protocols against this virus, and affordability has not been challenging.

The virus species is classified within *Parvoviridae*, subfamily *Parvovirinae*, and genus *Protoparvovirus,* a virus family known for its high pathogenicity [4,5]. Despite the knowledge of the circulation of canine parvovirus subtypes in Nigeria and routine vaccination of dogs, some vaccinated dogs still come down with Canine Parvoviral Enteritis (CPE). The polyvalent vaccine DHLPP (Distemper Hepatitis Leptospirosis

Parvovirus Parainfluenza) for dog vaccination against CPV in Nigeria is mainly adopted. The CPV subtype in most vaccines is either the wild-type CPV or CPV-2b [6].

These may cause the outbreak of the disease in vaccinated dogs since vaccination of puppies with heterologous subtypes of the virus has been shown to yield a lower antibody titer than the homologous virus [7]. As such, some commercial CPV vaccines that contain only one or two subtypes or wild-type CPV do not confer significant immunity against CPV. Moreover, CPV-2a, the most prevalent serotype of CPV in Nigeria, has been reported as preponderant, despite the surge in the CPV-2c serotypes recorded lately [2].

Vaccine break or low immunity leads to full-blown CPE, which clinically presents with hemorrhagic diarrhoea and vomiting. Severe intestinal crypt cell damage, erosion of enteric blood vessels and massive haemorrhage in the gastrointestinal tract are sequels of the viral invasion of cells [2]. Host cells undergo cell cycle arrest, apoptosis and necrosis of intestinal crypt cells [8]. Supportive care is the primary therapeutic protocol adopted, focusing on mitigating diarrhoea and vomiting. Lost electrolytes are restored via fluid therapy, and antibiotics are administered to treat opportunistic secondary bacterial infections. Other supportive care is given based on clinical signs observed [9]. However, the economic implication of therapy is usually very high with extensive days of treatment [10,11].

From the foregoing, developing alternative therapies from affordable and available sources within the environment is pertinent. Due to viral resistance, viral latency, and contradictory efficacy in recurrent infection of susceptible populations, developing antiviral medicines, mainly, has been challenging [12]. The outbreaks of viral diseases have been on a rampage within animal populations globally, with incidences of emerging and re-emerging virulent virus strains [13]. Therefore, it is vital to prioritize discovering new antiviral agents, especially those that can ameliorate the cytopathic effects of the virus.

Medicinal plants are potential sources for discovering remedies for various disease pathogens, including viruses. One such plant is *Lagenaria breviflora* Roberts (Family Cucurbitaceae), a plant reported to have demonstrated antiviral activities against Newcastle disease and measles viruses [14,15]. It is a perennial climber that grows in the wild in tropical Africa, mounting up the forest canopy and occupying the regions from Senegal to West Cameroons. The fruits have been reportedly used in folkloric medicine for prophylaxis and viral infection therapy, including measles, smallpox, human chickenpox, and Newcastle disease in poultry [5,16]. Previous reports have also documented its anti-ulcerogenic [17], haematinic and immunostimulatory [18], antidiarrhoiec and intestinal smooth muscle relaxant effects [19].

Therefore, in the quest to discover alternative therapies for CPE, this study investigated the antiviral potential of *L. breviflora* Roberts' whole fruit against CPV in embryonated chicken eggs.

2. Materials and Methods

2.1. Preparation of viral inoculum

The viral inoculum was prepared from a diarrheic faecal sample collected from a dog diagnosed with canine parvovirus (CPV) infection at the Veterinary Teaching Hospital, University of Ibadan. The sample was stored at −80°C until processing immediately. Viral presence was confirmed using an immunochromatographic test kit (BioNote, Inc., Gyeonggi, Republic of Korea; Catalog No. VCHECK® CPV Ag), following the manufacturer's instructions. A sterile viral transfer medium (VTM) was prepared by combining 500 mL glycerol (Sigma-Aldrich, St. Louis, MO, USA; Catalog No. G5516), 600 mg penicillin (Sigma-Aldrich; Catalog No. P3032), 5 g streptomycin (Sigma-Aldrich; Catalog No. S9137), 280 mg gentamycin (Sigma-Aldrich; Catalog No. G1272), and 100 mg amphotericin B (Sigma-Aldrich; Catalog No. A2942) in a 500 mL sterile bottle. The pH was adjusted to 7.2 using 1M NaOH (Sigma-Aldrich; Catalog No. S8045) and verified with a calibrated pH meter (Hanna Instruments, HI2211).

For sample processing, 1 g of faecal sample was suspended in 500 µL of VTM and vortexed (Scientific Industries Vortex Genie 2) for 2 min at maximum speed. The suspension was centrifuged at 6,000 × g for 15 min at 4°C (Eppendorf Centrifuge 5810R, rotor F-45-30-11). The supernatant was filtered through a 0.22 µm pore-size syringe filter (Millex®-GP, Millipore, Bedford, MA, USA; Catalog No. SLGP033RB)

under laminar flow to remove bacterial contaminants. The labelled CPV inoculum filtrate was aliquoted into 1.5 mL sterile microcentrifuge tubes (Eppendorf) and stored at −20°C until use.

2.2. Quantification of viral inoculum using spectrometry

Concentration of viral particle was estimated as described by Maizel *et al.* (1968) with a slight modification [20], and optical density of 1.00 AU (1cm pathlength) at 260nm, matching 1.1 x 10^{12} viral particles/mL was considered appropriate. Absorbance unit at 260nm and 320nm were determined from the spectrometric measurement using a NanoDrop™ 2000 spectrophotometer (Thermo Fisher Scientific). Corrected values of A260 absorbance were computed by subtracting the obtained values (A260 – A320) and then, the virus concentration for each of the inoculation hours was calculated using the expression:

Virus concentration [vir/mL] = corrected A260 × 1.1×10^{12}

-A260 represent the optical density at 260nm.

-A320 represent the optical density (background and scatter correction) and

-1.1×10^{12} is the number of virus particles per mL per 1 AU at 260nm.

2.3. Preparation of Lagenaria breviflora Extract

Fresh fruits of *L. breviflora* (40–50 balls) were harvested from the Teaching and Research Farm, University of Ibadan, Nigeria. A taxonomist confirmed Botanical identification, and a voucher specimen (Voucher No. LB-2023-001) was deposited at the Herbarium, Department of Botany, University of Ibadan. The fruits were washed with distilled water, sliced into small cubes measuring approximately 1 cm × 1 cm × 1 cm (1 cm^3), and air-dried at 25°C for 48 h.

About extraction, 500 g of dried material was soaked in 2 L of 96% methanol (Sigma-Aldrich; Catalog No. 322415) in a glass amber bottle for 72 h at 25°C with occasional shaking. The mixture was filtered through Whatman No. 1 filter paper (GE Healthcare), and the filtrate was concentrated under reduced pressure at 40°C using a rotary evaporator (BUCHI R-300, Switzerland; water bath set at 40°C, vacuum pressure: 175 mbar). Residual methanol was removed by placing the extract in an oven (Memmert UN110) at 40°C for 24 h. The extract was neutralized to pH 7.0 by adding 0.2 mL of 1M NaOH per 10 mL of extract, then sterilized by filtration through a 0.45 μm microbial filter (Millipore) and stored in sterile amber bottles at 4°C.

The extract was reconstituted with an antibiotic solution containing Penicillin, Streptomycin, Gentamycin, and Amphotericin B (PSGA), and solutions were refrigerated for 1h at 4°C. Stock solution of 1000 mg/ml of the fruit extracts was diluted in PSGA to a working concentration of 250 mg/ml and further diluted to 200 mg/ml in PSGA. Further, 1:2 dilutions were made to achieve final extract concentrations of 100, 50, 25, 12.5, 6.25, 3.125, and 1.5625mg/ml. The extract was reconstituted with the virus inoculum (1:1) and cooled at 40C for 4 hours before introduction into embryonated eggs [19].

2.4. Experimental Design

Fertilized specific-pathogen-free (SPF) eggs were purchased from a commercial breeder (Amo Farm Sieberer, Ibadan, Oyo State). The eggs were disinfected with 70% ethanol, arranged in an egg crate, and subjected to incubation within a humidified incubator (G.Q.F Manufacturing Incubator) at 370C with the air sac facing upwards with 60% relative humidity.

On the eighth day of incubation, the eggs were candled to assess fertility. An egg was deemed fertile if a thin blood vessel leading to a bean-shaped embryo with visible eyes was observed while infertile eggs were sorted out and discarded.

On day 10, the eggs were randomly allocated into 11 groups (n = 5 eggs/group). Group 1 served as the uninoculated control (0.2 mL sterile PBS), while Group 2 received CPV inoculum only (0.2 mL). Groups 3 and 4 were inoculated with *L. breviflora* extract at 25 or 50 mg/mL, respectively. Groups 5, 6, 7, 8, 9, 10 and 11 were embryonated eggs inoculated with the virus-extract suspension containing graded concentrations of the extract, respectively: 100, 50, 25, 12.5, 6.25, 3.125, and 1.5625mg/ml to establish the antiviral effect of this plant extract. The eggs were drilled at the air sac, ending using a sterile 23-G needle for inoculation. Each egg received a volume of 0.2 ml of virus-extracted inoculum via the drilled hole into the chorioallantoic cavity. This was, afterwards, sealed with sterile paraffin wax.

The eggs were incubated for 24 h at 37°C and then chilled at 4°C to constrict chorioallantoic membrane (CAM) blood vessels. Post-chilling, the eggshells were cracked open, and the embryo with CAM was harvested aseptically. The gross pathologies were photographed and eventually fixed in 10% formalin for histopathology for 48 h [21].

Histopathology

The (CAM) tissue and embryo were fixed in formalin for 48 h, dissected and placed in labelled cassettes. These tissues underwent dehydration in increasing ethanol concentrations (70%, 90%, 100%), followed by xylene clearing to remove alcohol. They were then infiltrated with molten paraffin wax at 56°C, moulded, and solidified for microtome sectioning (Leica RM2235) at 5 μm thickness. Thin wax sections were stained with hematoxylin and eosin (H & E).

The staining process involved dewaxing in xylene, rehydration in decreasing alcohol concentrations, washing, staining, dehydration, and mounting in DPX. Finally, the slides were air-dried and examined microscopically with a microscope (Olympus BX53) at 100x and 400x magnification [22].

3. Results

3.1. Morphology and Gross Pathology

No visible lesions were observed in the uninoculated untreated embryos, the yolk sac, and albumin, while the inoculated untreated embryos presented as a congealed hemorrhagic mass. Embryos inoculated with CPV, treated with 1.562mg/ml and 3.125mg/ml of L. breviflora (LB) extract, showed whitish and cloudy albumin, respectively. A slight haemorrhage and congestion were equally observed at both concentrations. The group inoculated and treated with 6.25mg/ml of LB extract presented with slight congestion in some membranous vessels on the embryo, while inoculated embryos treated with 12.5mg/ml of LB extract showed a rounded embryo with severely congested membranous vessels and slightly cloudy albumin. Inoculated embryos treated with 25mg/ml and 50mg/ml showed haemorrhage and an edematous appearance within the embryo and membrane, mixed with a gelatinous yolk sac and albumin. There was severe congestion around the yolk sac and mild ecchymosis on the surface of embryos treated with 25mg/ml. The albumin of embryos treated with 50mg/ml of LB extract was clear with mild haemorrhage. Inoculated embryos treated with 100mg/ml of LB extract lost embryonic comma shape; the yolk sac and albumin had merged, with a yellow tinge of the yolk sac (Figure 3.1).

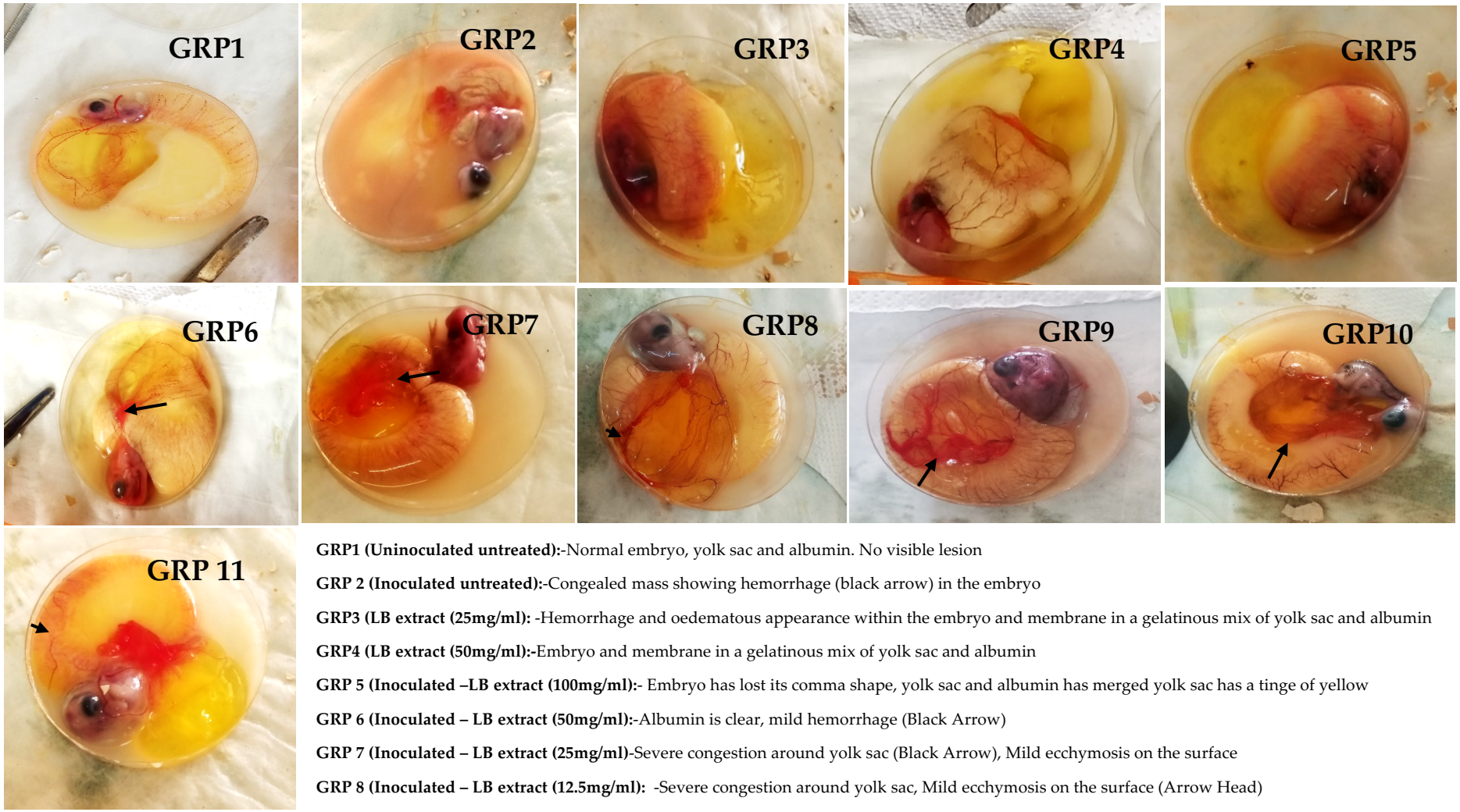

GRP1 (Uninoculated untreated):-Normal embryo, yolk sac and albumin. No visible lesion

GRP 2 (Inoculated untreated):-Congealed mass showing hemorrhage (black arrow) in the embryo

GRP3 (LB extract (25mg/ml): -Hemorrhage and oedematous appearance within the embryo and membrane in a gelatinous mix of yolk sac and albumin

GRP4 (LB extract (50mg/ml):-Embryo and membrane in a gelatinous mix of yolk sac and albumin

GRP 5 (Inoculated –LB extract (100mg/ml):- Embryo has lost its comma shape, yolk sac and albumin has merged yolk sac has a tinge of yellow

GRP 6 (Inoculated – LB extract (50mg/ml):-Albumin is clear, mild hemorrhage (Black Arrow)

GRP 7 (Inoculated – LB extract (25mg/ml)-Severe congestion around yolk sac (Black Arrow), Mild ecchymosis on the surface

GRP 8 (Inoculated – LB extract (12.5mg/ml): -Severe congestion around yolk sac, Mild ecchymosis on the surface (Arrow Head)

GRP 9 (Inoculated – LB extract (6.25mg/ml):-Slight congestion on some membranous vessels

GRP 10 (Inoculated – LB extract (3.125mg/ml): -Albumin is cloudy, slight congestion

GRP 11 (Inoculated – LB extract (1.5625mg/ml)-slight hemorrhage (Arrow head), Albumin is whitish

Figure 3.1: Gross pathology of chicken embryonated eggs inoculated with CPV and treated with L. breviflora whole fruit extract (X100)

3.2. Histopathology of Embryo Head

The membrane of the uninoculated-untreated embryo head was intact with normal integrity of parenchymatous cells. In contrast, the inoculated-untreated group showed a distorted membrane and disruption of neuronal layer arrangement. Embryos were inoculated but treated with 1.5625mg/ml of LB extract, which showed neuronal layer disruption and areas of spongiosis. Compared, extended cavernous spaces containing bloody spots were observed for inoculated-treated embryos at 3.125mg/ml. Inoculated-treated embryos with 6.25mg/ml of LB extract showed areas of mild blood accumulation. However, a relatively normal and parenchymatous cell membrane integrity was observed at 12.5mg/ml LB extract of inoculated-treated embryos. Inoculated embryos treated with 25mg/ml of LB extract presented as membrane-bound accumulation of blood and areas of spongiosis.

In contrast, the inoculated-treated group at 50mg/ml of LB extract maintained normal parenchymatous cell integrity. In addition, embryos treated with LB extract at 25mg/ml had focal points of severe necrosis in the parenchyma, while the group treated with 50mg/ml showed neuronal layer arrangement disruption. Finally, embryos inoculated and treated with 100mg/ml of LB extract revealed disruption of neuronal layer arrangement and a mild area of spongiosis (Figure 3.2).

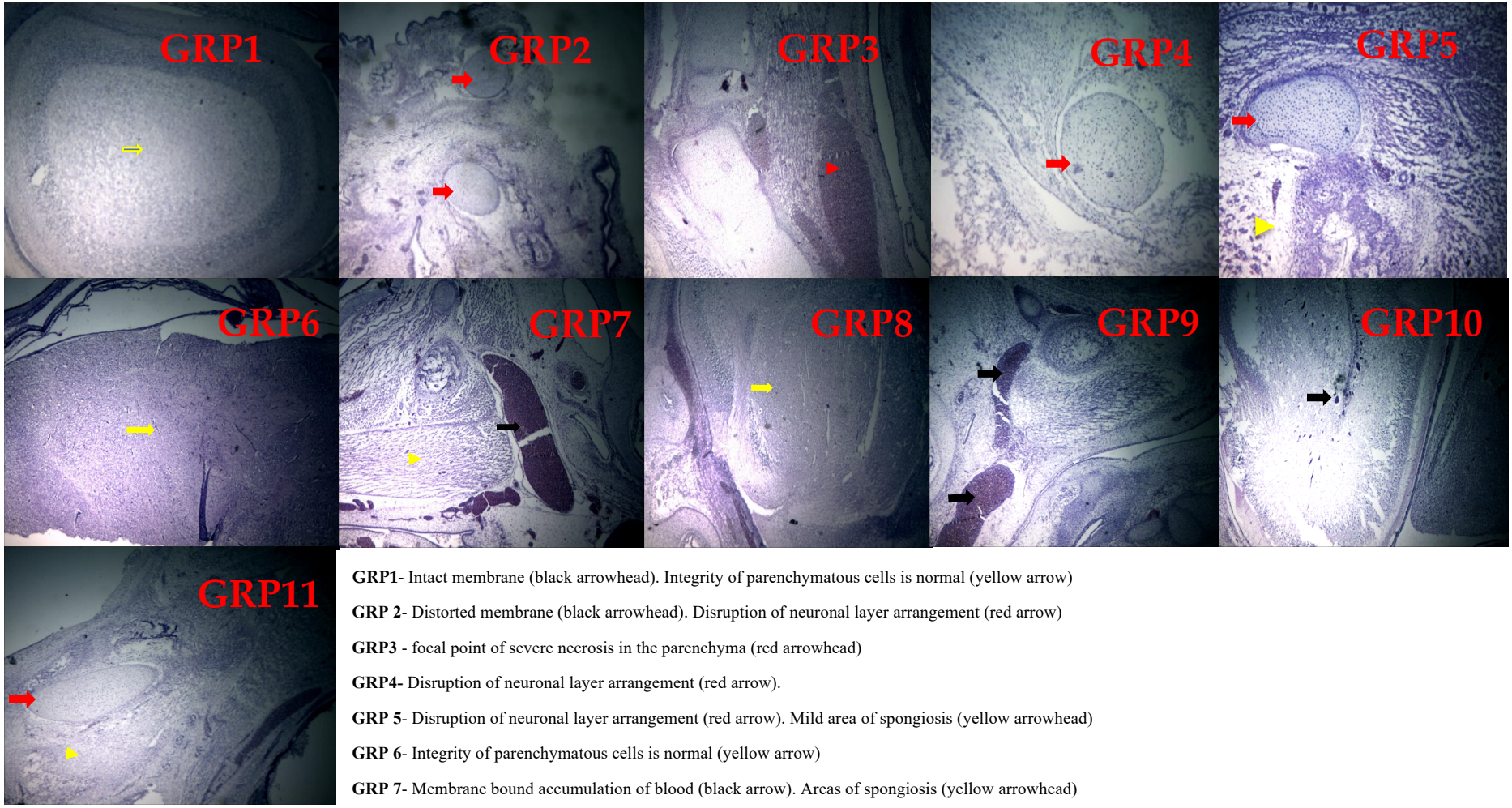

GRP1- Intact membrane (black arrowhead). Integrity of parenchymatous cells is normal (yellow arrow)

GRP 2- Distorted membrane (black arrowhead). Disruption of neuronal layer arrangement (red arrow)

GRP3 - focal point of severe necrosis in the parenchyma (red arrowhead)

GRP4- Disruption of neuronal layer arrangement (red arrow).

GRP 5- Disruption of neuronal layer arrangement (red arrow). Mild area of spongiosis (yellow arrowhead)

GRP 6- Integrity of parenchymatous cells is normal (yellow arrow)

GRP 7- Membrane bound accumulation of blood (black arrow). Areas of spongiosis (yellow arrowhead)

GRP 8 - Fairly normal membrane (black arrowhead). Integrity of parenchymatous cells is normal (yellow arrow)

GRP 9- Areas of mild accumulation of blood (black arrows)

GRP 10- Mildly extended cavernous spaces containing bloody spots (black arrows)

GRP 11- Disruption of neuronal layer arrangement (red arrow). Areas of spongiosis (yellow arrowhead)

Figure 3.2: Histopathology of the head of chicken embryos inoculated with Parvovirus and treated with Lagenaria breviflora whole fruit extract (H&E, X100)

3.3. Histopathology of Embryo Body

The integrity of parenchymatous cells of the embryo body in the uninoculated, untreated embryos was observed to be expected, as shown by prominent cavernous areas filled with embryonic blood. However, the inoculated-untreated embryos showed severe necrosis of parenchymatous cells and prominent cavernous areas filled with embryonic blood. Inoculated and treated embryos with 1.5625mg/ml of LB extract showed mild degeneration of parenchymatous cells. In contrast, prominent cavernous areas filled with embryonic blood and mild degeneration of parenchymatous cells were observed for embryos treated with 3.125 and 6.25 mg/mL, respectively. Nonetheless, the integrity of parenchymatous cells was expected, with a prominent cavernous area filled with embryonic blood in the group inoculated and treated with 12.5mg/ml LB extract. The embryos inoculated and treated with 25 mg/mL LB extract presented mild necrosis of parenchymatous cells and moderate cavernous areas filled with embryonic blood. In addition, embryonic-treated groups with 25 and 50mg/ml LB extract had mild disruption of parenchymatous arrangement and some cell necrosis. Likewise, inoculated and treated embryos with 50mg/ml LB extract showed severe necrosis of parenchymatous cells and prominent cavernous areas filled with embryonic blood. Finally, parenchymatous cell integrity was expected in the group inoculated and treated with 100mg/ml of LB extract (Figure 3.3).

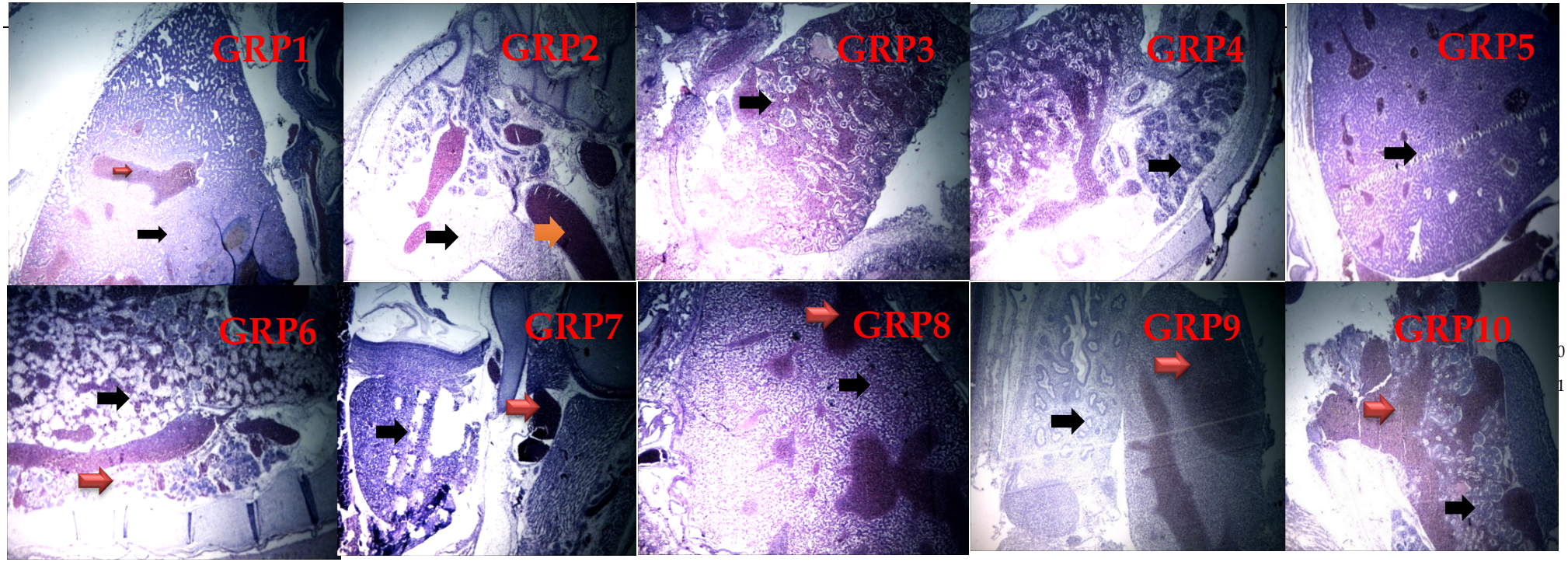

GRP1- Integrity of parenchymatous cells is normal (black arrow). Prominent cavernous areas filled with embryonic blood (red arrow).

GRP 2- Prominent cavernous areas filled with embryonic blood (red arrow). severe necrosis of parenchymatous cells (black arrow)

GRP3 - Mild disruption of parenchymatous arrangement and there is also cell necrosis

GRP4- Mild disruption of parenchymatous arrangement and there is also cell necrosis

GRP 5- Integrity of parenchymatous cells is normal

GRP 6- severe necrosis of parenchymatous cells (black arrow). Prominent cavernous areas filled with embryonic blood (red arrow).

GRP7- mild necrosis of parenchymatous cells (black arrow). Moderate cavernous area filled with embryonic blood (red arrow)

GRP 8 - Integrity of parenchymatous cells is normal (black arrow). Prominent cavernous area filled with embryonic blood (red arow)

GRP 9 -prominent cavernous area filled with embryonic blood (red arrow). mild degeneration of the parenchymatous cells (black arrow)

GRP 10- prominent cavernous area filled with embryonic blood (red arrow), mild degeneration of the parenchymatous cells (black arrow)

GRP 11- mild degeneration of the parenchymatous cells (black arrow)

Figure 3.3: Histopathology of the body of chicken embryos inoculated with Parvovirus and treated with Lagenaria breviflora whole fruit extract (H&E, X100)

3.4. Histopathology of Chorioallantoic Membrane

The uninoculated untreated CAM presented with normal blood vessels connecting the embryo to the yolk. On the other hand, the inoculated untreated embryos showed a copious presence of proteinaceous materials within the membranous spaces. Inoculated embryos treated with 1.5625mg/ml of LB extract revealed a severely necrotic membrane, while inoculated embryos treated with 3.125mg/ml of LB extract showed a degenerated fetal membrane with remnants of clots. There was severe fetal membrane necrosis at 6.25mg/ml and 12.5mg/ml LB in the inoculated-treated embryos. The fetal membrane appeared thickened in the group inoculated and treated with 25mg/ml of LB extract. Embryos inoculated and treated with 50mg/ml of LB extract presented with an intact membrane, a mild presence of proteinaceous materials within the membranous spaces, and mild congestion of blood vessels. However, embryos inoculated with 25mg/ml of LB extract showed thickened fetal membranes and prominent blood vessels, which were congested, while severe necrosis with blood accumulation was observed with 50mg/ml of LB extract. Finally, inoculated embryos treated with 100mg/ml of LB extract showed an intact membrane and mild congestion of blood vessels (Figure 3.4).

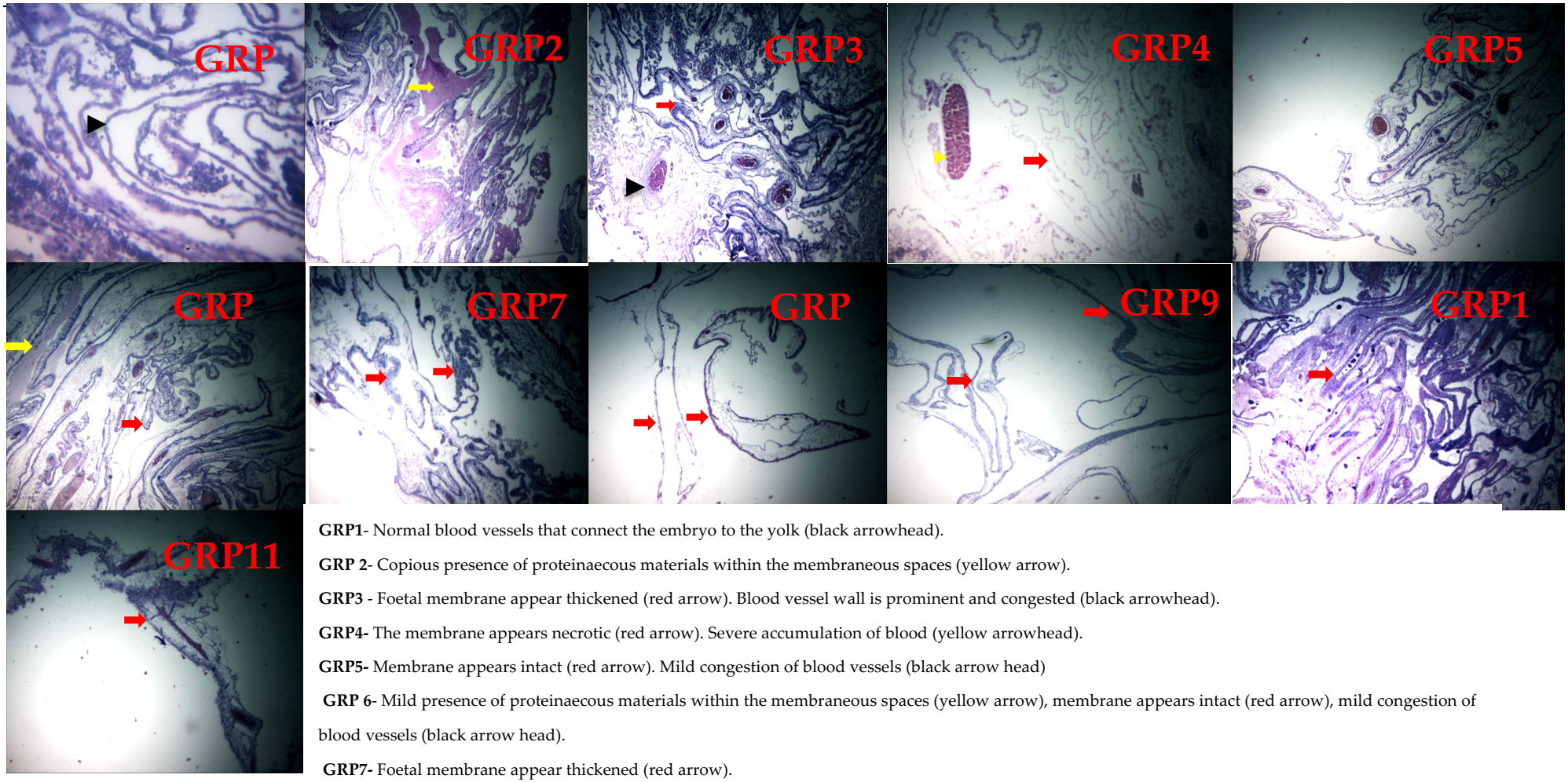

GRP1- Normal blood vessels that connect the embryo to the yolk (black arrowhead).

GRP 2- Copious presence of proteinaecous materials within the membraneous spaces (yellow arrow).

GRP3 - Foetal membrane appear thickened (red arrow). Blood vessel wall is prominent and congested (black arrowhead).

GRP4- The membrane appears necrotic (red arrow). Severe accumulation of blood (yellow arrowhead).

GRP5- Membrane appears intact (red arrow). Mild congestion of blood vessels (black arrow head)

GRP 6- Mild presence of proteinaecous materials within the membraneous spaces (yellow arrow), membrane appears intact (red arrow), mild congestion of blood vessels (black arrow head).

GRP7- Foetal membrane appear thickened (red arrow).

GRP 8 - Foetal membrane appears severely necrotic (red arrow).

GRP 9 - Foetal membrane appears severely necrotic (red arrow).

GRP 10- Foetal membrane appears degenerated with fossils of clots. (red arrow).

GRP 11-): Foetal membrane appears severely necrotic (red arrow).

Figure 3.4: Histopathology of the chorionallantoic membrane of chicken embryos inoculated with *Parvovirus* and treated with *Lagenaria breviflora* whole fruit extract (H&E x100)

4. Discussion

In this study, the methanol extract of *L. breviflora* whole fruit exhibited significant antiviral properties against CPV in embryonated chicken eggs. Notably, the extract inhibited the growth of the virus, leading to reduced cytopathic changes and increased survival rates in treated embryos compared to the untreated infected embryos. These findings indicated the antiviral potential of *L. breviflora* extract, particularly against CPV, which is in agreement with its folkloric antiviral claim [23]. This study further corroborates a previous report of the antiviral activity of the extract demonstrated against Newcastle disease [15].

Canine Parvovirus is recognized for its high contagion and mortality rates in dogs. It causes severe disease characterized by replication in rapidly dividing cells such as bone marrow, lymphoid tissues, and intestinal crypts (24, 25). Typical pathological manifestations of CPE include congestion, haemorrhage, and oedema in infected tissues [26]. This study is in tandem with reported pathological features of CPE, as seen in the untreated infected embryos, which presented with significant lesions and mortality.

However, the observed virus-induced pathologies were prevented in the extract-treated embryos in a dose-dependent manner, aligning with the study by Oridupa *et al.* [15], which demonstrated the antiviral efficacy of ethanol extracts of *L. breviflora* fruit against Newcastle Disease Virus. The lower concentrations inhibited CPV growth and maintained embryo viability, suggesting an optimal therapeutic window for the extract's antiviral activity (3.125-12.5 mg/ml). While the antiviral benefits of *L. breviflora* extract were apparent at lower concentrations, higher concentrations (25-100 mg/ml) introduced toxicity. Embryos exposed to these concentrations showed mild haemorrhage, severe congestion, and significant histopathological changes such as spongiosis, necrosis, and severe neuronal and parenchymatous cell arrangement disruption. These findings are consistent with previous reports by Oridupa *et al.* [15], which highlighted the embryotoxic potentials of various parts of the *Lagenaria breviflora* fruit (100mg/ml). Thus, while the extract is effective at lower doses, its application must be carefully managed to avoid toxic effects.

The gross pathology results in this study indicated that embryos treated with 3.125-12.5 mg/ml of the extract exhibited no haemorrhage and only slight congestion, contrasting sharply with the severe lesions seen in untreated infected embryos. Histopathology of treated embryos showed relatively normal membranes and mildly degenerated parenchymatous cells, further substantiating the protective effect of the extract at these concentrations. Conversely, higher doses (25-100 mg/ml) resulted in moderate to severe virus-induced damage, reinforcing the necessity for dose optimization.

This study demonstrates a notable antiviral activity of *L. breviflora* whole fruit methanol extract against CPV, particularly at concentrations of 3.125, 6.25 and 12.5 mg/ml, effectively inhibited viral growth and mitigated virus-induced damage in embryonated chicken eggs infected with canine parvovirus. This aligns with previous findings on its efficacy against other viral pathogens. The potential of the extract as an antiviral agent is evident, provided that its application is carefully regulated to mitigate associated toxicities.

5. Conclusions

The findings of this study suggest that *L. breviflora* extract holds promise as an antiviral agent against canine parvovirus and for the treatment of enteritis, with significant efficacy observed at lower concentrations. However, the observed toxicity at higher doses necessitates further investigation for the safe therapeutic range and mechanisms underlying both the antiviral and toxic effects. Future research should also explore the specific active compounds within the extract responsible for these effects, potentially leading to more refined antiviral therapies..

Author Contributions: Conceptualization, Olayinka Oridupa and Olusegun Fagbogun; methodology, Blessing Ayeni and Olusegun Fagbohun; software and Imaging, Oluwasanmi Aina.; validation, Olawale Olawumi Ola, Oluwasanimi Aina and Olusegun Fagbohun; investigation, Blessing Ayeni, Olawale Ola.; resources, Tolulope Olakojo; writing—original draft preparation, Tolulope Olakojo.; writing—review and editing, Tolulope Olakojo , Olayinka Oridupa, Oluwasanmi Aina and Olusegun Fagbohun.; visualization, Oluwasanmi Aina, Olawale Ola.; supervision, Olayinka Oridupa; project administration, Blessing Ayeni.

All authors have read and agreed to the published version of the manuscript.

Funding: This research received no external funding

Institutional Review Board Statement: Not applicable.

Acknowledgments: We acknowledge the support of the entire members of technical staff of the Virology Laboratory of the Department of Veterinary Microbiology, Histology unit of Veterinary Anatomy Laboratory and Histopathology unit of Veterinary Pathology, University of Ibadan for their support all through this research.

Conflicts of Interest: The authors declare no conflict of interest.

References

1. Qi, S.; Zhao, J.; Guo, D.; Sun, D. A mini-review on the epidemiology of canine parvovirus in China. Front Vet Sci. **2020**, 7, 5.
2. Ogbu, K.I.; Chukwudi, I.C.; Mira, F.; Eze, U.U.; Di Bella, S.; Olaolu, O.S.; Tion, M.T.; Purpari, G.; Cannella, V.; Nwosuh, I.C.; Guercio, A.; Anene, B.M. Current status and risk factors of canine parvovirus type 2 in North Central Nigeria. Comp Immunol Microbiol Infect Dis. **2021**, 74.
3. Sykes, J.E. Immunization. In: Greene's Infectious Diseases of the Dog and Cat. Elsevier, **2021**; pp. 238–55.
4. Cotmore, S.F.; Tattersall, P. Parvoviruses: small does not mean simple. Annu Rev Virol. **2014**, 1, 517–37.
5. Pénzes, J.J.; Söderlund-Venermo, M.; Canuti, M.; Eis-Hübinger, A.M.; Hughes, J.; Cotmore, S.F.; Harrach, B. Reorganizing the family Parvoviridae: a revised taxonomy independent of the canonical approach based on host association. Arch Virol. **2020**, 165, 2133–46.
6. Fagbohun, O.A.; Omobowale, T.O. Sequence and phylogenetic analysis of canine parvovirus-2 isolates in dogs revealed circulation of three subtypes in Nigeria. Virusdisease. **2018**, 29, 411–5.
7. Larson, L.J.; Schultz, R.D. Canine and feline vaccinations and immunology. Infectious disease management in animal shelters. **2021**, 191–220.
8. Afumba, R.; Liu, J.T.; Dong, H. Apoptosis mechanisms induced by parvovirus infections. Acta Virologica **2022**, 66(2), 101-109
9. Mazzaferro, E.M. Update on canine parvoviral enteritis. Veterinary Clinics: Small Animal Practice. **2020**, 50(6), 1307–25.
10. Kelman, M.; Ward, M.P.; Barrs, V.R.; Norris, J.M. The geographic distribution and financial impact of canine parvovirus in Australia. Transbound Emerg Dis. **2019**, 66(1), 299–311.
11. Kelman, M.; Barrs, V.R, Norris, J.M.; Ward, M.P. Canine parvovirus prevention and prevalence: Veterinarian perceptions and behaviors. Prev Vet Med. **2020,** 174, 104817.
12. Pandit, M.; Latha, N. In silico studies reveal potential antiviral activity of phytochemicals from medicinal plants for the treatment of COVID-19 infection. PREPRINT (Version 1) available at Research Square [https://doi.org/10.21203/rs.3.rs-22687/v1] (14 April 2020)

13. Adamson, C.S.; Chibale, K.; Goss, R.J.M.; Jaspars, M.; Newman, D.J.; Dorrington, R.A. Antiviral drug discovery: preparing for the next pandemic. Chem Soc Rev. **2021**, 50(6), 3647–55.
14. Renner, S.S.; Schaefer, H. Phylogeny and evolution of the Cucurbitaceae. Genetics and genomics of Cucurbitaceae. **2017**, 13–23.
15. Oridupa, O.A.; Saba, A.B.; Sulaiman, L.K. Preliminary report on the antiviral activity of the ethanolic fruit extract of Lagenaria breviflora Roberts on Newcastle disease virus. Tropical Vet. **2011**, 29(1), 22–33.
16. Adedapo, A.A.; Adewuyi, T.; Sofidiya M. Phytochemistry, anti-inflammatory and analgesic activities of the aqueous leaf extract of Lagenaria breviflora (Cucurbitaceae) in laboratory animals. Rev Biol Trop. **2013**, 61(1), 281–90.
17. Onasanwo., SA.; Singh, N.; Saba, A.B.; Oyagbemi, A.A.; Oridupa, O.A.; Palit, G. Anti-ulcerogenic and in vitro antioxidant activities of Lagenaria breviflora (LB) whole fruit ethanolic extract in laboratory animals. Pharmacognosy Res. **2011**, 3(1), 2-8
18. Ekunseitan, D.A.; Ayoola, A.A.; Jimoh, S.A.; Adegoke, T.O.; Adeniran, K.A. Resposta das aves à administração aquosa de extrato de abóbora manchada. Archivos de zootecnia. **2019**, 68(262), 214–9.
19. Oridupa, O.; Saba, A. Relaxant effect of *Lagenaria breviflora* Roberty fruit pulp and seeds on isolated rabbit ileum. Sokoto Journal of Veterinary Sciences. **2013**, 11(2), 21-27
20. Sobotka, P.; Przychodzki, M.; Uściło, K.; Woliński, T.R.; Staniszewska, M. Effect of ultraviolet light C (UV-C) radiation generated by semiconductor light sources on human beta-coronaviruses' inactivation. Materials. **2022**, 15(6), 2302.
21. Ribatti, D. The chick embryo chorioallantoic membrane (CAM) assay. Reproductive toxicology. **2017**, 70, 97–101.
22. Jedelska, J.; Strehlow, B.; Bakowsky, U.; Aigner, A.; Hoebel, S.; Bette, M.; Roessler, M.; Franke, N.; Teymoortash, A.; Werner, J.A.; Eivazi, B.; Mandic, R. The chorioallantoic membrane assay is a promising ex vivo model system for the study of vascular anomalies. In Vivo (Brooklyn). **2013**, 27(6), 701–5.
23. Saba, A.B.; Oridupa, O.A.; Oyagbemi, A.A.; Alao, E.O. Serum biochemical changes accompanying prolonged administration of ethanolic extract of whole fruit of Lagenaria breviflora (Benth) Roberty in Wistar rats. Afr J Biotechnol. **2010**, 9(42), 7128–33.
24. Parrish, C.R.; Sykes, J.E. Canine parvovirus infections and other viral enteritides. In: Greene's Infectious Diseases of the Dog and Cat. Elsevier: 2021; pp. 341–351.
25. Tuteja, D.; Banu, K.; Mondal, B. Canine parvovirology–A brief updated review on structural biology, occurrence, pathogenesis, clinical diagnosis, treatment and prevention. Comp Immunol Microbiol Infect Dis. **2022**, 82, 101765.
26. Fagbohun, O.A.; Jarikre, T.A.; Alaka, O.O.; Adesina, R.D.; Ola, O.O.; Afolabi, M.; Oridupa, O.A.; Omobowale, T.O.; Emikpe, B.O. Pathology and molecular diagnosis of canine parvoviral enteritis in Nigeria: case report. Comp Clin Path**.** **2020**, 29, 887–93.

CVJ CLUJ VETERINARY JOURNAL

Article

Evaluation of 14-3-3σ as a Prognostic Marker in Canine Mammary Tumors

Ana Hîruța [1], Andrada Negoescu[1]*, Zoltán-Miklós Gál[2], Alexandru Raul Pop[2] and Cornel Cătoi [1]

[1] Faculty of Veterinary Medicine, Pathology Department, University of Agricultural Sciences and Veterinary Medicine, Cluj-Napoca, 400372, Cluj, Romania.
[2] Faculty of Veterinary Medicine, Reproduction Department, University of Agricultural Sciences and Veterinary Medicine, Cluj-Napoca, 400372, Cluj, Romania;
* Correspondence: andrada.negoescu@usamvcluj.ro; Tel.: +4 0745613960

Abstract: 14-3-3σ is a regulatory protein involved in cell cycle control and has been implicated in both tumor-suppressive and tumor-promoting roles, depending on the biological context. While extensively studied in human cancers, limited information is available regarding its expression in canine mammary gland tumors. This study aimed to assess the immunohistochemical expression of 14-3-3σ in canine mammary tumors and evaluate its potential association with malignancy indicators such as histological grade and mitotic index. A total of 62 tumor samples were analyzed using immunohistochemistry, and the area of 14-3-3σ expression was digitally quantified. Statistical comparisons were performed using non-parametric tests. An inverse trend was observed between 14-3-3σ expression and both tumor grade ($p = 0.051$) and mitotic ($p = 0.0090$) activity. These findings suggest a potential link between decreased 14-3-3σ expression and increased malignancy, supporting its relevance as a candidate prognostic marker in canine mammary tumors. Further studies with larger cohorts are needed to validate these observations.

Keywords: 14-3-3 σ, immunohistochemistry, canine mammary gland tumor.

Received: 07.07.2025
Accepted: 09.07.2025
Published: 15.07.2025

DOI: 10.52331/v30i20s71

1. Introduction

The 14-3-3 protein family comprises highly conserved regulatory molecules present in all eukaryotic cells, playing essential roles in key physiological processes[1]. To date, over 200 target proteins have been identified, including those involved in mitogenic signaling, cell survival, cell cycle regulation and apoptosis. Notably, the interaction of 14-3-3 proteins with various oncogenes and tumor suppressor genes highlights their potential involvement in cancer development and progression[2]. The 14-3-3 protein family comprises seven isoforms (β, ε, η, γ, τ, σ, and ζ), each ranging in size from 28 to 33 kDa, which are highly conserved and widely expressed across various tissues[3].

The 14-3-3 σ protein, also known as stratifin or human mammary epithelial marker (HME1), is a negative regulator of the cell cycle and has been closely associated with tumor development. It is unique among the seven 14-3-3 isoforms for its strong link to oncogenesis[4]. Its expression is regulated by the tumor suppressor protein p53 in response to DNA damage, functioning to inhibit mitosis by sequestering the cdc2–cyclin B1 complex in the cytoplasm and preventing its translocation to the nucleus. 14-3-3σ is involved in both G1/S and G2/M cell cycle arrest through p53-dependent transactivation in response to DNA damage[5]. In this way, it induces G2 arrest, providing time for the repair of damaged DNA.

In humans, both reduced [6,7] and elevated levels [8,9] of 14-3-3 σ expression have been implicated in various cancers. Furthermore, both upregulation and downregulation of 14-3-3 σ have been reported in various tumor types, suggesting a context-dependent role in tumorigenesis [3]. Notably, breast cancer cells lacking 14-3-3σ expression exhibit a significantly higher frequency of G2-type chromosomal aberrations compared to cells that express the protein. These findings suggest that 14-3-3σ plays a critical role in G2 checkpoint control in breast epithelial cells. The loss of 14-3-3σ gene expression may contribute to breast cancer

development by permitting the accumulation of genetic damage that promotes malignant transformation [10].

In canine mammary tissues 14-3-3 σ has been detected in 97% of samples, localizing to both epithelial (ECs) and myoepithelial cells (MECs)[4]. Studies have shown that this isoform is specifically expressed in epithelial cells under normal conditions.

Mammary cancer is the most frequently diagnosed malignancy in both women and female dogs[11]. Owing to its significant clinical impact, mammary gland tumors have been extensively investigated. Since ethical constraints limit experimental research in humans, animals with naturally occurring mammary tumors represent valuable models for the development of in vitro systems and the advancement of cancer research [4]. Given the inconsistent and seemingly random pattern of 14-3-3 σ staining in epithelial cells (ECs) [12], the authors hypothesized that its expression might be associated with the degree of malignancy. To explore this possibility, histological grade and mitotic count—both established indicators of malignancy—were analyzed in relation to the level of 14-3-3 σ expression.

This study aimed to investigate the expression of 14-3-3 σ protein in neoplastic canine mammary tissue and to evaluate its potential as a malignancy marker for epithelial cells (ECs).

2. Materials and Methods

This study included 55 female canine patients diagnosed with mammary gland tumors. All patients underwent clinical examination, thoracic imaging, and either unilateral or total mastectomy. A total of 64 tumor specimens were collected, routinely fixed in 10% neutral buffered formalin, processed, and embedded in paraffin wax. Tissue sections were stained with hematoxylin and eosin (H&E) and evaluated histopathologically according to the Zappulli classification and grading system [13]. For each sample, the mitotic count was determined by evaluating ten high-power fields (40× magnification) and recording the number of mitotic figures observed.

For the immunohistochemical analysis, two-micrometer-thick sections were cut from formalin-fixed, paraffin-embedded tissue blocks and immunolabeled using mouse monoclonal antibodies against 14-3-3σ (clone 5D7, 1:40; Santa Cruz Biotechnology, Heidelberg, Germany). Heat-induced epitope retrieval was carried out in a pH 6 buffer (Bond ER1; Leica) for 20 minutes at 90 °C. Visualization was performed using the Bond Polymer Refine Detection Kit (Leica), with hematoxylin used as a counterstain. Positive labeling was identified by the presence of brown staining of the cytoplasm.

The quantitative analysis was performed using the ImageJ software, version 1.54f (Wayne Rasband and contributors, National Institutes of Health, USA). For each case, ten microscopic fields were captured at 40X magnification using an Olympus UC-30 digital camera and Stream Basic software, maintaining the same light intensity throughout. For statistical consistency, the mean percentage value across the ten analyzed fields was calculated for each sample and used in subsequent analyses.

To assess the association between the immunolabeled area and histological grade, the Kruskal–Wallis non-parametric test and the Jonckheere–Terpstra trend test were employed. The correlation between the labeled area and mitotic count was analyzed using Spearman's rank correlation and Kendall's tau non-parametric tests.

3. Results

The mean age of the patients was 9.19 years. The majority of female dogs were mixed-breed (11/55), followed by German Shepherds (7/55) and Yorkshire Terriers (7/55). The database included the following histological subtypes of mammary carcinomas: complex carcinomas (n=19), tubular carcinomas (n=15), tubulopapillary carcinomas (n=1), inflammatory carcinoma (n=1), mixed carcinomas (n=9), solid carcinomas (n=4), invasive micropapillary carcinoma (n=1), intraductal papillary carcinomas (n=9), and ductal carcinomas (n=2). Additionally, four cases were classified as special types: lipid-rich carcinoma (n=1), carcinosarcoma (n=1), comedocarcinoma (n=1) and adenosquamous carcinoma (n=1). **Immunohistochemical expression of 14-3-3σ varied across histological subtypes of canine mammary carcinomas.** Positive labeling was observed in the vast majority of complex carcinomas (18/19), tubular carcinomas (13/15), and all cases of tubulopapillary carcinoma (1/1), invasive micropapillary carcinoma (1/1), intraductal papillary carcinomas (9/9), and ductal carcinomas (2/2). Mixed carcinomas exhibited positive labeling in 6 out of 9 cases. Among solid carcinomas, only 1 of 4 cases showed immunoreactivity. In contrast, none of the special carcinoma

subtypes—lipid-rich carcinoma (n=1), carcinosarcoma (n=1), comedocarcinoma (n=1), and adenosquamous carcinoma (n=1)—showed any detectable expression of 14-3-3σ.

Across the examined samples, the cytoplasmic staining pattern of the cells was variable (Figure 1). Notably, in terms of immunolabeling, the cytoplasm of epithelial cells from the three most aggressive histological subtypes—lipid-rich carcinoma, carcinosarcoma, and adenosquamous carcinoma—showed a complete absence of detectable staining for 14-3-3σ.

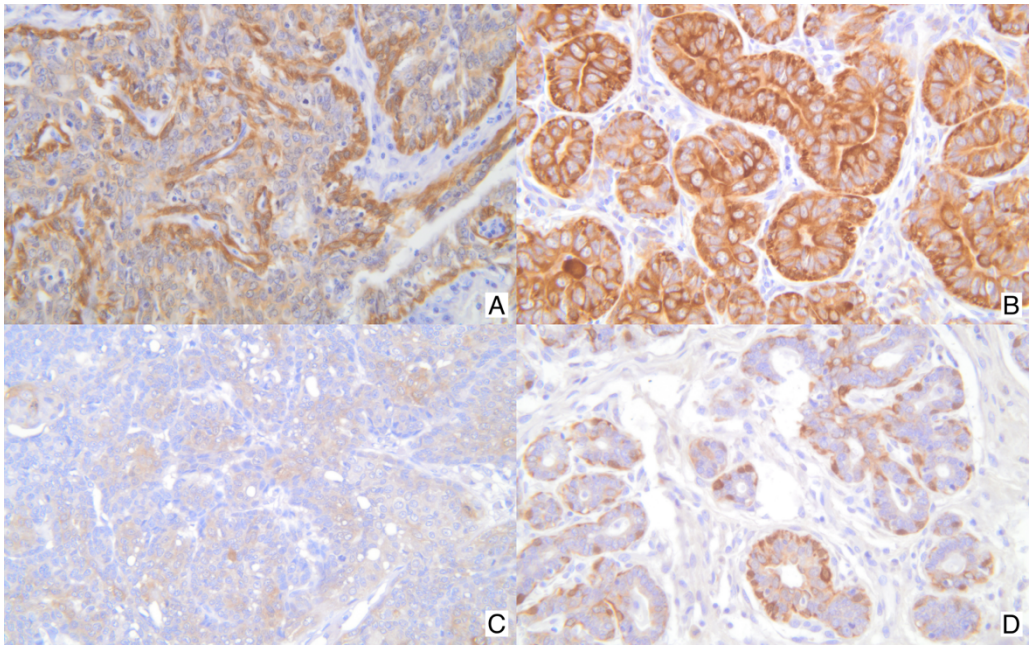

Figure 1. Immunohistochemical patterns showing varying labeling intensities.

The Kruskal–Wallis test did not show statistically significant differences in the area of expression among the three histological grades (H = 3.51, p = 0.171). However, the Jonckheere–Terpstra test revealed a trend toward decreasing expression with increasing tumor grade (z = –1.951, p = 0.051), suggesting a potential association between reduced expression area and higher tumor aggressiveness (Figure 2-left).

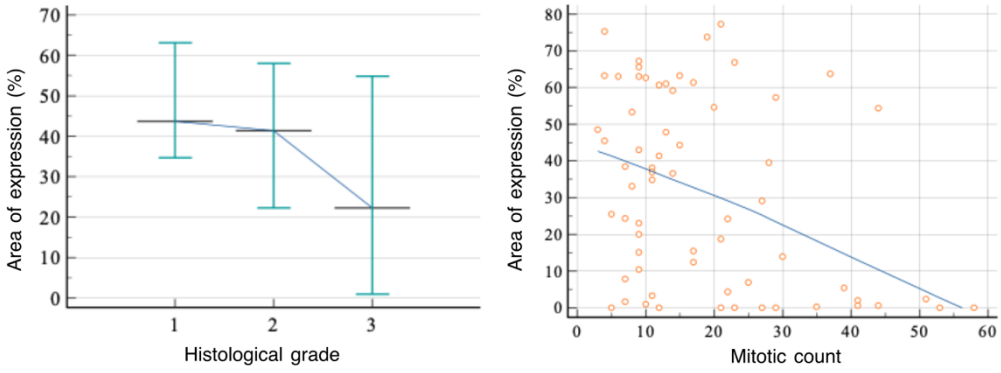

Figure 2. Graphical representation of the relationship between expression area and histological grade (left) and mitotic count (right).

Left: vertical error bars- Indicate variability, blue line- connects the central values (medians), visually indicating a decreasing trend in expression from Grade 1 to Grade 3.

Right: X-axis**:** Represents the number of mitotic figures observed per tumor, Y-axis**:** represents the percentage of IHC marked area, trend line**:** a linear regression line showing the general direction of the relationship.

A statistically significant moderate inverse correlation was found between 14-3-3σ expression and mitotic activity. As the mitotic count increased, the area of epithelial immunolabeling decreased. This relationship was demonstrated by both Spearman's rank correlation coefficient ($\rho = -0.323$, $p = 0.0086$; 95% CI: –0.526 to –0.086) and Kendall's tau ($\tau = -0.221$, $p = 0.0090$; 95% CI: –0.385 to –0.018), indicating that higher proliferative activity is associated with reduced 14-3-3σ expression in epithelial cells (Figure 2, right).

4. Discussion

14-3-3 sigma is a regulatory protein involved in cell cycle control, particularly at the G2/M checkpoint, and has been shown to play dual roles in cancer biology—functioning either as a tumor suppressor or having oncogenic potential depending on the cellular context. It is also implicated in tumor invasion and metastasis pathways [14,15].

Although traditionally classified as a tumor suppressor, a 2013 study revealed that in basal-like breast cancer (BLBC) in humans, 14-3-3 sigma can adopt a pro-tumorigenic role. Its expression increases progressively during malignant transformation, promoting tumor cell migration and invasion, independent of cell proliferation [16]. Additionally, in invasive ductal carcinoma, reduced 14-3-3 sigma expression is associated with decreased patient survival. Likewise, in ductal carcinoma in situ, higher levels of 14-3-3 sigma expression are linked to poorer patient outcomes [17]. These features suggest the complex biological behaviour of this particular protein when different types of breast neoplasms are involved.

In veterinary oncology, 14-3-3 sigma has also been explored in various species and tumor types. Notably, studies have documented its expression in canine mammary, gastric, and renal cell carcinomas and equine penile squamous cell carcinoma [4,12,18,19]

An intriguing finding across both squamous cell carcinoma and renal cell carcinoma is the observation of aberrant nuclear immunolabeling of 14-3-3 sigma. This nuclear localization is suggested to correlate with increased metastatic potential, serving as a potential marker of aggressive tumor behavior [19,20]. Similar features were observed in a recent study on canine gastric carcinoma, in which aberrant immunolabeling was noted in pleomorphic neoplastic cells, indicating a higher potential for metastasis [21]. Despite these associations, no significant correlation was found between 14-3-3 sigma expression and tumor grade or mitotic index in some studies [19]. In contrast, a positive correlation was observed in canine mammary neoplasms between 14-3-3 sigma expression and the number of mitotic figures(In contrast, a positive correlation was observed in canine mammary neoplasms between 14-3-3 sigma expression and the number of mitotic figures, degree of invasion, and presence of vascular emboli.). Authors should discuss the results and how they can be interpreted from the perspective of previous studies and of the working hypotheses. The findings and their implications should be discussed in the broadest context possible. Future research directions may also be highlighted.

Our study suggests that immunohistochemical labeling of 14-3-3σ may be associated with malignancy markers such as tumor grade and mitotic count. Although statistical analyses did not reach conventional levels of significance, the results approached relevance, and the observed inverse trend between tumor grade, mitotic figures, and the area of positive labeling indicates a potential biological relationship. These findings imply that the lack of statistical significance may be attributed to the limited sample size, and further studies with larger cohorts are warranted to validate this association.

5. Conclusions

This study indicates a possible association between 14-3-3σ expression and malignancy features, such as tumor grade and mitotic activity, in canine mammary tumors. While statistical significance was not reached, the inverse trends observed suggest biological relevance. These findings, in line with previous research, underscore the need for further studies with larger cohorts to better define the prognostic value of 14-3-3σ.

Author Contributions: Conceptualization, A.H. and A.N.; methodology, A.H. and A.N.; statistical analysis, Z.-M.G.; resources, C.C..; data curation, A.H.; writing—original draft preparation,., A.H., A.N. and Z.-M.G.; writing—review and editing, A.N.; supervision, C.C. All authors have read and agreed to the published version of the manuscript.

Funding: This research was founded by the Discipline of Veterinary Pathology at the Faculty of Veterinary Medicine Cluj-Napoca.

Acknowledgments: The authors extend their gratitude to the Discipline of Animal Reproduction at the Faculty of Veterinary Medicine Cluj-Napoca, and the private practice reproduction referral clinic Quantas Repro Vet SRL in Cluj-Napoca for their help in collecting the samples.

Conflicts of Interest: The authors declare no conflict of interest.

References

1. Fu, H.; Subramanian, R.R.; Masters, S.C. 14-3-3 Proteins: Structure, Function, and Regulation. *Annu. Rev. Pharmacol. Toxicol.* **2000**, *40*, 617–647, doi:10.1146/annurev.pharmtox.40.1.617.
2. Tzivion, G.; Avruch, J. 14-3-3 Proteins: Active Cofactors in Cellular Regulation by Serine/Threonine Phosphorylation. *Journal of Biological Chemistry* **2002**, *277*, 3061–3064, doi:10.1074/jbc.R100059200.
3. Tzivion, G.; Gupta, V.S.; Kaplun, L.; Balan, V. 14-3-3 Proteins as Potential Oncogenes. *Seminars in Cancer Biology* **2006**, *16*, 203–213, doi:10.1016/j.semcancer.2006.03.004.
4. Suárez-Bonnet, A.; Herráez, P.; Mulas, J.M.D.L.; Rodríguez, F.; Déniz, J.M.; Monteros, A.E.D.L. Expression of 14-3-3 σ Protein in Normal and Neoplastic Canine Mammary Gland. *The Veterinary Journal* **2011**, *190*, 345–351, doi:10.1016/j.tvjl.2010.12.015.
5. Simpson, P.T.; Gale, T.; Reis-Filho, J.S.; Jones, C.; Parry, S.; Steele, D.; Cossu, A.; Budroni, M.; Palmieri, G.; Lakhani, S.R. Distribution and Significance of 14-3-3σ, a Novel Myoepithelial Marker, in Normal, Benign, and Malignant Breast Tissue. *The Journal of Pathology* **2004**, *202*, 274–285, doi:10.1002/path.1530.
6. Iwata, N.; Yamamoto, H.; Sasaki, S.; Itoh, F.; Suzuki, H.; Kikuchi, T.; Kaneto, H.; Iku, S.; Ozeki, I.; Karino, Y.; et al. Frequent Hypermethylation of CpG Islands and Loss of Expression of the 14-3-3 σ Gene in Human Hepatocellular Carcinoma. *Oncogene* **2000**, *19*, 5298–5302, doi:10.1038/sj.onc.1203898.
7. Mhawech, P.; Benz, A.; Cerato, C.; Greloz, V.; Assaly, M.; Desmond, J.C.; Koeffler, H.P.; Lodygin, D.; Hermeking, H.; Herrmann, F.; et al. Downregulation of 14-3-3σ in Ovary, Prostate and Endometrial Carcinomas Is Associated with CpG Island Methylation. *Modern Pathology* **2005**, *18*, 340–348, doi:10.1038/modpathol.3800240.
8. Guweidhi, A. Enhanced Expression of 14-3-3sigma in Pancreatic Cancer and Its Role in Cell Cycle Regulation and Apoptosis. *Carcinogenesis* **2004**, *25*, 1575–1585, doi:10.1093/carcin/bgh159.
9. Perathoner, A.; Pirkebner, D.; Brandacher, G.; Spizzo, G.; Stadlmann, S.; Obrist, P.; Margreiter, R.; Amberger, A. 14-3-3σ Expression Is an Independent Prognostic Parameter for Poor Survival in Colorectal Carcinoma Patients. *Clinical Cancer Research* **2005**, *11*, 3274–3279, doi:10.1158/1078-0432.CCR-04-2207.
10. Ferguson, A.T.; Evron, E.; Umbricht, C.B.; Pandita, T.K.; Chan, T.A.; Hermeking, H.; Marks, J.R.; Lambers, A.R.; Futreal, P.A.; Stampfer, M.R.; et al. High Frequency of Hypermethylation at the 14-3-3 σ Locus Leads to Gene Silencing in Breast Cancer. *Proc. Natl. Acad. Sci. U.S.A.* **2000**, *97*, 6049–6054, doi:10.1073/pnas.100566997.
11. Ferreira, T.; Miranda, M.; Pinto-Leite, R.; Mano, J.F.; Medeiros, R.; Oliveira, P.A.; Gama, A. Integrated Study of Canine Mammary Tumors Histopathology, Immunohistochemistry, and Cytogenetic Findings. *Veterinary Sciences* **2024**, *11*, 409, doi:10.3390/vetsci11090409.
12. Suárez-Bonnet, A.; De Las Mulas, J.M.; Herráez, P.; Rodríguez, F.; De Los Monteros, A.E. Immunohistochemical Localisation of 14-3-3 σ Protein in Normal Canine Tissues. *The Veterinary Journal* **2010**, *185*, 218–221, doi:10.1016/j.tvjl.2009.05.014.
13. *Mammary Tumors*; Zappulli, V., Ed.; Surgical pathology of tumors of domestic animals / edited by M. Kiupel; Davis-Thompson DVM Foundation: Gurnee, Illinois, 2019; ISBN 978-1-73374-911-4.
14. Ko, S.; Kim, J.Y.; Jeong, J.; Lee, J.E.; Yang, W.I.; Jung, W.H. The Role and Regulatory Mechanism of 14-3-3 Sigma in Human Breast Cancer. *J Breast Cancer* **2014**, *17*, 207, doi:10.4048/jbc.2014.17.3.207.
15. Mikami, T.; Maruyama, S.; Abé, T.; Kobayashi, T.; Yamazaki, M.; Funayama, A.; Shingaki, S.; Kobayashi, T.; Jun, C.; Saku, T. Keratin 17 Is Co-Expressed with 14-3-3 Sigma in Oral Carcinoma in Situ and Squamous Cell Carcinoma and Modulates Cell Proliferation and Size but Not Cell Migration. *Virchows Arch* **2015**, *466*, 559–569, doi:10.1007/s00428-015-1735-6.

16. Boudreau, A.; Tanner, K.; Wang, D.; Geyer, F.C.; Reis-Filho, J.S.; Bissell, M.J. 14-3-3σ Stabilizes a Complex of Soluble Actin and Intermediate Filament to Enable Breast Tumor Invasion. *Proc. Natl. Acad. Sci. U.S.A.* **2013**, *110*, doi:10.1073/pnas.1315022110.
17. Yoon, N.K.; Seligson, D.B.; Chia, D.; Elshimali, Y.; Sulur, G.; Li, A.; Horvath, S.; Maresh, E.; Mah, V.; Bose, S.; et al. Higher Expression Levels of 14-3-3σ in Ductal Carcinoma in Situ of the Breast Predict Poorer Outcome1. *CBM* **2009**, *5*, 215–224, doi:10.3233/CBM-2009-0106.
18. Suárez-Bonnet, A.; Herráez, P.; Aguirre, M.; Suárez-Bonnet, E.; Andrada, M.; Rodríguez, F.; Espinosa De Los Monteros, A. Expression of Cell Cycle Regulators, 14-3-3σ and P53 Proteins, and Vimentin in Canine Transitional Cell Carcinoma of the Urinary Bladder. *Urologic Oncology: Seminars and Original Investigations* **2015**, *33*, 332.e1-332.e7, doi:10.1016/j.urolonc.2015.04.006.
19. Suárez-Bonnet, A.; Willis, C.; Pittaway, R.; Smith, K.; Mair, T.; Priestnall, S.L. Molecular Carcinogenesis in Equine Penile Cancer: A Potential Animal Model for Human Penile Cancer. *Urologic Oncology: Seminars and Original Investigations* **2018**, *36*, 532.e9-532.e18, doi:10.1016/j.urolonc.2018.09.004.
20. Suárez-Bonnet, A.; Lara-García, A.; Stoll, A.L.; Carvalho, S.; Priestnall, S.L. 14-3-3σ Protein Expression in Canine Renal Cell Carcinomas. *Vet Pathol* **2018**, *55*, 233–240, doi:10.1177/0300985817738097.
21. Hardas, A.; Suárez-Bonnet, A.; Beck, S.; Becker, W.E.; Ramírez, G.A.; Priestnall, S.L. Canine Gastric Carcinomas: A Histopathological and Immunohistochemical Study and Similarities with the Human Counterpart. *Animals* **2021**, *11*, 1409, doi:10.3390/ani11051409.

CVJ CLUJ VETERINARY JOURNAL

Article

The First Spermatological Examination of New Commercial Fish Species of the Mediterranean: Randall's Threadfin Bream, *Nemipterus randalli* Russell, 1986

Şükrü Güngör[1,*], Feyzanur Mart[1], Muhammed Enes İnanç[1] and Deniz İnnal[2]

1 Burdur Mehmet Akif Ersoy University, Faculty of Veterinary Science, Istiklal Campus, 15030, Burdur, Türkiye; sukrugungor@mehmetakif.edu.tr, feyzanurmart@gmail.com, enesinanc@mehmetakif.edu.tr
2 Burdur Mehmet Akif Ersoy University, Department of Biology, Istiklal Campus, 15030, Burdur, Türkiye; denizinnal@mehmetakif.edu.tr
* Correspondence: sukrugungor@mehmetakif.edu.tr; Tel.: +90 248 2132183

Abstract: Determining spermatological characteristics in fish is critical for understanding species' reproductive biology, protecting fish stocks, increasing reproductive success, and ensuring fish farming efficiency. While reproductive biology research on native fish species of Mediterranean is restricted, there is no information on the spermatological characteristics of invasive Mediterranean species. Samples were collected from trawl surveys conducted in the Gulf of Antalya (Mediterranean-Turkey) between March and April 2024. The fish samples were promptly transported to the laboratory at the Department of Biology, Burdur Mehmet Akif Ersoy University. The individuals' sex determination, lengths, and weights were recorded. 17 (65.38%) males, 9 (34.62%) females were determined. Male specimens of N. randalli, ranging in size from 19 to 27.2 cm in total length and weighing between 80 and 270.5 g, were analyzed. Nemipterus randalli sperm viability and concentration were evaluated. Male fish gonads were handled, and testes were dissected in a tube containing 1 ml PBS. Sperm concentration was done with haemocytometric method. The viability of spermatozoa was analysed using a Cytoflex Flow Cytometry device and a Sybr-14/PI double staining method. Spermatozoa concentration of male individuals obtained from the Gulf of Antalya was 160.0±45.63 × 106 spz/ml and the viability rate were 51.71±17.01%. As a result, some spermatological characteristics of Nemipterus randalli, which is recorded as an invasive species and has a serious economic value, were revealed for the first time.

Keywords: Commercial species; Nemipteridae; Lessepsian fish; sperm parameters

Received: 14.03.2025
Accepted: 27.03.2025
Published: 15.07.2025

DOI:10.52331/v30i2881

1. Introduction

The recruitment of wild fish populations and the controlled production in aquaculture systems are biological processes intrinsically linked to reproductive success, specifically through the fertilization of mature oocytes. Following this, further stages of the life cycle, such as successful larval development, particularly during critical periods like the initial intake of food, play a key role in recruitment dynamics. Typically, fish undergo seasonal gametogenesis and exhibit synchronized reproductive behaviors, resulting in the release of gametes into the aquatic environment for external fertilization. The success of fertilization is influenced by both the intrinsic characteristics of the gametes, such as quality and quantity and the environmental conditions at the site of gamete fusion. Consequently, fertilization serves as a complex integrative outcome of multiple interacting factors, potentially masking variations in the inherent quality of sperm. Recent comprehensive reviews Cabrita, Engrola [1], Bobe and Labbé [2] have demonstrated that while various sperm characteristics collectively influence overall sperm quality, none of these attributes

alone is sufficient to fully describe the fertilization potential of spermatozoa. Additionally, the evaluation of sperm quality can significantly benefit from the standardization of analytical methodologies and techniques.

In mammals, alterations in sperm structure, including changes in flagellum length or head size, have been observed under various conditions. During the 1990s, image analysis techniques were adapted for the study of mammalian sperm morphology, leading to the development of Automated Sperm Morphology Analysis (ASMA). This approach was first utilized to evaluate fish sperm by Van Look and Kime [3], who examined the impact of increasing mercury concentrations on sperm quality. Subsequently, ASMA has been applied in diverse contexts, such as evaluating the influence of HCG on spermiation in European eel [4], and exploring potential correlations between sperm morphology and swimming performance [5]. In thıs study we also observed N. randalli spermatozoa under the light microscobe (Figure 2).

Spermatozoa concentration in semen can be measured using various techniques, including microscopic counting, spectrophotometry, flow cytometry, and spermatocrit evaluation (as reviewed by Alavi, Psenicka [6]). However, each of these methods has certain limitations. Microscopic counting, considered the fundamental approach, provides sperm counts with reasonable accuracy, though subject to variability stemming from dilution and counting errors. For instance, an error margin of approximately 6% has been reported when counting 300 spermatozoa per observation using a 1/500 diluted sample over three repetitions [7]. While this method is the most cost-effective for measuring sperm concentration, its primary drawback is its labor-intensive nature, which makes it less practical for downstream applications such as sperm preservation or partitioning for genetic cross-breeding studies.

At the subcellular level, sperm quality is often evaluated based on the integrity of the spermatozoa's plasma membrane, which plays a crucial role in regulating ion and water exchange between the intracellular and extracellular environment, thereby influencing axonemal motion as described by Cosson, Groison [8] and Inaba [9]. Practically, membrane integrity has been examined using dye-penetration assays such as eosin/nigrosin or eosin staining alone, followed by microscopic observation, particularly in studies on mammals [10] and fish [11]. More recent approaches involve the use of fluorescent DNA-binding dyes like Hoechst 33258 and Propidium Iodide (PI), or more sophisticated kits with markers such as Sybr-14/PI, which enable concurrent visualization of both live and dead sperm cells. Viability percentages have been determined through direct counting or image analysis under the microscope [4, 12], flow cytometric analysis [13, 14].

The colonization of Red Sea species in the Mediterranean began sometime after the opening of the Suez Canal in 1869, a process that has had bioecological and economic impacts that continue today [15-18].

Nemipterus randalli Russell, 1986 is a Red Sea Lessepsian species [19]. It has a wide geographical distribution from the coasts of eastern and western India to Pakistan, the Persian Gulf, the Red Sea, the Gulf of Aden, East Africa, Seychelles and Madagascar in the western Indian Ocean [17, 20-22]. Golani and Sonin [23] recorded first time in the Mediterranean under the name N. japonicus in Israel. After a short time, it spread westward and was discovered in Lebanon by Lelli, Colloca [24], in Iskenderun Bay [20, 21], in Antalya Bay [25], in Gökova Bay [26], in the Mediterranean coast of Egypt [27], and in Greece [28].

Nemipterus randalli is a bottom fish that lives on sandy or muddy bottoms at depths ranging from 22 to 225 meters. It has an ellipsoid body shape and a silvery pink tint with three or four faint yellow stripes. The upper rays are recognized by a forked caudal fin with a long filament [29]. It feeds mostly on crustaceans, with minor amounts of small fish, polychaetes, molluscs, and spiny skins [21, 30, 31].

The number of studies on the distribution and ecology of N. randalli in the Mediterranean has increased in recent years [17, 20, 21, 23-27, 30-40].

There are limited studies on the reproductive biology of N. randalli [22, 31, 41]. In these studies, information on important reproductive parameters such as sex ratios, gonadasomatic index (GSI) values, fecundity values, etc. were presented. Ozen [42] provided histological information on male and female gonads. There are no studies on sperm parameters. Determination of sperm parameters is an important biological phenomenon in terms of understanding invasion biology. At the same time, this economically important species will also contribute to the evaluation of aquaculture potentials in the future. With this study, spermatological parameters will be determined for the first time in N. randalli species.

2. Materials and Methods

2.1. Ethics statement

This study follows all relevant international, national, and institutional guidelines for the collection and experimental use of fish samples. The fish species examined are not listed in the IUCN Red List of Threatened Species and are not classified as endangered, vulnerable, rare, or protected in Türkiye. Additionally, the sampling sites are situated outside of any designated protected areas, making an ethics statement unnecessary.

2.2 Study design

Samples were collected from trawl surveys conducted in the Gulf of Antalya (Mediterranean-Turkey) between March and April 2024. The fish samples were promptly transported to the laboratory at the Department of Biology, Burdur Mehmet Akif Ersoy University. The individuals' lengths (total length, TL; measured to a precision of 1 mm) and weights (total weight, W; measured to the nearest 0.1 g) were recorded (Figure 1). Gonads were examined macroscopically and microscopically, and sex was determined. After sex determination, sperm concentration and flow cytometric dead-live analysis were performed in terms of spermatological parameters with samples taken from males at Mehmet Akif Ersoy University Reproduction and Artificial Insemination Clinic. Gonads were separated from the fish by dissection and the weights of the gonads were recorded. A total of 9 male fish were analyzed. Testes were dissected in a tube containing 1 ml PBS and allowed to stand for two minutes to allow semen to come out of the tissue into the liquid.

Figure 1. A specimen of *Nemipterus randalli*

2.3 Sperm Concentration

The concentration of semen was determined using the haemocytometric method [43]. The testis was trimmed in 1 ml PBS and incubated in an incubator at 37°C for 2 hours. Subsequently, 10 µl of sperm sample was added to 490 µl of Hayem's solution, and the number of spermatozoa was counted using a Thoma counting chamber. The sperm concentration was expressed as the number of spermatozoa per ml. (spz. / ml) (Figure 3).

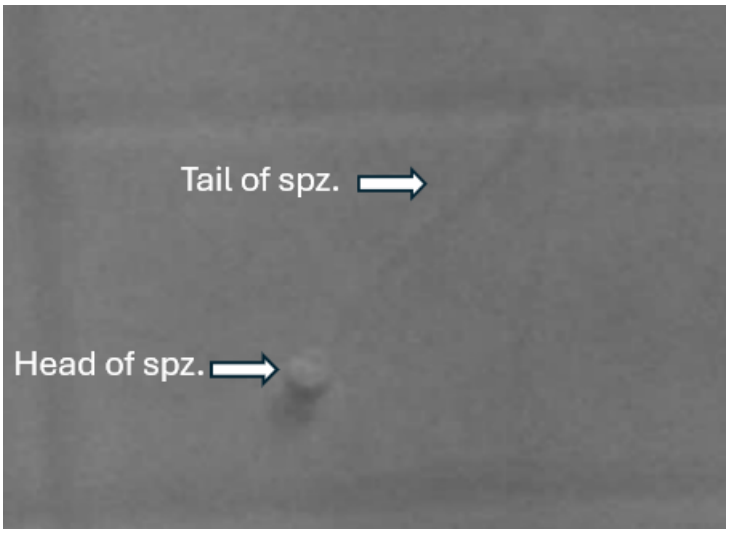

Figure 2. Sections of *N. randalli* spermatozoon

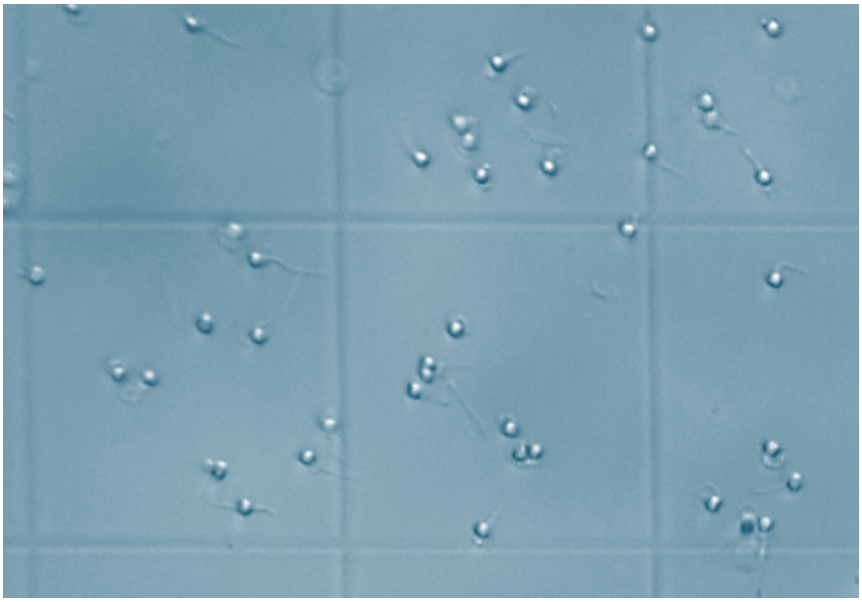

Figure 3. *N. randalli* sperm concentration analysis

2.4. Sperm Viability

The viability of spermatozoa was analysed using a Cytoflex Flow Cytometry device (Beckman Coulter, CA, USA) and a Sybr-14/PI (L7011, Invitrogen, CA, USA) double staining method. 50 µL of sperm sample, and 5 µL of Sybr-14 and 3 µL of PI stain were added to 442 µL of PBS solution. The mixture was then incubated in a dark room at 37 °C in a water bath for 5 minutes. The ratio of live to dead sperm was determined using CytExpert 2.3 software (Figure 4).

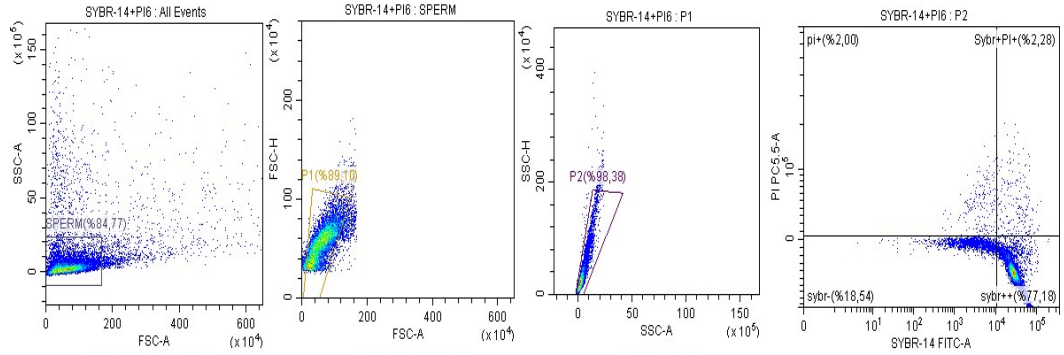

Figure 4. *N. randalli* flow cytometry viability analysis

2.5 Statistical analysis

All parameters, statistical analyses were performed using IBM Corp.'s SPSS (v.22, New York, NY, USA). Datas were given as MEAN±SEM.

3. Result

Based on the sex determination of *N. randalli*, we recorded 17 (65.38%) males, 9 (34.62%) females. The male–female ratio for all fish combined was 1.89:1 and differed statistically from the expected 1:1 ($P < 0.05$). During the study period, 17 male specimens of *N. randalli*, ranging in size from 19 to 27.2 cm in total length and weighing between 80 and 270.5 g, were analyzed.

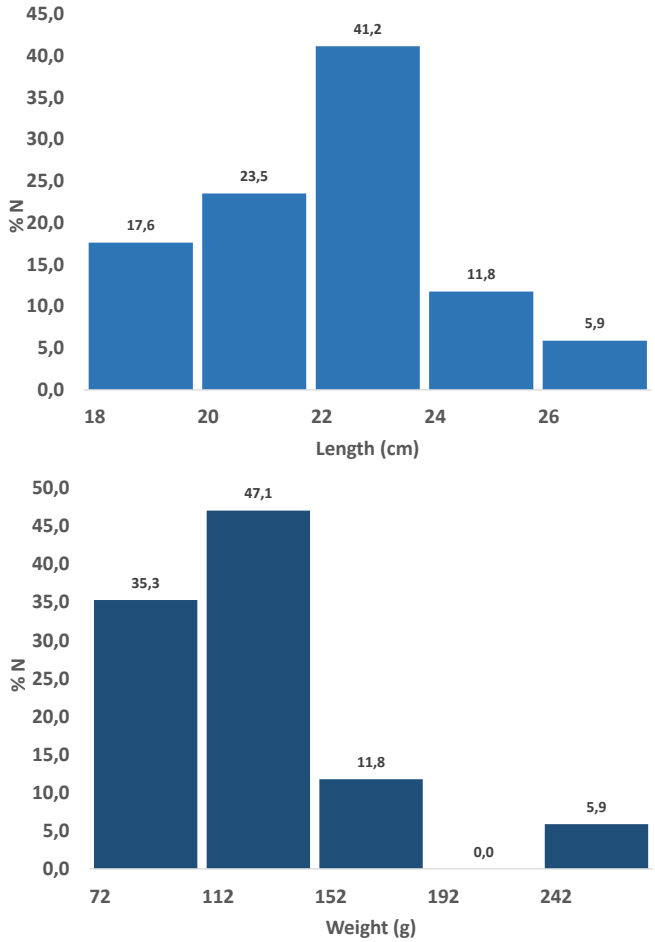

Figure 5. Length and weight distribution of *N. randalli* male specimens

The spermatozoa concentration was determined to be 160.0±45.63×10⁶ spz/ml. The flow cytometric determination of the sperm viability was 51.71±17.01% (Table 1).

Table 1. Total length (TL), total weight (W), sperm concentration, sperm viability values of male *N. randalli* species (Mean±SEM).

Mean Total length (mm)	21.75±0.50
Mean Weight (g)	131.31±10.75
Sperm Concentration (x10⁶/ml)	160.0±45.63
Sperm Viability (%)	51.71±17.01

4. Discussion

N. randalli, an Indo-Pacific fish migrating to the Mediterranean Sea, has established a sustainable population in the Gulf of Antalya, Turkey. No data on spermatological parameters of *N. randalli* were found in the literature. Therefore, in this study, the mean viability and concentration values of spermatozoa of *N. randalli* were investigated for the first time.

Reproductive biology studies on *N. randalli*, which has recently entered the Mediterranean Sea, revealed that reproductive periods differ according to habitats. Ozen [42] showed that the breeding period of *N. randalli* in the Gulf of Antalya is between June and October and the peak breeding period is between July and August. Taylan and Yapıcı [22] indicated that the reproductive activity of both female and male *N. randalli* occurs during the spring and summer months, with females being active

from April to August and males from April to July. Uyan [44], determine the spawning period of the species between May and June. Demirci, Demirci and Şimşek [41], in their study to determine the reproductive period, showed that the gonadosomatic index value of the species increased in February and reached the highest value in April and May. The result of this study that male individuals of *N. randalli* are dominant over female individuals is similar to other studies [17, 21, 22, 31, 35, 44, 45]. To better understand the importance of sperm quality in *N. randalli* reproductive performance, it should be compared with many parameters. In this study, viability and sperm concentrations were revealed. *N. randalli* sperm concentration was found to be 160.0±45.63×10^6 spz/ml. Flow cytometric analysis of sperm viability resulted in a value of 51.71±17.01%. In the literature, spermatozoa concentration values are given for some species. The spermatozoa concentration of Barbus barbus (Teleostei: Cyprinidae) decreased from 18.81× 10^9 spz/ml to 12.45 × 10^9 spz/ml in March to in May and decreased towards the end of the breeding season [6]. Hatipoğlu [46] determined that the average concentration of Abant trout was 17.85x10^9 spz/ml. While the concentration of spermatozoa in rainbow trout was found to be 11.80x10^9 spz/ml, reported it as 6.90 x 10^9 spz/ml by hemacytometric method in their study on the same species[47].

In *N. randalli* viability analysis by flow cytometric method was found 51.71±17.01%. There are some studies on spermatozoa viability rates in natural fish stocks. Trigo, Merino [48] was found the spermatozoa viability in rainbow trout (Oncorhynchus mykiss) 95.1 ± 0.68%. Also Nynca, Dietrich [49] reported that rainbow trout sperm viability was 97.00 ± 0.99% by flow cytometry and 86.22 ± 1.16% by fluorescence microscopy analyse. In a study conducted on Galaxias argenteus, a giant cockle grown in farms, sperm viability was determined to have 4.621 live cells and 1.168 dead cells by flow cytometry [50]. In these studies, it was determined that spermatozoa viability rates differed between species.

Differences in sperm concentration and sperm viability between species may be due to changing habitat conditions and abiotic parameters such as temperature, pH, salinity and dissolved oxygen. For some populations, sperm analyses cover a single sampling period. This may alter sperm values. In addition to seasonality and habitat conditions, the observed variation in sperm parameters may be due to biological characteristics of fish species, sex ratio, invasiveness, reproductive strategies, sampling and analysis methods.

Ozen [42] showed that the breeding period of *N. randalli* in the Gulf of Antalya is between June and October and the peak breeding period is between July and August. Taylan and Yapıcı [22] stated that both female and male *N. randalli* are reproductively active during the spring and summer, with the spawning season for females lasting from April to August and for males from April to July. Likewise, Demirci, Demirci and Şimşek [41] observed in their study on the species' reproductive period that the gonadosomatic index started rising in February and reached its highest levels in April and May.

During the present study males were more abundant in the catch of *N. randalli*. In the *N. randalli* populations under study, the sex ratio which varies from population to population within the same species was 1.89 males to 1 females. The small sample size prevented a clear determination of the gender ratio. According to Bohlen, Freyhof and Nolte [51], the sex ratio in a population can change from year to year, suggesting that genetics or environmental variables play a role in its determination. There are a variety of potential causes for this variation, such as seasonal variations, feeding and

maturation schedules, disparities in male and female growth rates, mortality differences between the sexes, and potentially size-selective impacts of fishing gear.

5. Conclusions

Determining fish sperm parameters is a crucial scientific phenomenon that helps comprehend the biology of invasion. The first information on spermatological characteristics of *N. randalli*, such as spermatozoa concentration and viability, was reported in this study. These data will help determine the invasion ecology, assess the possibility for aquaculture in the future, and comprehend the reproductive biology of this commercially significant species. The normospermic traits of this species will be determined in part by analyzing spermatological traits over time and with a larger number of individuals.

Supplementary Materials: Figure S1: A specimen of Nemipterus randalli, Figure S2: Sections of N. randalli spermatozoon, Figure S3: N. randalli sperm concentration analysis, Figure S4: N. randalli flow cytometry viability analysis, Figure S: Length and weight distribution of N. randalli male specimens, Table S1: Total length (TL), total weight (W), sperm concentration, sperm viability values of male N. randalli species (Mean±SEM)

Author Contributions: Gungor S.: Conceptualization, sampling, methodology, investigation, formal analysis, writing—original draft, writing—review and editing. Mart F.: Methodology, validation, formal analysis, writing—original draft. Inanc ME: Formal analysis, original draft, writing—review and editing. Innal D.: Conceptualization, sampling, methodology, writing—original draft, writing—review and editing.

Funding: This research received no external funding.

Institutional Review Board Statement: This study follows all relevant international, national, and institutional guidelines for the collection and experimental use of fish samples. The fish species examined are not listed in the IUCN Red List of Threatened Species and are not classified as endangered, vulnerable, rare, or protected in Türkiye. Additionally, the sampling sites are situated outside of any designated protected areas, making an ethics statement unnecessary.

Acknowledgments: The authors have no support to report.

Conflicts of Interest: The authors declare no conflict of interest.

References

1. Cabrita, E., et al., Successful Cryopreservation of sperm from sex-reversed dusky grouper, Epinephelus marginatus. *Aquaculture*, **2009**. 287: p. 152-157. 10.1016/j.aquaculture.2008.10.019
2. Bobe, J. and C. Labbé, Egg and sperm quality in fish. *General and Comparative Endocrinology*, **2010**. 165(3): p. 535-548. https://doi.org/10.1016/j.ygcen.2009.02.011
3. Van Look, K.J.W. and D.E. Kime, Automated sperm morphology analysis in fishes: the effect of mercury on goldfish sperm. *Journal of Fish Biology*, **2003**. 63(4): p. 1020-1033. https://doi.org/10.1046/j.1095-8649.2003.00226.x
4. Asturiano, J.F., et al., Effects of hCG as spermiation inducer on European eel semen quality. *Theriogenology*, **2006**. 66(4): p. 1012-20. 10.1016/j.theriogenology.2006.02.041
5. Tuset, V.M., E.A. Trippel, and J. De Monserrat, Sperm morphology and its influence on swimming speed in Atlantic cod. *Journal of Applied Ichthyology*, **2008**. 24(4): p. 398-405. https://doi.org/10.1111/j.1439-0426.2008.01125.x
6. Alavi, S.M.H., et al., Changes of sperm morphology, volume, density and motility and seminal plasma composition in Barbus barbus (Teleostei: Cyprinidae) during the reproductive season. *Aquat Living Resour*, **2008**. 21(1): p. 75-80. https://doi.org/10.1051/alr:2008011

7. Suquet, M., M.H. Omnes, Y. Normant, and C. Fauvel, Assessment of sperm concentration and motility in turbot (Scophthalmus maximus). *Aquaculture*, **1992**. 101(1): p. 177-185. https://doi.org/10.1016/0044-8486(92)90241-C
8. Cosson, J., et al., Marine fish spermatozoa: racing ephemeral swimmers. *Reproduction*, **2008**. 136(3): p. 277-94. 10.1530/rep-07-0522
9. Inaba, K., Molecular mechanisms of the activation of flagellar motility in sperm. 2008; 267-279.
10. Björndahl, L., I. Söderlund, and U. Kvist, Evaluation of the one-step eosin-nigrosin staining technique for human sperm vitality assessment. *Hum Reprod*, **2003**. 18(4): p. 813-6. 10.1093/humrep/deg199
11. Zilli, L., et al., Adenosine Triphosphate Concentration and β-d-Glucuronidase Activity as Indicators of Sea Bass Semen Quality. *Biology of Reproduction*, **2004**. 70(6): p. 1679-1684. 10.1095/biolreprod.103.027177
12. Flajšhans, M., J. Cosson, M. Rodina, and O. Linhart, The application of image cytometry to viability assessment in dual fluorescence-stained fish spermatozoa. *Cell Biology International*, **2004**. 28(12): p. 955-959. https://doi.org/10.1016/j.cellbi.2004.07.014
13. De Baulny, B.O., Y. Le Vern, D. Kerboeuf, and G. Maisse, Flow cytometric evaluation of mitochondrial activity and membrane integrity in fresh and cryopreserved rainbow trout (Oncorhynchus mykiss) spermatozoa. *Cryobiology*, **1997**. 34(2): p. 141-149.
14. Cabrita, E., et al., Evaluation of DNA damage in rainbow trout (Oncorhynchus mykiss) and gilthead sea bream (Sparus aurata) cryopreserved sperm. *Cryobiology*, **2005**. 50(2): p. 144-153. https://doi.org/10.1016/j.cryobiol.2004.12.003
15. Galil, B.S., et al., 'Double trouble': the expansion of the Suez Canal and marine bioinvasions in the Mediterranean Sea. *Biol Invasions*, **2015**. 17: p. 973-976. http://dx.doi.org/10.3391/mbi.2016.7.2.01
16. Golani, D., The marine ichthyofauna of the Eastern Levant—history, inventory, and characterization. *Isr J Ecol Evol*, **1996**. 42(1): p. 15-55. https://doi.org/10.1080/00212210.1996.10688830
17. Innal, D., et al., Age and growth of Nemipterus randalli from Antalya Gulf-Turkey. *Int J Fish Aquat Stud*, **2015**. 2(4): p. 299-303.
18. Spanier, E. and B.S. Galil, Lessepsian migration: a continuous biogeographical process. *Endeavour*, **1991**. 15: p. 102-106. https://doi.org/10.1016/0160-9327(91)90152-2
19. Tikochinski, Y., et al., Reduced genetic variation of the Red Sea fish, Randall's threadfin bream Nemipterus randalli, invasive in the Mediterranean Sea. *Aquat Invasions*, **2019**. 14(4): p. 716-723. https://doi.org/10.3391/ai.2019.14.4.10
20. Bilecenoglu, M. and B.C. Russell, Record of Nemipterus randalli Russell, 1986 (Nemipteridae) from Iskenderun Bay, Turkey. *Cybium*, **2008**. 32(3): p. 279-280. https://doi.org/10.26028/cybium/2008-323-014
21. Erguden, D., et al., Age and growth of the Randall's threadfin bream Nemipterus randalli (Russell, 1986), a recent Lessepsian migrant in Iskenderun Bay, northeastern Mediterranean. *J Appl Ichthyol*, **2010**. 26(3): p. 441-444. https://doi.org/10.1111/j.1439-0426.2009.01387.x
22. Taylan, B. and S. Yapıcı, Reproductive biology of non-native Nemipterus randalli Russell, 1986 and native Pagellus erythrinus (Linnaeus, 1758) from the Aegean Sea. **2021**.
23. Golani, D. and O. Sonin, The Japanese threadfin bream Nemipterus japonicus, a new Indo - Pacific fish in the Mediterranean
24. Lelli, S., F. Colloca, P. Carpentieri, and B. Russell, The threadfin bream Nemipterus randalli (Perciformes: Nemipteridae) in the eastern Mediterranean Sea. *J Fish Biol*, **2008**. 73(3): p. 740-745. http://dx.doi.org/10.1111/j.1095-8649.2008.01962.x
25. Gökoglu, M., et al., First records of Nemichthys scolopaceus and Nemipterus randalli and second record of Apterichthus caecus from Antalya Bay, Southern Turkey. *Mar Biodivers Rec*, **2009**. 2: p. e29. http://dx.doi.org/10.1017/S175526720800033X
26. Gülşahin, A. and A. Kara, Record of Nemipterus randalli Russell, 1986 from the southern Aegean Sea (Gokova Bay, Turkey). *J. Appl. Ichthyol*, **2013**. 29( ): p. 933–934. http://dx.doi.org/10.1111/jai.12187
27. ElHaweet, A.E.A., Biological studies of the invasive species Nemipterus japonicus (Bloch, 1791) as a Red Sea immigrant into the Mediterranean. *Egypt J Aquat Res*, **2013**. 39(4): p. 267-274. https://doi.org/10.1016/j.ejar.2013.12.008
28. Kampouris, T.E., N. Doumpas, I. Giovos, and I.E. Batjakas, First record of the Lessepsian Nemipterus randalli Russell, 1986 (Perciformes, Nemipteridae) in Greece. *Cah Biol Mar*, **2019**. 60(6): p. 559-561. http://dx.doi.org/10.21411/CBM.A.53CEC126
29. Russell, B.C., *FAO Species Catalogue: Nemipterid Fishes of the World (Threadfin Breams, Whip Tail Breams, Monocle Breams, Dwarf Monocle Breams and Coral Breams*; FAO, 1990.
30. Gurlek, M., et al., Feeding habits of indo-pacific species Nemipterus randalli Russel, 1986 (Nemipteridae) in Iskenderun bay, Eastern Mediterranean Sea. *Rapp p.-v. réun - Cons. int. explor mer*, **2010**. 39: p. 539.
31. Yapıcı, S. and H. Filiz, Biological aspects of two coexisting native and nonnative fish species in the Aegean Sea: Pagellus erythrinus vs. Nemipterus randalli. *Mediterr Mar Sci*, **2019**. 20(3): p. 594-602. https://doi.org/10.12681/mms.19658

32. Akgun, Y. and E. Akoglu, Randall's Threadfin Bream (Nemipterus randalli, Russell 1986) Poses a Potential Threat to the Northeastern Mediterranean Sea Food Web. *Fishes*, **2023**. 8(8): p. 402.
33. Ali, M., A. Saad, C. Reynaud, and C. Capapé. Fırst Records Of Randall's Threadfın Bream Nemıpterus Randallı (Osteıchthyes: Nemıpterıdae) Off The Syrıan Coast (Eastern Medıterranean)/Prıme Segnalazıonı Dı Nemıpterus Randallı (Osteıchthyes: Nemıpterıdae) Al Largo Della Costa Della Sırıa (Medıterraneo Orıentale). in *Ann Ser Hist Nat*. 2013. Scientific and Research Center of the Republic of Slovenia.
34. Aydın, İ. and O. Akyol, Occurrence of Nemipterus randalli Russell, 1986 (Nemipteridae) off Izmir Bay, Turkey. *Egypt J Aquat Res*, **2016**. 18(39): p. 267-74. https://doi.org/10.1111/jai.13331
35. Özen, M.R. and O. Çetinkaya, Population Composition, Growth and Fisheries of Nemipterus randalli Russell, 1986 in Antalya Gulf, Mediterranean Sea, Turkey. *Acta Aquat Turc*, **2020**. 16(3): p. 330-337. https://doi.org/10.22392/actaquatr.681309
36. Tartar, Ü. and H. Yeldan, Some population dynamic parameters of Northeastern Mediterranean (Iskenderun Bay) threadfin bream, Nemipterus randalli Russell, 1986. *Acta Aquat Turc*, **2022**. 35(3): p. 3-1-7.
37. Uyan, U., et al., Fish length and otolith size of in Nemipterus randalli Russel, 1986 (Actinopterygii: Perciformes: Nemipteridae) collected from Gökova Bay, Turkey. *Thalass Sal*, **2019**. 41: p. 137-146. http://dx.doi.org/10.1285/i15910725v41p137
38. Yazıcı, R., et al., The length-weight (LWR) and length-length (LLR) relationships of Nemipterus randalli (Russel, 1986), an invasive species in Iskenderun Bay. *Acta Bio Turc*, **2024**. 37(1): p. 7-1-7.
39. Yazici, R., Sex ‐ linked variations in the sagittal otolith biometry of Nemipterus randalli (Russell, 1986) from the eastern Mediterranean Sea. *J Fish Biol*, **2023**. 102(1): p. 241-247. https://doi.org/10.1111/jfb.15256
40. Stern, N., et al., Distribution and population structure of the alien Indo ‐ Pacific Randall's threadfin bream Nemipterus randalli in the eastern Mediterranean Sea. *J Fish Biol*, **2014**. 85(2): p. 394-406. https://doi.org/10.1111/jfb.12421
41. Demirci, S., A. Demirci, and E. Şimşek, Spawning season and size at maturity of a migrated fish, Randall's Threadfin Bream (Nemipterus randalli) in Iskenderun Bay, Northeastern Mediterranean, Turkey. *Fresenius Environ Bull*, **2018**. 27(1): p. 503-507. https://dx.doi.org/10.17582/journal.pjz/20180327130349
42. Ozen, M.R., Some histological reveals on reproduction of one of the lessepsian species, Nemipterus randalli in Antalya (Turkey). **2021**. https://doi.org/10.3906/vet-2007-96
43. Caille, N., et al., Quantity, motility and fertility of tench Tinca tinca (L.) sperm in relation to LHRH analogue and carp pituitary treatments. *Aquac Int*, **2006**. 14(1): p. 75-87. http://dx.doi.org/10.1007/s10499-005-9015-0
44. Uyan, U., Nemipterus Randalli Russell, 1986nin Gökova Körfezinde bazı biyolojik özelliklerinin belirlenmesi. PhD Thesis, PhD Thesis, University of Muğla Sıtkı Koçman, Muğla, 2017.
45. Al-Kiyumi, F., S. Mehanna, and N. Al-Bulush, Growth, mortality and yield per recruit of the Randall's threadfin bream Nemipterus randalli (Russell, 1986) from the Arabian Sea off Oman. *Thalassas*, **2014**. 30(1): p. 67-73.
46. Hatipoğlu, T., Abant Alabalığında (salmo trutta abanticus) bazı reprodüktif özelliklerin saptanması, spermanın kısa süreli saklanması ve dölverimi. **2007**.
47. Seçer, S., E. Akçay, Y. Bozkurt, and S. Kayam, Gökkuşağı Alabalıklarında (Oncorhynchus mykiss W., 1792) Yaşın Spermatolojik Özellikler Üzerine Etkisi. *Turk J Vet Anim Sci*, **2003**. 27: p. 37-44.
48. Trigo, P., et al., Effect of short ‐ term semen storage in salmon (O ncorhynchus mykiss) on sperm functional parameters evaluated by flow cytometry. *Andrologia*, **2015**. 47(4): p. 407-411. https://doi.org/10.1111/and.12276
49. Nynca, J., et al., Usefulness of a portable flow cytometer for sperm concentration and viability measurements of rainbow trout spermatozoa. *Aquaculture*, **2016**. 451: p. 353-356. http://dx.doi.org/10.1016/j.aquaculture.2015.09.027
50. Pearce, J., et al., Assessing sperm membrane viability using flow cytometry in farmed New Zealand giant kokopu Galaxias argenteus. *N Z J Mar Freshw Res*, **2018**. 52(3): p. 362-371. https://doi.org/10.1080/00288330.2017.1394883
51. Bohlen, J., J. Freyhof, and A. Nolte, Sex ratio and body size in Cobitis elongatoides and Sabanejewia balcanica (Cypriniformes, Cobitidae) from a thermal spring. *Folia Zool*, **2008**. 57(1/2): p. 191.

CVJ CLUJ VETERINARY JOURNAL

Article

Pathological findings of an eye anomaly in Randall's threadfin bream *Nemipterus randalli* Russell, 1986 from the Mediterranean Sea (Antalya Gulf-Türkiye)

Şükrü Güngör [1], *, Özlem Özmen [1] and Deniz İnnal[2]

1 Burdur Mehmet Akif Ersoy University, Faculty of Veterinary Science, Istiklal Campus, 15030, Burdur, Türkiye; ozlemoz@mehmetakif.edu.tr
2 Burdur Mehmet Akif Ersoy University, Department of Biology, Istiklal Campus, 15030, Burdur, Türkiye; denizinnal@mehmetakif.edu.tr
* Correspondence: sukrugungor@mehmetakif.edu.tr ; Tel.: +90 248 2132183

Abstract: Genetic, environmental and nutritional conditions seriously affect the health of natural fish stocks. In addition, increasing human pressure on aquatic systems in recent years is threatening fish populations. Under the influence of increasing environmental pressures and other factors, different types of abnormalities are observed in fish. Among these, morphological abnormalities, pigmentation abnormalities, eye abnormalities, visceral abnormalities and reproductive abnormalities are commonly observed. There is limited information on eye abnormalities in Mediterranean fish species. In the present study, the body abnormality observed in a trawl-caught specimen of Randall's threadfin bream, in which the eyes were missing, and its causes are reported and the pathological findings discussed.

Keywords: Red Sea; Lessepsian; Randall's threadfin bream; ocular abnormalities

Received: 25.02.2025
Accepted: 28.02.2025
Published: 15.07.2025

DOI:10.52331/v30i2k31

1. Introduction

Several types of abnormalities have been reported in fish. These abnormalities include morphological abnormalities, pigmentation abnormalities, ocular abnormalities, visceral abnormalities and reproductive abnormalities[1, 2]. These abnormalities may be due to genetic, environmental, nutritional and stress factors. Abnormalities observed in fish can affect the health and quality of life of the fish in several ways. These effects can often have a negative impact on the fish's general physiological functions, growth rate, reproductive ability and even survival rate [3, 4]. Among the abnormalities observed in fish, ocular abnormalities have a very important impact on fish health. It is reported that microphthalmia, anophthalmia, cataract, abnormalities in eye size and location are common among eye abnormalities. Eye abnormalities in fish have been reported under both aquaculture conditions and from natural stocks [5].

This paper describes the physical body abnormality observed in an individual (*Nemipterus randalli*) without its eyes, collected from the Gulf of Antalya, in the Mediterranean Sea, on 18 March 2024. The number of studies on the distribution and ecology of N. randalli in the Mediterranean has increased in recent years [6-11]. As far as it is known, this study is the first record of eye deformity of Randall's threadfin bream along the Mediterranean. Simultaneously, this report constitutes the pathological findings of this deformity.

2. Materials and Methods

2.1. Ethics statement

This study follows all relevant international, national, and institutional guidelines for the collection and experimental use of fish samples. The fish species examined are not listed in the IUCN Red List of Threatened Species and are not classified as endangered, vulnerable, rare, or protected in Türkiye. Additionally, the sampling sites are situated outside of any designated protected areas, making an ethics statement unnecessary.

2.2. Study design

The specimen of *N. randalli* obtained from the Gulf of Antalya was caught during trawl surveys on 18 March 2024. Fish samples were transported directly to the lab, where measurements were made of their weight (total weight W to the nearest 0.1 g) and length (total length cm TL, precision 1 mm). The gonads were examined both macroscopic and microscopic to determine the sex. During the necropsy, the eyes of the fish were examined grossly and then carefully enucleated. The eye samples were collected, and the fish were fixed in 10% neutral formalin. Normal fish eye were also collected for comparison. The formalin-fixed tissues were embedded in paraffin following standard processing with an automatic tissue processor (Leica ASP300S; Leica Microsystems, Nussloch, Germany). Using a Leica RM 2155 rotary microtome (Leica Microsystems, Nussloch, Germany), serial sections with a thickness of 5 μm were cut. Hematoxylin and eosin (HE) staining was applied to each section, and each was inspected under a light microscope. The Database Manual Cell Sens Life Science Imaging Software System (Olympus Corporation, Tokyo, Japan) was used for microphotography.

3. Results

Abnormality was recorded in one specimen of *N. randalli* obtained from Antalya Gulf. The Randall's threadfin bream specimen was obtained from with trawl surveys. The specimen had a normal body shape, but eyes were missing with no injury (Figure 1). The total body length was 18.4 cm, and the total weight was 69.3 g.

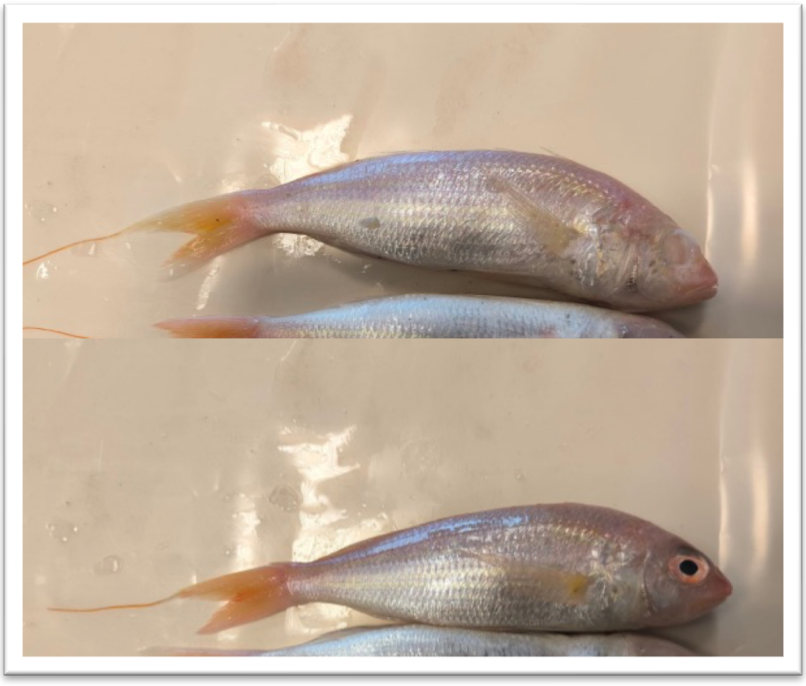

Figure 1. Macroscopic appearance of normal and anomalous fish, iris and pupil of the normal fish and no iris and pupil of anomalous fish.

3.1. Gross Findings

During the macroscopic examination of the normal fish eye, a distinct yellow-orange iris and a prominent black pupil in the center were observed. In the eye of the anomalous fish, only scleral structures within the orbit were observed (Figure 1).

Macroscopic examination of the anomalous fish's body revealed normal body appearance but during the opening of the abdominal cavity, the organs appeared atrophic compared the normal fish (Figure 2).

Figure 2. Appearance of abdominal organs of the normal and anomalous fish.

Microscopic examination revealed that only the sclera was present in the eye. The retinal layer was completely undeveloped. No melanocytes were observed. Only a hypoplastic, small lens remnant was noted. No other ocular structures were seen (Figure3).

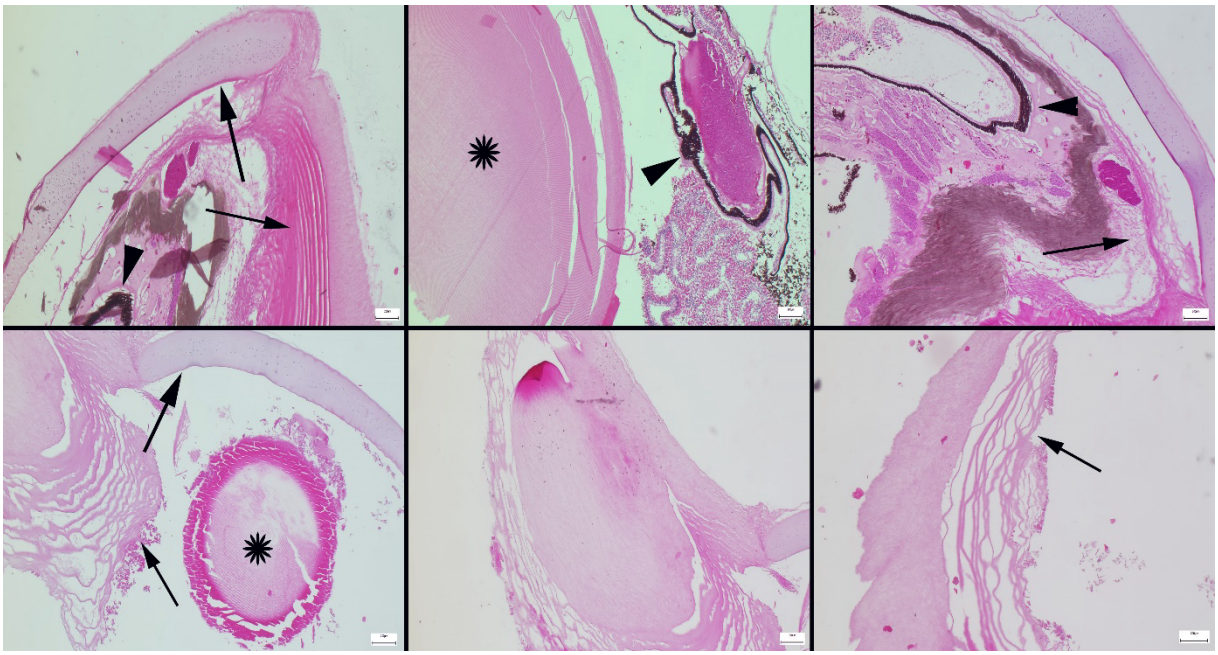

Figure 3. Normal (upper row) and anomalous eyes (below row) histopathology findings. Scleral cartilages (thick arrows), and scleral stroma (thin arrows), normal lens of normal fish and atrophic lens in anomalous fish (stars) and retinal layer (arrowhead) in normal fish but no retina in anomalous fish, HE, scale bars= 200µm.

4. Discussion

Nemipterus randalli has a wide geographical distribution from the coasts of eastern and western India to Pakistan, the Persian Gulf, the Red Sea, the Gulf of Aden, East Africa, Seychelles and Madagascar in the western Indian Ocean [10, 12-14]. *N. randalli* was first recorded in Israel in the Mediterranean. In the following years, it showed a widespread distribution in the Mediterranean. This species, which has been caught in high density in the Mediterranean coast of Turkey in recent years, is economically utilized. It has a high economic value due to its similarity to coral species. This species, which has been caught in high density in the Mediterranean coast of Turkey in recent years, is economically utilized.

Some abnormalities have been reported due to different reasons in the natural habitat of this species and in the Mediterranean Sea. Pigment anomaly was reported in the natural distribution area of Nemipterus [15]. Pugheadness anomaly was reported in Gökova (Muğla) populations of Nemipterus which introduced to the Mediterranean Sea [16]. A number of factors have been identified as contributing to fish abnormalities, including unfavourable abiotic conditions; and pollutants such as pesticides, chlorinated hydrocarbons, organophosphates, heavy metals, infectious agents, inappropriate nutrition and genetic factors [2, 3, 17].

According to Smith, Donahue [5], the abnormalities found in fish eyes include opaque or cloudy eyes, exophthalmia, missing eyes, hemorrhagic eyes, emboli, and gas bubbles in the eye. A number of factors, such as gas imbalances that cause exophthalmos, toxicants that cause hyperemia, cataract, retinitis, and keratitis, low temperatures and osmotic imbalances that cause cataract, on the other hand

nutritional deficiencies that cause cataract, retinal and corneal, diseases, parasitemias that cause exophthalmos, keratitis, cataract, radiation damage that causes keratitis, cataract, trauma from iatrogenic factors, and injuries from uncontrolled culture systems, can lead to eyes lesions[18]. When the abnormalities reported in this species were analysed, it was found that no eye anomaly had been reported before. In the study, it was determined that the eyes abnormalities one speciemen of *N. randalli* showed macroscopic and microscopic differences compared to normal individuals. It is thought that this situation negatively affects the fish physiologically.

5. Conclusions

To the best of our knowledge, this survey reports the first eye abnormalities in *Nemipterus randalli*. The causes of the eye anomaly found in *N. randalli* are unknown. In countries bordering the Mediterranean Sea, increasing human activities are changing the quality of seawater. Numerous physiological and morphological changes in marine organisms have been reported as a result of water quality. Nervous necrosis virus (NNV), which is reported to infect about 40 fish species worldwide, was detected in *N. randalli* in a study conducted in the Mediterranean Sea [19]. NNV infection targets the central nervous system, including the brain, spinal cord and eye. Due to the fact that the Randall's threadfin bream is commercial species, further studies are needed in order to assess the eye abnormalities in Mediterranean populations.

Author Contributions: Gungor S.: Conception and design of the study, Gungor S., Ozmen O., and Innal D.; acquisition and analysis of data, interpretation of data. Ozmen O., Gungor S., and Innal D. drafting of manuscript. Gungor S., and Innal D. revision of the manuscript. All authors read and approved the final manuscript.

Funding: The authors have no funding to report.

Institutional Review Board Statement: This study follows all relevant international, national, and institutional guidelines for the collection and experimental use of fish samples. The fish species examined are not listed in the IUCN Red List of Threatened Species and are not classified as endangered, vulnerable, rare, or protected in Türkiye. Additionally, the sampling sites are situated outside of any designated protected areas, making an ethics statement unnecessary.

Acknowledgments: The authors have no support to report.

Conflicts of Interest: The authors declare no conflict of interest.

References

1. Dawson, C.E., *A Bibliography of Anomalies of Fishes.* Gulf and Caribbean Research, 1964. **1**: p. 308-399.
2. Eissa, A.E., et al., *A comprehensive overview of the most common skeletal deformities in fish.* Aquaculture Research, 2021. **52**(6): p. 2391-2402.
3. Boglione, C., et al., *Skeletal anomalies in reared E uropean fish larvae and juveniles. Part 2: main typologies, occurrences and causative factors.* Reviews in Aquaculture, 2013. **5**: p. S121-S167.
4. Divanach, P., et al., *Abnormalities in finfish mariculture: An overview of the problem, causes and solutions.* Special publication/European aquaculture society, 1996: p. 45-66.
5. Smith, S.B., et al., *Illustrated field guide for assessing external and internal anomalies in fish*, in *Information and Technology Report*. 2002, US Geological Survey.
6. Akgun, Y. and E. Akoglu, *Randall's Threadfin Bream (Nemipterus randalli, Russell 1986) Poses a Potential Threat to the Northeastern Mediterranean Sea Food Web.* Fishes, 2023. **8**(8): p. 402.

7. Ali, M., A. Saad, C. Reynaud, and C. Capapé. *First Records Of Randall's Threadfin Bream Nemipterus Randalli (Osteichthyes: Nemipteridae) Off The Syrian Coast (Eastern Mediterranean)/Prime Segnalazioni Di Nemipterus Randalli (Osteichthyes: Nemipteridae) Al Largo Della Costa Della Siria (Mediterraneo Orientale)*. in *Annales: Series Historia Naturalis*. 2013. Scientific and Research Center of the Republic of Slovenia.
8. ElHaweet, A.E.A., *Biological studies of the invasive species Nemipterus japonicus (Bloch, 1791) as a Red Sea immigrant into the Mediterranean.* The Egyptian Journal of Aquatic Research, 2013. **39**(4): p. 267-274.
9. Stern, N., et al., *Distribution and population structure of the alien Indo-Pacific Randall's threadfin bream Nemipterus randalli in the eastern Mediterranean Sea.* Journal of fish biology, 2014. **85**(2): p. 394-406.
10. Innal, D., et al., *Age and growth of Nemipterus randalli from Antalya Gulf-Turkey*. International Journal of Fisheries and Aquatic Studies, 2015. **2**(4): p. 299-303.
11. Yazici, R., et al., *The length-weight (LWR) and length-length (LLR) relationships of Nemipterus randalli (Russel, 1986), an invasive species in Iskenderun Bay.* Acta Biologica Turcica, 2024. **37**(1): p. 7-1-7.
12. Bilecenoglu, M., *Record of Nemipterus randalli Russell, 1986 (Nemipteridae) from Iskenderun Bay, Turkey.* Cybium, 2008. **32**(3): p. 279-280.
13. Erguden, D., et al., *Age and growth of the Randall's threadfin bream Nemipterus randalli (Russell, 1986), a recent Lessepsian migrant in Iskenderun Bay, northeastern Mediterranean.* Journal of Applied Ichthyology, 2010. **26**(3): p. 441-444.
14. Taylan, B. and S. Yapıcı, *Reproductive biology of non-native Nemipterus randalli Russell, 1986 and native Pagellus erythrinus (Linnaeus, 1758) from the Aegean Sea.* North-Western Journal of Zoology, 2021. **17**(2): p. 180-186.
15. Jawad, L.A., F. Mutlak, and A. Al-Faisal, *Partial and hyper-melanic pigmentation in fishes collected from the marine waters of Iraq, Arabian Gulf.* Thalassia Salentina, 2022. **44**: p. 27-40.
16. Jawad, L.A., M. Çelik, and C. Ateş, *Occurrence of scoliosis, pugheadness and disappearance of pelvic fin in three marine fish species from Turkey.* International Journal of Marine Science, 2017. **7**(28): p. 275-283.
17. Slooff, W., *Skeletal anomalies in fish from polluted surface waters.* Aquatic toxicology, 1982. **2**(3): p. 157-173.
18. Hargis Jr, W.J., *Disorders of the eye in finfish.* Annual Review of Fish Diseases, 1991. **1**: p. 95-117.
19. Lampert, Y., et al., *Indigenous versus Lessepsian Hosts: Nervous Necrosis Virus (NNV) in Eastern Mediterranean Sea Fish.* Viruses, 2020. **12**(4): p. 430.

1
2

CVJ CLUJ VETERINARY JOURNAL

Case Report

Percutaneous balloon valvuloplasty for management of pulmonic stenosis in four dogs: First experience in Veterinary Medicine in Romania

Florin Leca [3], Altin Cala [2], , Stefan A. Geanta[3], Mihaela C. Ivanciu[3], Alina Nechifor[4], Ana Maria Vlas[3]*, Luigi Venco[1]

[1] Ospedale Veterinario Città di Pavia, Pavia, Italy; luigivenco@libero.it
[2] The Ralph Veterinary Referral Centre, Marlow, Buckinghamshire, UK
[3] Doctor's Vet Univers Clinic , Bucharest, Romania, leca_florin2000@yahoo.com
[4] Dr. Bercaru Veterinary Clinic, Bucharest, Romania

* Correspondence: leca_florin2000@yahoo.com

Abstract: Pulmonic stenosis (PS) is one of the most common congenital heart diseases (CHD) in dogs, accounting for approximately 32% of all congenital cardiac defects diagnosed in this species [9]. If severe and left undiagnosed or untreated, PS can lead to signs of right-sided congestive heart failure (R-CHF) and, ultimately, death [7]. This paper describes aspects of the palliative management of PS using percutaneous balloon valvuloplasty (BVP) in four dogs, which, to the authors' knowledge, has not been previously performed in Romania. The minimally invasive procedures were performed between December 2021 and February 2023, at the first Interventional Veterinary Radiology Laboratory in Romania., specialized and optimised for Interventional Veterinary Cardiology (Doctor's Vet Univers Clinic, Bucharest). All patients were referred for signs of exercise intolerance or syncope due to haemodinamic effects of PS. The population included 2 females and 2 males aged between 18 and 72 months. Three dogs who underwent BVP showed a reduction in pressure gradient between 28 and 50 percent and a positive outcome. In one dog, the BPV failed to reduce the pressure gradient, and the patient subsequently suffered a sudden cardiac death (SCD). These findings are comparable with previously reported data in the literature and support the use of BVP as an effective palliative option for managing PS in dogs. Although the learning curve is important for improving outcomes, continued experience remains crucial for achieving consistent success.

Keywords: BVP, minimally invasive, catheterisation, Veterinary Interventional Cardiology

Received: 12.07.2025
Accepted: 14.07.2025
Published: 15.07.2025

DOI:10.52331/v30i2d79

1. Introduction

Pulmonic stenosis is a congenital heart disease, characterized by an obstruction localized at the level of the right ventricular outflow tract. Pulmonic stenosis is the most commonly diagnosed congenital malformation in dogs [2,8,9], accounting for up to 32% of all congenital conditions. In some studies it surpasses subaortic stenosis and patent ductus arteriosus. It can affect both sexes equally and is more commonly described in certain breeds: Boxer, Mongrel, English Bulldog, French Bulldog, Pincher, German Shepherd, Beagle, West Highland White Terrier. [4]

Depending on the location of the stenotic lesion, PS can be classified as subvalvular, valvular and supravalvular. The most common of these is the valvular form and its classified itself into 3 types. Type A is characterized by a normal annulus, but fusion of the cusps with a dome-like appearance during systole. Type B includes valves with thickened cusps and reduced mobility and annulus hypoplasia. The mixed/intermediate type is used to describe condition that have common characters of both types A and B [8,7,4]

The clinical signs observed in dogs with PS are usually related to their severity. In mild forms, clinical signs may be absent, while in moderate to severe forms exercise intollerance, syncope, and signs of R-CHF, such as ascites, pleural effusion and subcutaneous oedema are frequently detected. In most severe cases with marked ventricular hypertrophy leading to myocardial hypoxia, arrhythmias as well as sudden cardiac death may occur [10].

The diagnosis and assessment of the severity of stenosis is achieved by echocardiography, based on morphologic changes of the valve and pressure gradient at this level, in conjunction with other associated changes (right ventricular concentric hypertrophy due to pressure overload, right atrial dilatation frequently associated with tricuspid valve regurgitation and/or post-stenotic dilatation of the pulmonary trunk [10,2]

The most widely used guidelines for classifying the severity of PS were established by Bussadori et al. in 2000. These guidelines define three severity categories based on the maximum pressure gradient measured across the pulmonary valve: mild stenosis corresponds to a peak pressure gradient between 20–49 mmHg, moderate stenosis is defined by a gradient of 50–80 mmHg, and severe stenosis is diagnosed when the pressure gradient exceeds 80 mmHg [4].

Currently, in veterinary medicine, two types of procedures are relatively commonly performed to palliate or alleviate PS: balloon valvuloplasty using different types of catheters, including cutting and high-pressure balloons and transpulmonary stent implantation. Other minimally invasive techniques described in dogs include pulmonary valve implantation, such as the Melody valve. In addition to interventional approaches, some cardiologists employ beta-blocker therapy with the aim of improving diastolic function, reducing right ventricular inotropism and the transvalvular pressure gradient, and thereby decreasing myocardial oxygen consumption [1,3,5,6].

2. Cases

2.1 Case description

Four dogs aged between 18 and 72 months, two males and two females, from three different breeds (one German Shepherd, two West Highland White Terriers and one Lagotto Romagnolo), were included in the present case study. They were diagnosed with valvular pulmonary stenosis type A. Three of them showed syncope on physical efforts at the time of diagnosis.

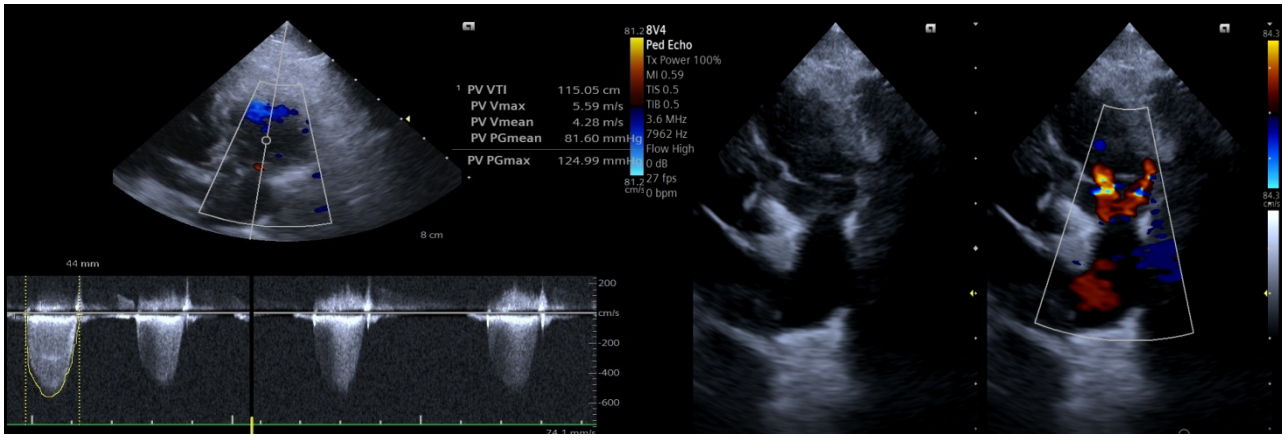

(a) (b)

Fig 1. (Case 1): (a) Right parasternal, short axis view, Continuous wave Doppler at the pulmonary valve level, showing high pressure gradient, suggestive pulmonic stenosis; (b) Right parasternal, short axis view, 2D image and color Doppler during ventricular diastole, showing the presence two pulmonary regurgitation jets and the thickened and fused appearance of the sigmoids.

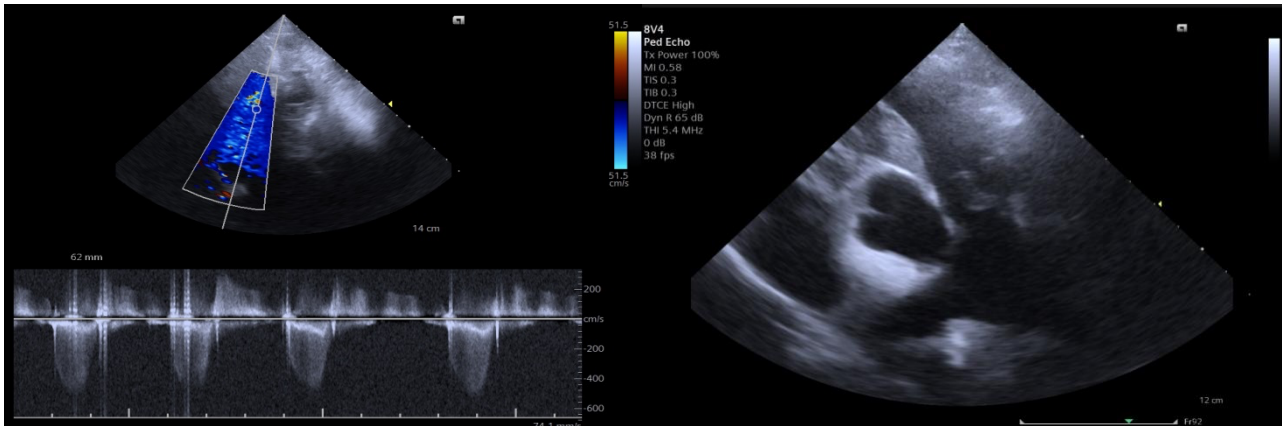

(a) (b)

Fig 2. (Case 2): (a) Right parasternal, short axis view, Continuous wave Doppler at the pulmonary valve level, showing high pressure gradient; (b) Left parasternal, short axis view, 2D image and during ventricular diastole, showing thickened valve sigmoids.

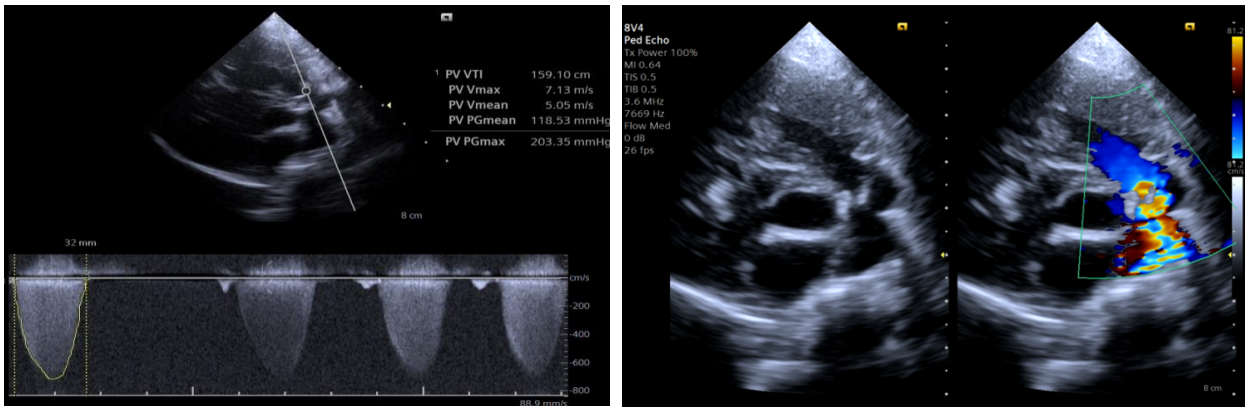

(a) (b)

Fig 3. (Case 3): (a) Right parasternal, short axis view, Continuous wave Doppler at the pulmonary valve level, showing the increased pressure gradient; (b) Right parasternal, short axis view, 2D image and color Doppler during ventricular systole, showing the turbulent flow across the pulmonary valve.

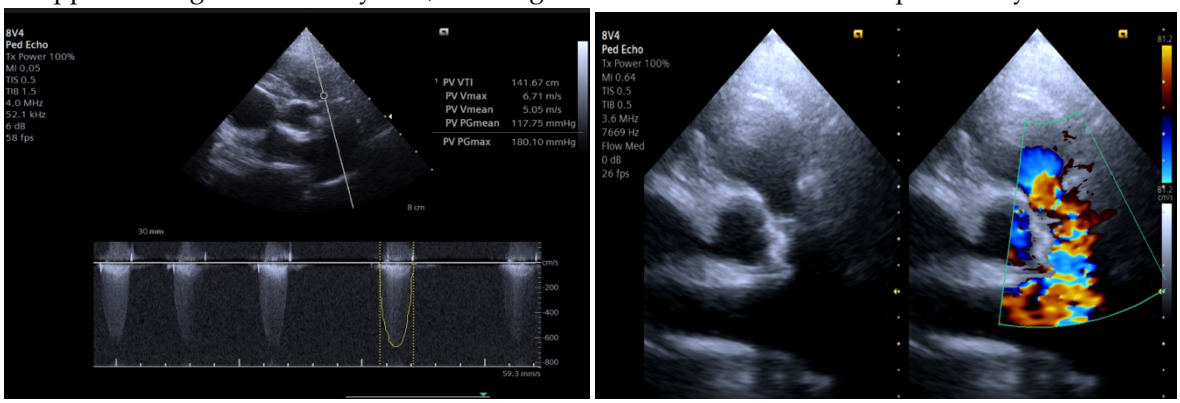

(a) (b)

Fig 4. (Case 4): (a) Right parasternal, short axis view, Continuous wave Doppler at the pulmonary valve level, showing the increased pressure gradient; (b) Right parasternal, short axis view, 2D image and color Doppler during ventricular systole, showing the turbulent flow across the pulmonary valve.

2.2 Procedure description

The vascular access was performed using the surgical cut-down technique, exposing the right external jugular vein, under general anesthesia, with the patient positioned in left lateral recumbency. Using the modified Seldinger technique or venotomy (the vein is exposed and the temporary haemostasis is obtained by placing two - cranially and caudally - umbilical tapes, silk or sterile rubber band in a single loop technique), an introducer sheath is placed and an angiography catheter was inserted through in order to perform angiography, aiming to localize the stenosis and to exclude coronary malformations. Either a diagnostic catheter or a hydrophilic guidewire (inserted through the lumen of the catheter) was advanced to the pulmonary trunk. The hydrophilic guidewire was then replaced with a rigid Rosen guidewire or a rigid guidewire was inserted through the diagnostic catheter into the pulmonary arteries. Subsequently (after removal of the angiography catheter, if necessary) the pressure balloon was inserted "over the wire". The balloon was selected individually according to the diastolic diameter of the stenosis (using the ratio Balloon/ring diameter = 1.2 or 1.3 and taking into account the size of the access port required for the balloon in relation to the patient's size). After positioning the pressure balloon at the stenosis level, the balloon inflation procedure followed. In each case the balloon was inflated 5 times successively, aiming for the "waist" appearance of the balloon to completely disappear during the last series of dilations. Finally, after the final emptying of the contrast solution from the balloon, the balloon and guidewire were withdrawn from the heart and then from the blood vessel, followed by the removal of the access port, ligation of the blood vessel or venoplasty and suture of the skin.

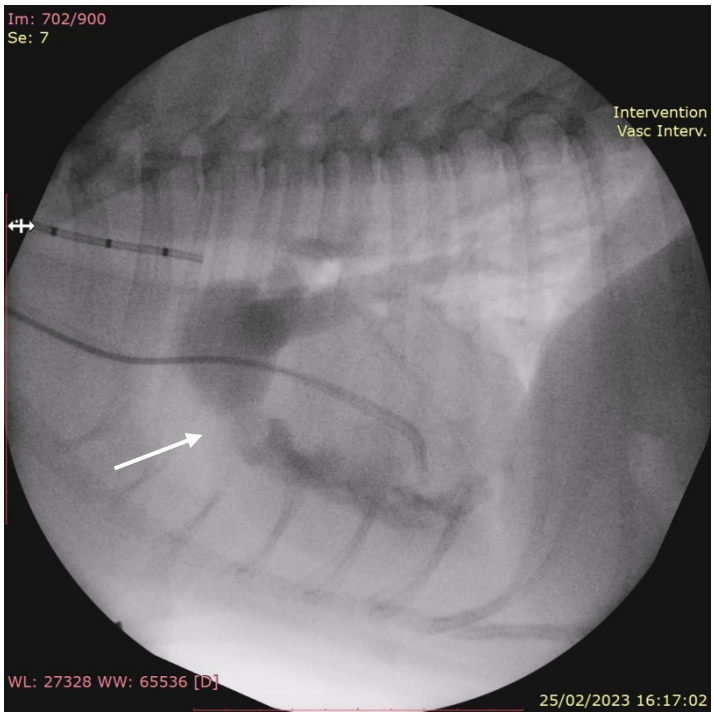

Fig. 5: Fluoroscopic image showing the angiogram taken during the procedure. The stenosis is indicated by an arrow (original)

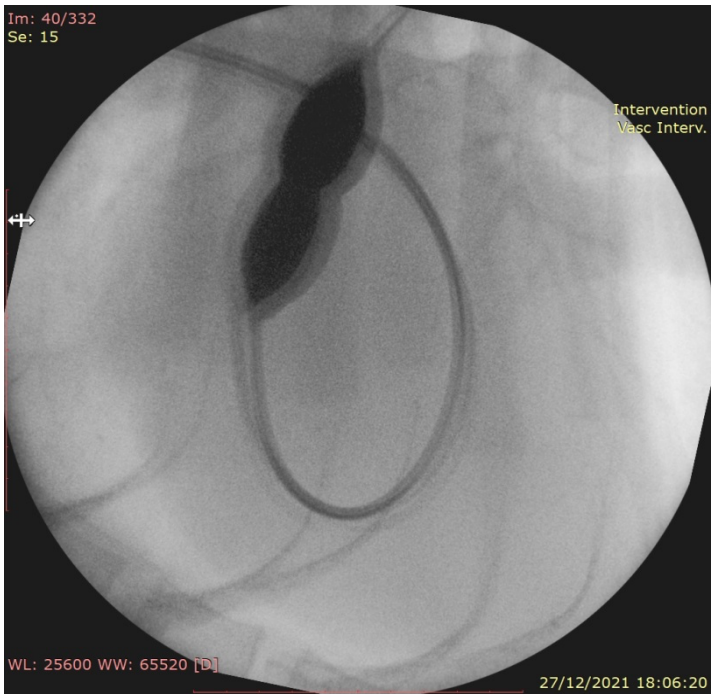

Fig. 6: Fluroscopic image showing the "waist" aspect of the pressure balloon when inflated at the level of the stenotic valve (original)

3. Results

Table 1. Echocardiographic values of each case, measured before and after the procedure

	Pulmonic valve peak pressure gradient before balloon valvuloplasty	Pulmonic valve peak velocity before balloon valvuloplasty	Pulmonic valve peak pressure gradient after balloon valvuloplasty	Pulmonic valve peak velocity after balloon valvuloplasty	Pressure peak gradient reduction percentage
Case 1	130,42 mmHg	5,71 m/s	82,81 mmHg	4,55 m/s	36,50 %
Case 2	123,21 mmHg	5,55 m/s	88,36 mmHg	4,7 m/s	28,28 %
Case 3	212,58 mmHg	7,29 m/s	194,88 mmHg	6,98 m/s	8,32%
Case 4	172,11 mmHg	6,56 m/s	85,75 mmHg	4,63 m/s	50,17 %

Three patients who underwent balloon valvuloplasty showed a reduction in pressure gradient between 28 and 50 percent. This reduction was also associated with an improvement in clinical signs, in 2 of these patients the symptomatology completely resolved, while another patient continued to show episodes of lipotimia/syncope with onset triggered by hyperadrenergic episodes.

For the other patient, balloon valvuloplasty did not reduce significantly the pressure gradient of the stenotic valve. The patient continued to present clinical signs of syncope/lipothymia and cardiac medication was maintained.

Discussions

Balloon valvuloplasty, while generally considered safe, is not without risks. Although complications were rare in our group, it is important to recognize that balloon valvuloplasty carries risks, such as arrhythmias or valvular rupture.

Ventricular premature complexes (VPCs) were commonly observed during right heart catheterization. In one case, however, a severe bradycardia occurred immediately after balloon dilatation.

The patient exhibited a favorable response to atropine, and anesthesia recovery proceeded uneventfully, with no subsequent complications."

A key post-procedural pitfall was the difficulty in ensuring timely ultrasound follow-ups, not necessarily due to lack of compliance, but rather due to the considerable distance that owners were required to travel.

The outcome of the procedure depends on many factors. As regards clinical evolution, it is necessary to take into consideration: age of the subject, degree of right ventricular hypertrophy, presence of fibrosis, possible concomitant tricuspid regurgitation.

As far as the dilation of the stenotic valve and the reduction of the transvalvular peak velocity are concerned, it is necessary to consider the type of stenosis (A. B or mixed form), the level of fibrosis of the valvular leaflets and any dynamic components of the stenosis as well as the concomitant presence of stenosing elements above or below the valve.

As regards the balloons used, it is important to evaluate the balloon diameter/valve diameter ratio. The use of compliant or non-compliant balloons, inflation of the balloon manually or with an inflator device and pressure reached inside the balloon are critical factors that influence procedural success and the possible risk of complications such as balloon rupture.

References

1. Borenstein, N., Chetboul, V., Passavin, P., Morlet, A., Fernandez-Parra, R., Arias, L. C., Giannettoni, G., Saponaro, V., Poissonnier, C., Ghazal, S., Lefort, S., Trehiou-Sechi, E., Marchal, C., Cave, J. D., Vannucci, E., Behr, L., & Verwaerde, P. (2019). Successful transcatheter pulmonary valve implantation in a dog: first clinical report. Journal of Veterinary Cardiology, 26, 10–18. https://doi.org/10.1016/j.jvc.2019.10.001
2. Borgeat, K., Gomart, S., Kilkenny, E., Chanoit, G., Hezzell, M., & Payne, J. (2021). Transvalvular pulmonic stent angioplasty: procedural outcomes and complications in 15 dogs with pulmonic stenosis. *Journal of Veterinary Cardiology*, *38*, 1–11. https://doi.org/10.1016/j.jvc.2021.09.002
3. Buchanan, J. W., Anderson, J. H., & White, R. I. (2002). The 1st Balloon Valvuloplasty: An Historical note. *Journal of Veterinary Internal Medicine*, *16*(1), 116–117. https://doi.org/10.1111/j.1939-1676.2002.tb01616.x
4. Bussadori, C., Amberger, C., Bobinnec, G. L., & Lombard, C. (2000). Guidelines for the echocardiographic studies of suspected subaortic and pulmonic stenosis. Journal of Veterinary Cardiology, 2(2), 15–22. https://doi.org/10.1016/s1760-2734(06)70007-8
5. Gomart, S., MacFarlane, P., Payne, J. R., Hezzell, M. J., & Borgeat, K. (2022). Effect of preoperative administration of atenolol to dogs with pulmonic stenosis undergoing interventional procedures. *Journal of Veterinary Internal Medicine*, *36*(3), 877–885. https://doi.org/10.1111/jvim.16403
6. Johnson, M. S., Martin, M. (2004). Results of balloon valvuloplasty in 40 dogs with pulmonic stenosis. *Journal of Small Animal Practice*, *45*(3), 148–153. https://doi.org/10.1111/j.1748-5827.2004.tb00217.x
7. Locatelli, C., Spalla, I., Domenech, O., Sala, E., Brambilla, P. G., & Bussadori, C. (2013). Pulmonic stenosis in dogs: survival and risk factors in a retrospective cohort of patients. *Journal of Small Animal Practice*, *54*(9), 445–452. https://doi.org/10.1111/jsap.12113
8. Oliveira, P., Domenech, O., Silva, J., Vannini, S., Bussadori, R., & Bussadori, C. (2011). Retrospective review of congenital heart disease in 976 dogs. *Journal of Veterinary Internal Medicine*, *25*(3), 477–483. https://doi.org/10.1111/j.1939-1676.2011.0711.x
9. Schrope, D. P. (2015). Prevalence of congenital heart disease in 76,301 mixed-breed dogs and 57,025 mixed-breed cats. Journal of Veterinary Cardiology, 17(3), 192–202. https://doi.org/10.1016/j.jvc.2015.06.001
10. Tilley, L. P., Smith, F. W. K., Sleeper, M. M., & Kraus, M. (2025). *Manual of Canine and Feline Cardiology*. Saunders.